

CALIFORNIA STATE UNIVERSITY NORTHRIDGE

ENZYMATIC TRANSFORMATIONS OF RESVERATROL  
FROM RED WINE

A thesis submitted in partial fulfillment of the requirements  
for the degree of Master of Science  
in Family and Consumer Sciences

By

Jennifer Good Jensen

August 2017

The thesis of Jennifer Jensen is approved:

---

Dr. Annette Besnilian

---

Date

---

Dr. Yoko Mimura

---

Date

---

Dr. Scott Williams

---

Date

---

Dr. Gagik Melikyan, Chair

---

Date

## DEDICATIONS

I dedicate this work to the Haldeman brothers, Danny (CSUN alumni) and Jimmy, my beloved cousins who left this world far too soon and to an exceptional woman and dear friend, Patricia White, whom I had the great pleasure of knowing as we pursued our nutrition degrees together at CSUN. Patti, your aspirations to improve children's nutrition upon earning your masters was cut short but your loving spirit lives on in my heart and the memories we shared will always make me smile. This is for you.

## ACKNOWLEDGEMENTS

From the bottom of my heart, I would like to thank my Committee Chair, Dr. Gagik Melikyan for adopting me into his elite research team of organic chemistry scholars and for translating enzymatic chemistry into a language I could understand. His research and analytical labs were where my knowledge and analytical skills flourished and I am forever grateful for the vast research knowledge I acquired under his supervision. If you were fortunate enough to get a “Melikyan high-five,” it meant he wore his happy face and your work was stellar. At times, I felt inadequate in research when I put in exhaustive amounts of time chasing sought-after data but Dr. Melikyan always kept things positive, incorporating humor into our work together to add levity to what seemed impossible. He allowed boundless learning opportunities in analytical chemistry, all of which will serve me well in my future career endeavors. I am indebted for his mentorship, patience, and devotion to the student community. Thank you so much for believing in me and giving me a chance to prove myself when no one else in my department would and for keeping me grounded during the research process.

I would like to thank Dr. Sandra Chong, my department chair for being so instrumental in paving the way for me to pursue my food science education to unprecedented new heights, and by bending the rules despite department resistance. Because of her relentless support and powerful influence, it was because of her this project was made possible. A big thank you goes to Tami Abourezk, Associate Dean of the Health and Human Development department who further approved the decision for me to pursue a thesis outside of my department.

I would like to thank Dr. Scott Williams for his steadfast support in serving on my committee from the very beginning and for showing me how to visualize my dream of higher education.

From the encouraging words exchanged in Sequoia Hall to the inspiring office chats, he empowered me to keep my eye on the prize and to hold my chin up high.

I would like to thank Dr. Annette Besnlian for her mentorship and willingness to serve on my committee despite her toiling roles as a DI director, Executive director of the MMC, fulltime faculty member, and Mom. Our common interest in research had allowed us to work together for a short time and her genuine encouragement and concern for my personal growth and wellbeing has not gone unnoticed.

I wish to thank Dr. Yoko Mimura for holding her position on my committee despite her humble reservations. Her willingness to lend a hand with the scheduling for my thesis defense was truly appreciated. She was always genuinely interested to hear about my research progress and often inquired how she could assist. Your willingness to stick by me until the end truly meant so much!

I wish to acknowledge Hedy Carpenter in Research and Graduate Studies for awarding a research scholarship to purchase much needed materials for my research project; Lani and Tanya Kiapos in the Research and Graduate Studies department for their tireless patience and supportive role in answering endless graduate-related questions with a smile; Dr. Tom Cai for his continuous role in providing me with sound advice and lending an empathetic ear throughout my graduate career; Karen Sabbah for her friendship, imparting her graduate student wisdom, and keeping me employed within the FCS department so I could provide a Catholic education for my son; Professors Erin Matthews and Julie Ellis for their no-nonsense student advice on how to survive graduate school on my own terms. A special thank you goes to Sam Cappuchino for her analytical training and to Elenie Phillipas for helping me become better acclimated in the lab.

With heartfelt gratitude to my husband, Michael my superhero for caring for our son for so many days and nights while I was away from home, for always filling in, and for your unconditional love and financial support to make my formal education a reality. I wish to thank my son Connor (my IT guru) for your assistance with computer technicalities and for creating pristine data for my presentation. I know my absence was a huge adjustment for you both and I appreciate the sacrifices you made to help me succeed academically. I wish to extend my love and gratitude to my parents who have rooted for me all my life and gave me emotional support when I needed it most. Thank you for the pep talks which gave me strength in times of despair, and keeping me focused. Thank you to my brother, Chris who always kept me motivated and cheered me on to finish school, and to his lovely wife, Adri, for always being there to help with Connor's after school care. And lastly, my cat Blax, my shadow, who helped get me through writer's block with soothing purrs and infinite affection, a creature worthy of being immortal.

## TABLE OF CONTENTS

Signature Page	II
Dedication	III
Acknowledgments	IV
List of Figures	IX
List of Abbreviations	XIII
Abstract	XIV
I. LITERATURE REVIEW	
1.1. Introduction	1
1.2. Resveratrol origin	2
1.3. Natural abundance	2
1.4. Biological activity of resveratrol	4
1.5. Metabolism of resveratrol	11
1.6. Bioavailability	12
1.7. Availability of resveratrol as a dietary supplement	12
1.8. Conclusion	12
II. RESULTS AND DISCUSSION	
2.1. Introduction	14
2.2. Enzymatic transformations of resveratrol induced by human enzymes	20
2.3. Chemical transformation of piceatannol to piceatannol- <i>ortho</i> -quinone	53
2.4. Enzymatic transformation of piceatannol to piceatannol- <i>ortho</i> -quinone	63
2.5. Conclusion	65

III. EXPERIMENTAL	69
REFERENCES	102



## LIST OF FIGURES

Figure 1. Chemical structure of resveratrol <b>1</b> (RV)	2
Figure 2. Natural polyphenols	4
Figure 3. Chemical structure of piceatannol <b>7</b> (PIC)	15
Figure 4. HPLC chromatogram of resveratrol <b>1</b>	17
Figure 5. HPLC chromatogram of the co-injection of piceatannol <b>7</b> and resveratrol <b>1</b>	18
Figure 6. Chemical structure of piceatannol <i>ortho</i> -quinone <b>8</b> (Pic-Q)	19
Figure 7. HPLC chromatogram of a <i>crude</i> mixture of piceatannol- <i>ortho</i> -quinone <b>8</b>	19
Figure 8. Alimentary CYP450 human enzymes and their allocated, multi-organ expressions	21
Figure 9. CYP2C19 mapping diagram of enzymatic expression in human organ systems	23
Figure 10. HPLC chromatogram of a crude mixture of resveratrol <b>1</b> + CYP2C19 enzymatic reaction	24
Figure 11. HPLC chromatogram of a crude mixture of resveratrol <b>1</b> + CYP2C19 enzymatic reaction spiked with piceatannol <b>7</b>	24
Figure 12. CYP2D6 mapping diagram of enzymatic expression in human organ systems	26
Figure 13. HPLC chromatogram of a crude mixture of resveratrol <b>1</b> + CYP2D6 enzymatic reaction	27
Figure 14. HPLC chromatogram of a crude mixture of resveratrol <b>1</b> + CYP2D6 enzymatic reaction spiked with piceatannol <b>7</b>	28
Figure 15. CYP3A5 mapping diagram of enzymatic expression in human organ systems	29

Figure 16. HPLC chromatogram of a crude mixture of resveratrol <b>1</b> + CYP3A5 enzymatic reaction	30
Figure 17. HPLC chromatogram of a crude mixture of resveratrol <b>1</b> + CYP3A5 enzymatic reaction spiked with piceatannol <b>7</b>	31
Figure 18. CYP4F3A mapping diagram of enzymatic expression in various organ systems	32
Figure 19. HPLC chromatogram of a crude mixture of resveratrol <b>1</b> + CYP4F3A enzymatic reaction	32
Figure 20. HPLC chromatogram of a crude mixture of resveratrol <b>1</b> + CYP4F3A enzymatic reaction spiked with piceatannol <b>7</b>	33
Figure 21. HPLC chromatogram of a crude mixture of resveratrol <b>1</b> + CYP4F3A enzymatic reaction: “pumped” sample	33
Figure 22. CYP2E1 mapping diagram of enzymatic expression in human organ systems	35
Figure 23. HPLC chromatogram of a crude mixture of resveratrol <b>1</b> + CYP2E1 enzymatic reaction	36
Figure 24. CYP2C18 mapping diagram of enzymatic expression in human organ systems	37
Figure 25. HPLC chromatogram of a crude mixture of resveratrol <b>1</b> + CYP2C18 enzymatic reaction	38
Figure 26. CYP3A4 mapping diagram of enzymatic expression in human organ systems	39
Figure 27. HPLC chromatogram of a crude mixture of resveratrol <b>1</b> + CYP3A4 enzymatic reaction	40
Figure 28. CYP1A1 mapping diagram of enzymatic expression in human organ systems	42, 64

Figure 29. HPLC chromatogram of a crude mixture of resveratrol <b>1</b> + CYP1A1	
enzymatic reaction	42
Figure 30. CYP2A6 mapping diagram of enzymatic expression in human organ systems	44
Figure 31. HPLC chromatogram of a crude mixture of resveratrol <b>1</b> + CYP2A6	
enzymatic reaction	45
Figure 32. CYP2C9 mapping diagram of enzymatic expression in human organ systems	46
Figure 33. HPLC chromatogram of a crude mixture of resveratrol <b>1</b> + CYP2C9	
enzymatic reaction	47
Figure 34. CYP2C8 mapping diagram of enzymatic expression in human organ systems	48
Figure 35. HPLC chromatogram of a crude mixture of resveratrol <b>1</b> + CYP2C8	
enzymatic reaction	49
Figure 36. CYP4F12 mapping diagram of enzymatic expression in human organ systems	50
Figure 37. HPLC chromatogram of a crude mixture of resveratrol <b>1</b> + CYP4F12	
enzymatic reaction	51
Figure 38. Progression of piceatannol <i>ortho</i> -quinone <b>8</b> decay with resveratrol <b>1</b>	
as an internal reference	57
Figure 39. HPLC monitoring of spontaneous degradation of Pic-Q <b>8</b> with resveratrol <b>1</b>	
as an internal reference; <i>lapsed time: 0 hours</i>	57
Figure 40. HPLC monitoring of spontaneous degradation of Pic-Q <b>8</b> with resveratrol <b>1</b>	
as an internal reference; <i>lapsed time: 18 hours</i>	58
Figure 41. HPLC monitoring of spontaneous degradation of Pic-Q <b>8</b> with resveratrol <b>1</b>	
as an internal reference; <i>lapsed time: 26 hours</i>	58
Figure 42. HPLC monitoring of spontaneous degradation of Pic-Q <b>8</b> with resveratrol <b>1</b>	

as an internal reference; <i>lapsed time: 42 hours</i>	59
Figure 43. HPLC monitoring of spontaneous degradation of Pic-Q <b>8</b> with resveratrol <b>1</b> as an internal reference; <i>lapsed time: 67 hours</i>	59
Figure 44. HPLC monitoring of spontaneous degradation of Pic-Q <b>8</b> with resveratrol <b>1</b> as an internal reference; <i>lapsed time: 91 hours</i>	60
Figure 45. HPLC monitoring of spontaneous degradation of Pic-Q <b>8</b> with resveratrol <b>1</b> as an internal reference; <i>lapsed time: 116 hours</i>	60
Figure 46. HPLC monitoring of spontaneous degradation of Pic-Q <b>8</b> with resveratrol <b>1</b> as an internal reference; <i>lapsed time: 141 hours</i>	61
Figure 47. HPLC monitoring of spontaneous degradation of Pic-Q <b>8</b> with resveratrol <b>1</b> as an internal reference; <i>lapsed time: 165 hours</i>	61
Figure 48. Spontaneous disproportionation of Pic-Q <b>8</b> converting to Pic <b>7</b> over time span of 141 hours	62
Figure 49. HPLC chromatogram of a crude mixture of piceatannol <b>7</b> + CYP1A1 enzymatic reaction	65

## LIST OF ABBREVIATIONS

RV	resveratrol
PIC	piceatannol
PIC-Q	piceatannol- <i>ortho</i> -quinone
HPLC	High Pressure Liquid Chromatography
LC-MS	Liquid Chromatography – Mass Spectroscopy
LIFDI	Laser-Induced Field Desorption Ionization
ESI	Electro-Spray Ionization
NMR	Nuclear Magnetic Resonance
MS	Mass Spectroscopy
TLC	Thin Layer Chromatography
PTLC	Preparative Thin Layer Chromatography
DES	diethylstilbestrol
BPA	bis-phenol A
PE	Petroleum Ether
P	Pentane
E	Ether
ACN	acetonitrile
d	doublet
dd	doublet of doublets
s	singlet
t	triplet

## ABSTRACT

### ENZYMATIC TRANSFORMATIONS OF RESVERATROL FROM RED WINE

Jennifer Jensen

Master of Science in Family and Consumer Sciences

In the course of this study we established that cytochrome P450 enzymes are capable of converting resveratrol to its *ortho*-hydroxylated derivative, piceatannol, and piceatannol to its carcinogenic derivative, piceatannol *ortho*-quinone. Among 12 commercially available enzyme preparations, seven of them *ortho*-hydroxylated resveratrol with high conversion rates: (CYP2C18, 95%; CYP3A4, 96%; CYP1A1, 97%; CYP2A6, 97%; CYP2C9, 97%; CYP2C8; 98%; CYP4F12, 98%). Enzyme CYP1A1 was also able to convert piceatannol to its oxidized form, piceatannol *ortho*-quinone that belongs to the class of organic carcinogens, *ortho*-quinones. Feasibility of piceatannol oxidation to its respective *ortho*-quinone is corroborated by the chemical oxidation with manganese dioxide and full structural characterization by the totality of analytical methods. Stability studies on piceatannol *ortho*-quinone indicated that while its decomposition is rapid at room temperature in a solid form, or in contact with chromatographic sorbents, in a solution, at ambient temperatures, this potential carcinogen can survive for 141 hours, or almost 6 days. These experimental data suggest that consumption of resveratrol from dietary sources (wine, peanuts, berries), or through RV supplementation, represents a clear danger to public health. Given the abundance of cytochrome P450 enzymes in the human body, and their demonstrated ability to effect the resveratrol-*to*-piceatannol-*to*-piceatannol-*ortho*-quinone chemical sequence, it is conceivable that the same enzymatic transformations can also occur inside the human body, in multiple locations. *Ortho*-quinones thus formed could

potentially survive *in vivo* for days, and trigger tumor formation due to a well-known ability of *ortho*-quinones to react with DNA bases and render them biologically dysfunctional. The mechanism of carcinogenesis suggested for resveratrol is analogous to that established for female hormones, such as beta-estradiol. As a human carcinogen, estrogens are introduced into the list of carcinogens, which is maintained by the International Agency for Research on Cancer (IARC). The said carcinogenicity is the main reason why in the early 2000's the hormone-replacement therapy (HRT) was severely discredited, temporarily banned, and then re-evaluated for treatment of post-menopausal symptoms. This newly acquired knowledge on resveratrol enzymatics should be made available to the general public who is exposed to unrelenting advertisements on resveratrol and its supplements. In the long run, uncontrollable exposure to resveratrol may contribute to proliferation of various cancers, potentially becoming the next public health disaster. By its magnitude, it could be *on par* with asbestos, diethylstilbestrol (DES), thalidomide, bis-phenol A (BPA), or hexavalent chromium exposure.

## I. LITERATURE REVIEW

### 1.1. Introduction

Polyphenols that naturally exist in red wine have been extensively studied for many years and currently are well known to the general public for their alleged health claims.<sup>1a-c</sup> The star antioxidant in wine is resveratrol that has gained recognition in 1992 for its ability to protect the lining of coronary blood vessels.<sup>1a</sup> In particular, resveratrol was shown to increase high-density lipoprotein (HDL) or “good” cholesterol, decrease low-density lipoprotein (LDL) or “bad” cholesterol, and prevent arterial damage.<sup>1a</sup> To achieve the same therapeutic effects in humans as seen in mice, an individual would need to consume around 1,000 liters of wine every day.<sup>1b</sup> Resveratrol concentration in wine is dismal in comparison to therapeutic doses required, hence the supplement industry emerged with a pill form containing high doses of an active ingredient (100mg-2g) in order to entice the public that the heart benefits exhibited in animal studies could potentially be achieved in human subjects, a gross misconception at best. Experimental data on resveratrol did not support a multitude of health claims covered by the news media, nevertheless in 2006, a substantial surge in supplement sales was observed. Resveratrol has been touted as a “miracle pill” due to its anti-atherogenic, anti-estrogenicity, anti-inflammatory, and anti-platelet aggregation properties, as well as neuroprotection, blood sugar regulation, and prolonged endurance during exercise.<sup>1a,d-g</sup> Its most appraised attributes in the media today are an alleged anti-aging property and prevention of degenerative ailments such as dementia and Alzheimer’s disease.<sup>1h</sup> The latter is the sixth leading cause of death in the United States and the epidemic is projected to triple by 2050. This review identifies resveratrol’s plant-based origin, abundance in nature, biological properties, adverse effects, metabolism, bioavailability, data transferability from animal studies to humans, and health implications.



## 1.2. Resveratrol Origin

Resveratrol, a polyphenol called 3,5,4'-trihydroxystilbene (**1**), is produced in various plant species with the aid of stilbene synthase enzyme<sup>2a</sup> to protect the host from injury, herbivores, reactive oxygen species (ROS), and photosynthetic stress.<sup>1d</sup> In 1976, Langcake and Pryce<sup>2b</sup> identified resveratrol as a phytoalexin; it was first isolated in 1940 by Takaoka from white hellebore roots and again in 1963 from Japanese knotweed roots.<sup>2c</sup> *Trans*-resveratrol biosynthesis may be induced by ozone exposure, microbial infections, and UV radiation and is relatively stable when protected from light and high pH.<sup>2d</sup>

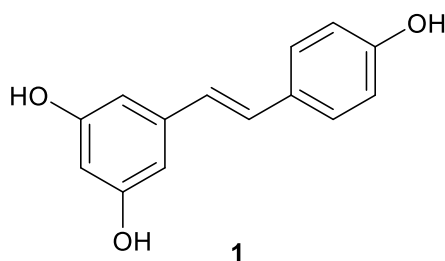


Figure 1. Chemical structure of resveratrol **1** (RV).

## 1.3. Natural Abundance

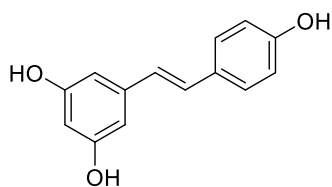
Over the last decade, resveratrol has retained its widespread popularity as a supplement due to its presence in grapes and red wine.<sup>3a</sup> Polyphenols, in general, are more abundant in fruits than vegetables, with concentrations as high as 1-2g per 100g of fresh weight. Resveratrol concentration is substantially elevated in grape skins,<sup>3b</sup> muscadine grapes and seeds,<sup>3c</sup> peanuts,<sup>3d</sup> cranberries,<sup>3e</sup> and pines.<sup>3f</sup> In particular, its content in muscadine grapes is reported to be as high as 40mg/L.<sup>3c,3g</sup> Resveratrol amounts in red wine are dependent upon its fermentation time (wine's contact time with grape skins), grape variety, geographic region, grape cultivar, and

fungal infection exposure.<sup>3b</sup> Some red varieties contain about 160µg of resveratrol per fluid ounce. One ounce of peanuts yields about 79µg of resveratrol<sup>3h</sup> and blueberries have roughly twice as much resveratrol as bilberries.<sup>3i</sup> Resveratrol in these berries constitutes ten percent of that found in grapes and can rapidly degrade, by up to 50%, at elevated temperatures.<sup>3i</sup> Resveratrol is also found in plums and to a lesser extent, in white wines.<sup>3j</sup>

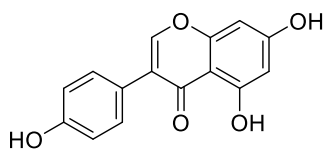
Resveratrol synthesized by grapevines (*Vitis vinifera*) and other plants<sup>2c</sup> is not as easily available due to its low yield and laborious, time-consuming extraction process.<sup>3k</sup> An average concentration of resveratrol in red wine is equal to 1.9±1.7mg per liter and spans from non-detectable levels up to 14.3mg per liter, with Pinot Noir and St. Laurent varieties containing the highest amounts of resveratrol.<sup>3l</sup>

Structurally, resveratrol **1** belongs to the family of natural non-steroidal phytoestrogens such as genistein **2**, daidzein **3**, quercetin **4**, and enterodiol **5**. These polyphenolic compounds are topologically similar to endogenous 17β-estradiol **6**, a female hormone generated from testosterone by an aromatization process, and are capable of binding to human estrogen receptors (ERs) and exhibiting estrogenic activities of various intensities (Figure 2).<sup>1c</sup> Overall, there are over 5,000 flavonoid compounds isolated from the plant kingdom, including catechins from tea, isoflavones from soy, anthocyanins from blueberries, flavanone from citrus, cumestans from alfalfa and clover sprouts, as well as lignans from flaxseeds and grains.<sup>1c</sup> Many of these compounds contain multiple sites for enzymatic transformations and, given their very nature, exhibit a wide array of biological activities.

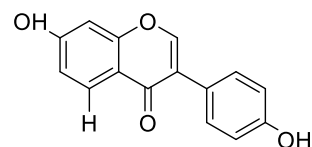
### Non-Steroidal Phytoestrogens



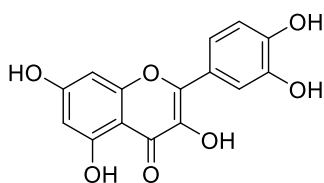
resveratrol **1** (wine)



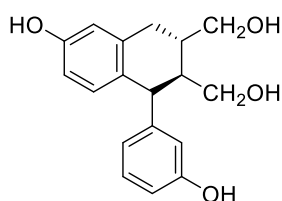
genistein **2** (soy)



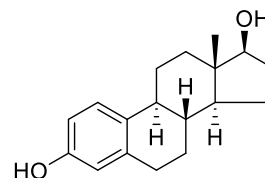
daidzein **3** (soy)



quercetin **4** (onions)



enterodiol **5** (flaxseeds)



$\beta$ -estradiol **6** (hormone)

Figure 2. Natural polyphenols.

### 1.4. Biological Activity of Resveratrol

**Resveratrol as an Anticancer Agent.** The protective role of plant-derived antioxidants acting as free radical scavengers has become a widely accepted theory in food science.<sup>1b,4a</sup> In particular, the antioxidant capacity for polyphenols is dependent upon redox properties of their hydroxyl groups and electron delocalization across the chemical structure.<sup>4b</sup> For resveratrol **1**, alternative antioxidant pathways suggested are as follows: (i) coenzyme-Q competition and down-regulation of the oxidative chain complex where reactive oxygen species (ROS) generation occurs, (ii) scavenging of mitochondrial-formed superoxide ( $O_2^{\cdot-}$ ) and hydroxyl ( $\cdot OH$ ) radicals, and (iii) inhibition of lipid peroxidation initiated by products of Fenton reactions.<sup>4c</sup>

From a practical point of view, the anticancer effect of resveratrol is best demonstrated for skin cancers and gastrointestinal tract tumors.<sup>4d</sup> In a two-stage mouse model, it prevented the laboratory carcinogen, 12-*o*-tetradecanoylphorbol-13-acetate (TPA), from forming tumors when

resveratrol **1** (1, 5, 10, or 25 $\mu$ mol) and TPA were administered twice weekly for 18 weeks. Two skin tumors per mouse (40% incidence) were observed, tumor shrinkage was 68, 81, 76, or 98%, respectively, and the percentage of mice with lesions declined in a dose-dependent manner (50, 63, 63, or 88%).<sup>4d</sup> Another study demonstrated that the pre-application of resveratrol on mouse skin permitted return of glutathione, hydrogen peroxide, myeloperoxidase, oxidized glutathione reductase, and superoxide dismutase levels back to those recorded prior to administering laboratory carcinogens.<sup>4e</sup> Direct contact of resveratrol with skin lesions may hold promise for future chemotherapeutic modalities in cancer treatment.

Jang and colleagues<sup>4f,g</sup> demonstrated resveratrol's anticancer and cytostatic properties at all three carcinogenetic stages (initiation, promotion, and progression). In particular, it hindered the initiation stage of DNA damage by acting as a free radical scavenger and by inducing quinone reductase synthesis, a phase II enzyme responsible for detoxifying carcinogens.<sup>4h</sup> In ovarian cancer cell lines, resveratrol **1** was shown to inhibit an uptake of glucose thus causing selective cancer cell death due to different energy requirements between healthy and malignant cells.<sup>4i</sup>

While no human clinical trials have been reported for resveratrol,<sup>4d</sup> multiple animal studies demonstrated its anti-cancer properties:<sup>4j</sup>

- administering the prophylactic doses of resveratrol (0.02-8mg/kg) reduced or prevented formation of the intestine and colon tumors in rats exposed to various carcinogens;<sup>4d</sup>
- mammary tumor formation in mice was inhibited with high doses of injectable resveratrol;<sup>4d</sup>
- in mice with pre-existing neuroblastomas, high-dose injections of resveratrol attenuated tumor growth;<sup>4d</sup>

- in various cells, resveratrol inhibited reactive oxygen intermediate (ROI) production and lipid peroxidation prompted by tumor necrosis factor (TNF);<sup>4k</sup>
- an *in vivo* study demonstrated resveratrol's antioxidant capacity in preventing renal oxidative DNA insult induced by the known kidney carcinogen, KBrO<sub>3</sub>; <sup>4l</sup>
- resveratrol inhibited growth of prostate cancer cell line, DU145, decreased nitric oxide (NO) production, and inhibited induction of nitric oxide synthase (iNOS);<sup>4m</sup>
- resveratrol down-regulated oxygen superoxide and H<sub>2</sub>O<sub>2</sub> production by macrophages stimulated by lipopolysaccharide (LPS) or TPA, and, in contrast, down-regulated COX-2 induction, arachidonic acid release, and prostaglandin (PG) formation.<sup>4n</sup>

It is also worthy to mention that in the presence of glutathione, resveratrol prevented hydroxyl radical generation and formation of glutathione disulfide, maintained intracellular glutathione concentrations in human blood cells,<sup>4o</sup> and raised the levels of the antioxidant enzymes, such as glutathione peroxidase, glutathione S-transferase, and glutathione reductase.<sup>4p</sup>

***Resveratrol and DNA Replication.*** Contrary to the studies presented thus far on resveratrol as a cancer cell mediator, resveratrol was found to be a strong DNA polymerase inhibitor, an essential enzyme for DNA replication.<sup>5a</sup> An antiproliferative outcome was observed in mammalian tumor cells where resveratrol suppressed ribonucleotide reductases,<sup>5b</sup> enzymes needed to reduce ribonucleotides into deoxynucleotides and which are essential during the S-phase of DNA synthesis.<sup>5c</sup> It also generated 2-4 times greater transcriptional activation in MCF-7 (breast) cancer cell lines and less activation than estradiol in BG-1 (ovarian) cancer cell lines, demonstrating that agonistic activity is cell-type specific.<sup>5d</sup> NFκB is an inducible transcription factor linked to immune and inflammatory responses and is directly associated with cancer cell proliferation in select cancer models.<sup>5e</sup> Resveratrol was first seen influencing the transcription

factor by Draczynska-Lusiak and colleagues where NFκB's binding activity was initiated by oxidized low density lipoprotein (LDL), thereby slowing the activation of NFκB in PC-12 (rat adrenal medulla) cell lines.<sup>5f</sup>

***Resveratrol as a Cardio-Protection Agent.*** Scientific evidence has shown that resveratrol can inhibit eicosanoids and lipid syntheses, which are attributed to atherosclerosis and inflammation, and lower cardiac arrhythmias.<sup>6a</sup> Researchers at Ohio State University and Northeast Ohio Medical University found that resveratrol is capable of slowing down cardiac fibrosis progression.<sup>6b</sup> In Sinclair's mouse study, resveratrol offset harmful effects of a high fat diet.<sup>6c</sup> The mice in the high fat plus resveratrol supplementation group consumed hydrogenated coconut oil (60% from fat energy), 30% more calories than the mice on the standard diet, and 22mg/kg of resveratrol compared to the control group. Analysis of gene expression indicated that resveratrol supplementation opposed the alteration of 144 out of 155 altered gene pathways. Interestingly, glucose and insulin levels in these mice were closer to the mice on the standard diet, however resveratrol supplementation didn't change the cholesterol and free fatty acid levels, which were considerably higher in mice on the high fat, supplemental diet.<sup>6c</sup>

***Exercise Endurance.*** Johan Auwerx's mouse endurance study conducted at the Institute of Genetics and Molecular Biology in France confirmed Sinclair's hypothesis that resveratrol activates the Sirtuin 1 (SIRT1) gene. Thus mice given resveratrol for 15 weeks had better overall treadmill endurance than the control group.<sup>7</sup> Interestingly, Finnish adults (n=123) who were born with high variations of SIRT1 genes, accompanied by expedient metabolisms, biologically recruited the same SIRT1 pathway activated in the aforementioned endurance study.<sup>7</sup>

***Resveratrol as a Neuroprotective Agent.*** In 2008, researchers at Cornell University demonstrated that oral resveratrol supplementation significantly lowered brain plaque formation

in a mouse model, a physical attribute responsible for Alzheimer's disease (AD) and other neurodegenerative diseases.<sup>8</sup> Researchers reported a vast reduction of plaque in the following regions of the brain: 90% reduction in the hypothalamus, 89% reduction in the striatum, and 48% reduction in the medial cortex. There are two theories that arise from neuroprotection and resveratrol supplementation: (1) that oral ingestion of resveratrol in humans may lower beta amyloid plaque formation attributed to aging populations and (2) the mechanism by which plaques are removed related to the resveratrol's ability to act as a copper chelator.<sup>8</sup>

***Other Biological Effects.*** In a human trial, 3-5 grams of resveratrol have been shown to drastically reduce blood sugar.<sup>9a</sup> Howitz and Sinclair (2003) demonstrated a significant, prolonged lifespan in yeast, *Saccaromyces cerevisiae* given resveratrol as a supplement.<sup>9b</sup> The fruit fly, *Drosophila melanogaster* and worm, *Caenorhabditis elegans* also demonstrated extended lifespans when fed with resveratrol.<sup>9c</sup> Another research group achieved reproducible results with *C. elegans*<sup>9d</sup> but a third group could not reproduce Sinclair's prolonged lifespan theory on either species.<sup>9e</sup> Contrary to Sinclair's findings,<sup>9b,c</sup> Gems and Partridge conducted large-scale studies on the fruit fly and worm and observed no lifespan effects with resveratrol supplementation;<sup>9e</sup> in an analogous setting, Pearson did not observe prolonged lifespan in mice.<sup>9f</sup>

***Estrogenicity and Antiestrogenicity.*** An in-depth review of over 100 clinical studies provided conclusive evidence that phytoestrogens support bone health (lowers osteoporosis), and supposedly preempt cardiovascular diseases and neurodegeneration.<sup>1a</sup> By capitalizing on these premises, supplement manufacturers have flooded the marketplace with the plant-based extracts which are endowed with estrogenic properties. There are legitimate health concerns for different population clusters in regards to exposure to estrogens, or natural estrogen-like chemicals. One of the most susceptible groups is infants' whose diet has been supplemented with soy-based

formulas during their first year of life. Neonatal soy formulas contain high amounts of isoflavones, which “are an order of magnitude greater than levels which have been shown to produce physiological effects” in adult females consuming a soy-rich diet.<sup>10a</sup> One collective view of existing, yet limited data suggest there are no adverse effects on human development or reproduction, however more precautionary views convey caution to parents as there is very little research on infant isoflavone consumption and potential long-term effects.<sup>10b</sup>

Resveratrol, due to its structure similar to that of the natural estrogens and estrogen mimics, is also found to be estrogenic.<sup>10c-f</sup> Some retailers of resveratrol now sell the supplement with a warning label that cautions expectant mothers or women of childbearing age as to possible consequences. Children should also not take resveratrol supplements due to the lack of studies on the effects of normal development.<sup>10c</sup> More detailed studies revealed that in different biological settings, resveratrol can exhibit a wide spectrum of activities further attesting to its alleged estrogenicity. Among them are: (a) acting as an agonist in MCF-7 cell lines;<sup>1a</sup> (b) stimulating the growth of estrogen-dependent T47D breast cancer;<sup>1a</sup> (c) suppressing proliferation of estrogen receptor (ER)-positive and -negative mammary cancer cells in humans;<sup>10g</sup> (d) exhibiting significant binding affinities to estrogen receptor- $\alpha$  (ER- $\alpha$ ) and estrogen receptor- $\beta$  (ER- $\beta$ ) receptors both expressed of human breast cancer cells and rodent uterine cells;<sup>10h</sup> (e) selectively down-regulating the ER- $\alpha$  subtype in Ishikawa (endometrial cancer) cells;<sup>10i</sup> and (f) exhibiting an estrogenic and bone-protective effects in (MC3T3-E1) mouse osteoblast cells.<sup>10j</sup> Further attesting to the dual nature of resveratrol, at high doses (575mg/kg body weight), it exhibited an antiestrogenic effect,<sup>1e</sup> and also functioned as a *Selective Estrogen Receptor Modulator* (SERM) demonstrating both estrogenic and anti-estrogenic properties in ER<sup>+</sup> mammary cancer cell lines.<sup>10k</sup>



***Pro-oxidant Properties, Genotoxicity, and Carcinogenicity.*** In a plasmid-based DNA cleavage assay, Fukuhara and Miyata first discovered the pro-oxidant activity of resveratrol on pBR322 DNA in the presence of Cu(II).<sup>11a</sup> Further studies have shown that resveratrol cleaves DNA by reducing Cu(II) to Cu(I) species which in turn generate DNA-derived oxidized products.<sup>11b</sup> The proposed mechanism challenged the conventional dogma that dietary supplements exclusively function as antioxidants. Burkitt and Duncan further challenged this view by providing evidence that resveratrol promotes the formation of hydroxyl radicals in tandem with DNA-bound copper species.<sup>11c</sup> It is well established that oxygen-centered radicals such as hydroxyl radical can wreak havoc on DNA and contribute to excessive lipid peroxidation.<sup>11d</sup> Galati and colleagues demonstrated that the observed effect is not limited to resveratrol, but is rather typical for plant polyphenols when they come into contact with peroxidases.<sup>11e</sup> In a Chinese hamster ovary (CHO) cell line, resveratrol causes endogenous oxidation and chromosomal insult at concentrations as low as 200 $\mu$ M.<sup>11f</sup> In intact peripheral blood lymphocytes (PBL's), a comet assay showed that DNA damage was induced by resveratrol in the presence of Cu(II) ions at much lower concentrations, i. e. 50 $\mu$ M.<sup>11g</sup> More interestingly, *even in the absence of copper*, resveratrol as well as epigallocatechin gallate (EGCG) from green tea could still induce DNA fragmentation at concentrations greater than 200 $\mu$ M.<sup>11h</sup> In isolated nuclei, the pro-oxidant nature of resveratrol relied on nuclear copper bound to chromatin that is primarily comprised of DNA, RNA, and protein moieties.<sup>11i</sup> It is worthy to mention that the essential role of copper ions was proved by reversal of DNA breakage in the presence of neocuproine, a copper chelator.<sup>11h</sup> In a rat model, oral copper supplementation resulted in copper accumulation in lymphocytes, which were then isolated and treated with resveratrol.<sup>11i</sup> An

extensive DNA degradation served as an experimental proof that endogenous copper played a critical role in resveratrol's pro-oxidant behavior.<sup>11i,j</sup>

### 1.5. Metabolism of Resveratrol

The cytochrome P-450, heme-containing enzymes are responsible for xenobiotic metabolism.<sup>12a,b</sup> In particular, enzymes CYP1A1, CYP2A6, and CYP3A4 are selective in metabolizing known classes of carcinogens such as aromatic hydrocarbons (PAHs).<sup>12b-d</sup> The subsequent metabolites are activated pro-carcinogens that can interact with DNA. Overexpressed P450 enzymes are found in breast, colon, and lung tumors of humans.<sup>12e-g</sup> The following aromatic hydrocarbons (AH): benzo[a]pyrene (B[a]P), 2,3,7,8-tetrachlorodibenzo-*p*-dioxin (TCDD), and dimethyl-benz[a]anthrazene (DMBA) induce CYP1A1 gene transcription by binding to the aryl hydrocarbon (Ah) receptor causing nucleus translocation, CYP1A1 gene promoter interaction, and up-regulation of CYP1A1, mRNA, and proteins. Resveratrol was shown to inhibit B[a]P, which activated the Ah receptor, from binding to the xenobiotic response element of the CYP1A1 promoter gene.<sup>12h,i</sup>

Contrary to these studies, resveratrol was also shown to act as an antagonist for the Ah receptor.<sup>12j</sup> It is also capable of inhibiting CYP450 isozymes responsible with enzymatic dealkylation processes. Thus, resveratrol was shown to inhibit the activation of CYP1A1 and CYP1A2, where CYP1A1 is a key extrahepatic enzyme known for its critical role in chemoprevention.<sup>12k</sup> It was demonstrated that resveratrol can decrease *o*-dealkylation activity of CYP1B1,<sup>12l</sup> and also can inactivate CYP3A4 in colon and liver cancers where this enzyme is overexpressed.<sup>12m</sup> From these inhibitory studies alone, resveratrol has clearly exhibited its direct, interceptive role in isozyme suppression as related to attenuation of cancer cell proliferation.

## 1.6. Bioavailability

Resveratrol absorption is most effective in humans by buccal administration (direct absorption by visceral tissue of the oral cavity).<sup>13a</sup> Due to its biotransformation and rapid elimination, resveratrol reports suggest that it has extremely low bioavailability. Metabolic reactions occur in the intestines and liver to generate, as conjugates, respective glucuronate and sulfonate.<sup>13b</sup> Less than 5ng/mL of resveratrol was detected in blood, followed by an oral ingestion of a 25-mg dose.<sup>13b</sup> High doses of resveratrol (2.5-5 g) yielded low blood concentrations and did not exhibit a chemotherapeutic effect,<sup>13c</sup> however 3-5 g of a proprietary formula, SRT-501 manufactured by Sirtris Pharmaceuticals was retained in the blood 5-8 times longer and demonstrated the needed concentration to exert cancer prevention effects in animal and in vitro studies.<sup>9a</sup>

## 1.7. Availability of Resveratrol as a Dietary Supplement

Chronologically, first resveratrol supplements were derived from desiccated, ground grape skins and seeds.<sup>14a</sup> Most supplements marketed in the United States today are made from Japanese knotweed root (*Polygonum cuspidatum*), as well as grape skin or red wine extracts. Doses of resveratrol in a single-pill form can range from 100 to 500mg. Safe and effective doses for human disease prevention remain unknown.<sup>14b</sup>

## 1.8. Conclusion

From a public health perspective, it is paramount to inform the general public that phytochemicals either consumed as supplements, extracts, or dietary sources, can have a deleterious impact on human health. Research has amply demonstrated that many natural

polyphenols have a dual nature, either by exhibiting genotoxic and estrogenic properties *in vitro*, or by displaying anti-carcinogenic properties through either enzymatic inhibition, by acting as antioxidants, or by inducing apoptosis in cancer cells. It is clear that genotoxicity of a variety of phytoestrogens and their metabolites can work through different mechanisms and that further investigations are warranted. To date, no long-term efficacy studies have been conducted on phytochemicals of polyphenolic nature and their actual ability to *prevent diseases*. Hence, investigators have yet to find safe and effective doses that could be recommended to the general public.

In case of resveratrol, biological effects vary widely and further investigations are warranted. Although a number of animal studies claim beneficial effects with supplementation, careful considerations with regard to transferability of evidence from animals to human subjects are needed. It is important to point out that animal tumors differ from those in humans, thus conclusions made with regard to animal studies should not be automatically carried over and presumed applicable, and beneficial, to humans. In today's society, resveratrol is overabundantly consumed as a dietary supplement despite the facts that its undesirable biological activities are well established, its metabolism is not fully understood, its bioavailability is extremely low, and its close structural analogs are known to be carcinogens. The current project was undertaken to shed light upon interaction of resveratrol with human enzymes located in alimentary canal and to assess potential dangers that an average person is exposed to because of the uncontrolled consumption of resveratrol supplements.

## II. RESULTS AND DISCUSSION

### 2.1. Introduction

Endogenous enzymes are capable of carrying out a multitude of biochemical transformations such as the conversion of food to energy, elimination of waste products, and the breakdown of drugs or supplements that we take. Among them, cytochrome P450 enzymes abbreviated as CYP are intended – by design – to conduct some of the most complex enzymatic reactions that take place inside the human body. Our project on resveratrol **1** was intended to study enzymatic transformations by human CYP450 enzymes located in alimentary canal. Prior studies by Potter's and Lucas' research teams<sup>15a,c</sup> revealed through HPLC and GC-MS analysis that resveratrol **1** can undergo aromatic hydroxylation by cytochrome P450 CYP1B1 and CYP1A2, forming three major metabolites: M1 (proposed to be 3,4,5,4'-tetrahydroxystilbene), M2 (piceatannol **7**, Fig. 3), and M3, a minor unknown metabolite, proposed to be a dihydroxylated derivative 3,4,5,3',4'-pentahydroxystilbene. The molecule of piceatannol **7** contains hydroxyl groups, which are positioned next to each other, making them susceptible to oxidation to carcinogenic *ortho*-quinones.<sup>15b</sup> To assess how common this problematic *ortho*-hydroxylation is among enzymes lining the alimentary canal, we identified 12 of them which were commercially available at the commencement of this project: CYP2C19, CYP2D6, CYP3A5, CYP4F3A, CYP2E1, CYP2C18, CYP3A4, CYP1A1, CYP2A6, CYP2C9, CYP2C8, and CYP4F12. The enzymes thus chosen span the human digestive tract and vary from each other by the level of expression. All of them were tested with resveratrol **1** acting as an enzymatic substrate, while piceatannol **7** was screened with CYP1A1 enzyme to test its ability to undergo a secondary oxidation to its respective *ortho*-quinone.

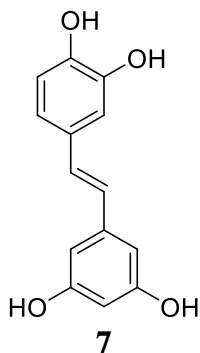


Figure 3. Chemical structure of piceatannol **7** (PIC).

The initial stage of the project consists of optimizing HPLC conditions for sufficient separation of resveratrol **1** and piceatannol **7**. There were numerous HPLC parameters that needed to be standardized such as flow rate, injection volume, sample preparation, solvent in which sample is dissolved, sample concentration, and composition of eluent. The only setting that remained constant was the wavelength controlled by the diode array detector (DAD). Both substrate and its hydroxylated derivative were detectable at 320nm with the reference absorption being set at 360/100nm. The flow rate was adjusted accordingly from 0.8 to 1.0 mL/min dependent on retention time ranges and peak separations. The injection volumes were adjusted based on sample type in order to minimize peak intensity. Reference samples were typically chosen between 1-10 microliters dependent upon the sample concentration in order to avoid column overload. All enzymatic samples had a standardized injection volume of 30 microliters because of low end-product concentrations. We experimented with several options for the isocratic mobile phase delivery: single (pre-mixed) versus dual solvent bottle delivery of various ratios of filtered acetonitrile and deionized water. System maintenance protocols were paramount to ensure optimal system performance: end-of-day needle washes and column flushes, as well as a reversal of solvent elution were routine operations in this project. Preparations of fresh mobile

phase solutions were rigorously mixed and allowed to reach room temperature prior to daily HPLC consecutive injections.

***Developing conditions for HPLC analysis of authentic, reference samples and enzymatic stock solutions. HPLC analysis of resveratrol 1.*** Resveratrol **1** reference samples were needed to determine retention times under optimized HPLC analytical conditions. Systematic reference sample runs were conducted on a weekly basis to check for reproducibility of retention time results prior to running enzymatic-related samples. To prepare a reference solution, commercially available resveratrol **1** (4.6mg, 0.02mmol) was dissolved in acetonitrile : deionized H<sub>2</sub>O, 1 : 3 (20mL, v/v). This ratio was analogous to the HPLC analytic conditions under isocratic mobile phase (Figure 4). For enzymatic samples, the solvent composition was chosen as acetonitrile : deionized H<sub>2</sub>O, 1 : 1 (6mL, v/v), that mimicked the solvent composition of the enzymatic reaction mixture. Originally, we prepared stock solutions with acetonitrile during preliminary trials, and later chose dimethyl sulfoxide (DMSO) as the exclusive medium for all enzymatic reactions. Hence, the stock solution consisted of resveratrol **1** (4.6 mg, 0.02 mmol) dissolved in 20mL of anhydrous DMSO (99.99% purity). Round-bottom flasks containing DMSO stock solutions were stored under refrigerated conditions initially, then later kept at room temperature covered with foil when not in use. The reason was that DMSO (mp 19°C) froze under refrigerated conditions, hence it was more efficient to store the solution under room temperature while conducting enzymatic reactions as the defrost step could be completely eliminated. Visual inspections of stock solutions related to color changes (from clear to clear yellow) were conducted prior to all enzymatic screenings. A color change signified stock solution decomposition, therefore fresh stock solutions were prepared if color changes were

noted. Retention times for resveratrol **1** were around 9 minutes (Figure 4), however fluctuations in elution times were not uncommon given the state of the column, its “age,” and number of parameters related to prior HPLC separations.

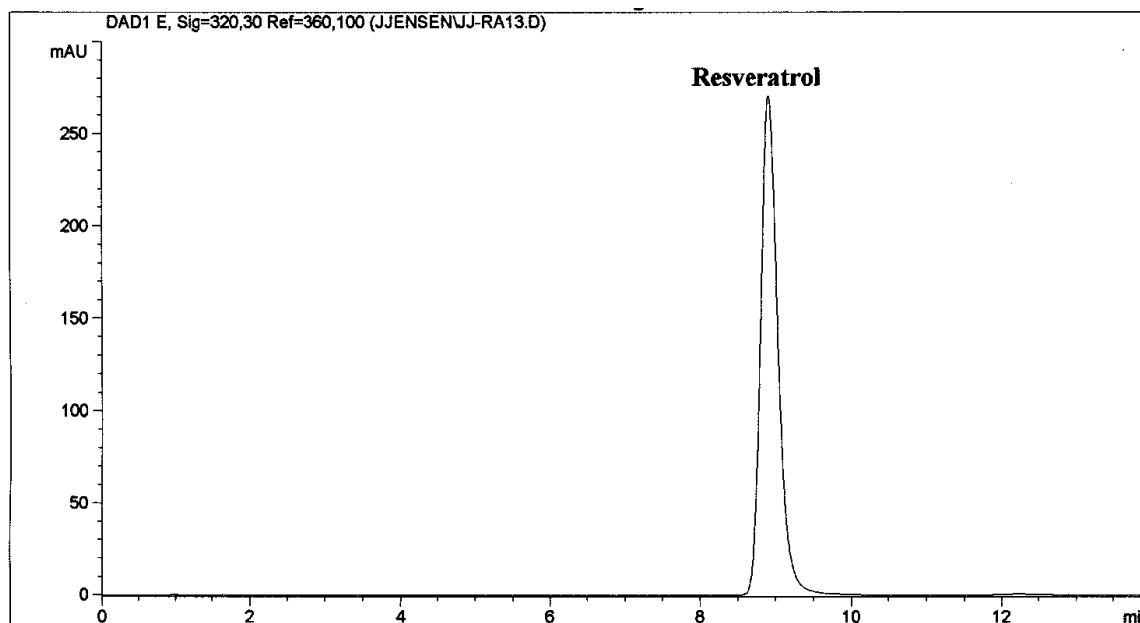


Figure 4. HPLC chromatogram of resveratrol **1** (1mM; solvent: acetonitrile : deionized H<sub>2</sub>O, 1 : 3, v/v; column: Zorbax SB-C18 reversed phase; dimension: 4.6 x 150mm, 5-micron; flow rate: 1mL/min; injection volume = 5 $\mu$ L; run time = 14min.;  $t_r$  = 8.91min).

**HPLC analysis of piceatannol 7.** Commercially available piceatannol **7** was dissolved in a mixture of acetonitrile : deionized H<sub>2</sub>O, 1 : 3 (v/v), and analyzed by HPLC on a weekly basis to determine its retention time and to check system performance. Similar to resveratrol, the solvent composition ratios were varied to determine ideal elution rates and retention times for this substrate. For enzymatic reactions, piceatannol **7** (2.3mg, 0.009mmol) was dissolved in DMSO (10mL) and solutions were kept at ambient temperatures.

To determine relative retention times for resveratrol **1** and piceatannol **7** within the *same sample*, an equimolar mixture was prepared by dissolving piceatannol **7** (12.2mg) and resveratrol **1** (11.4mg) in 6mL acetonitrile : deionized H<sub>2</sub>O, 1 : 1 (v/v). This ratio mimicked the solvent



composition of the enzymatic reaction. Final optimized HPLC conditions were as follows: (1) 1.0mL/min flow rate by a quaternary pump; (2) diode array detector (absorbance) signal of 320nm / reference 360nm, 100 nm; (3) injection volume - 30 $\mu$ L for all crude and pumped samples (excluding authentic, spiked, stock solution, and equimolar samples); and (4) single-bottle delivery of an isocratic mobile phase of acetonitrile : deionized water, 1 : 3, v/v. Under these conditions, a comfortable, 3-min separation was achieved between piceatannol **7** and resveratrol **1** (5.85 and 8.80 min, respectively; Fig. 5).

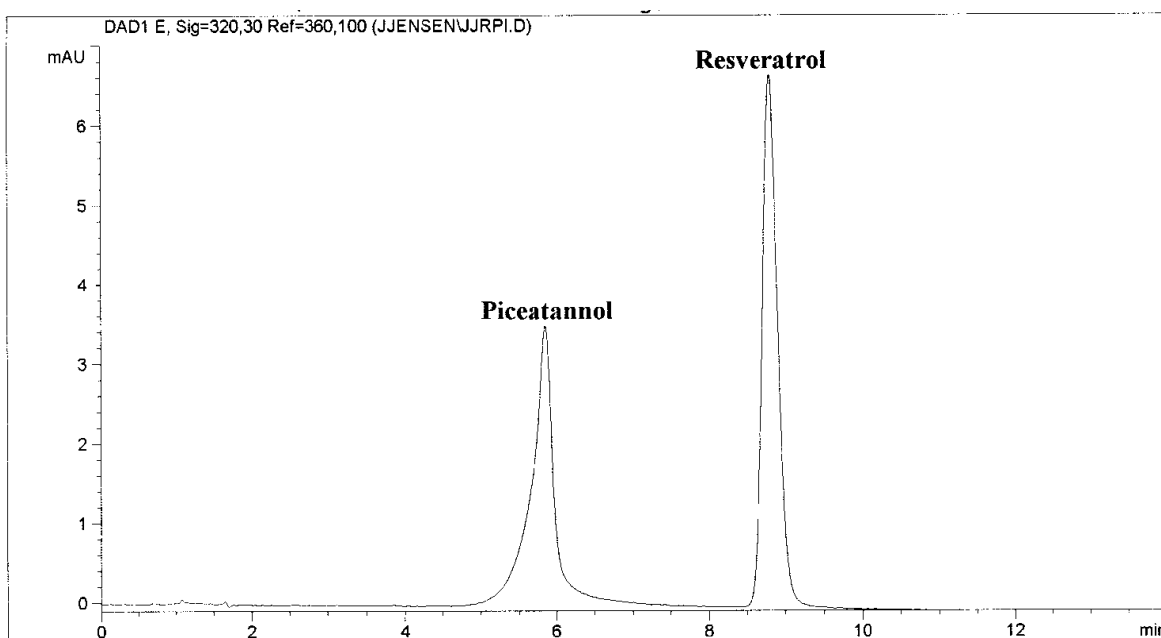


Figure 5. HPLC chromatogram of the co-injection of piceatannol **7** and resveratrol **1** (dissolved in acetonitrile : deionized H<sub>2</sub>O, 1 : 3, v/v; column: Zorbax SB-C18 reversed phase; dimension: 4.6 x 150mm, 5-micron; flow rate: 1mL/min; injection volume = 5 $\mu$ L; run time = 14min; piceatannol  $t_r$  = 5.85min, resveratrol  $t_r$  = 8.80min).

**HPLC analysis of piceatannol-derived ortho-quinone **8**.** Previously unknown piceatannol *ortho*-quinone **8** (Pic-Q; Figure 6) was synthesized in our laboratory by chemical means and structurally characterized by a totality of analytical methods (Subchapter 2.3). Under the

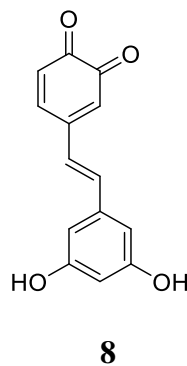


Figure 6. Chemical structure of piceatannol *ortho*-quinone **8** (Pic-Q).

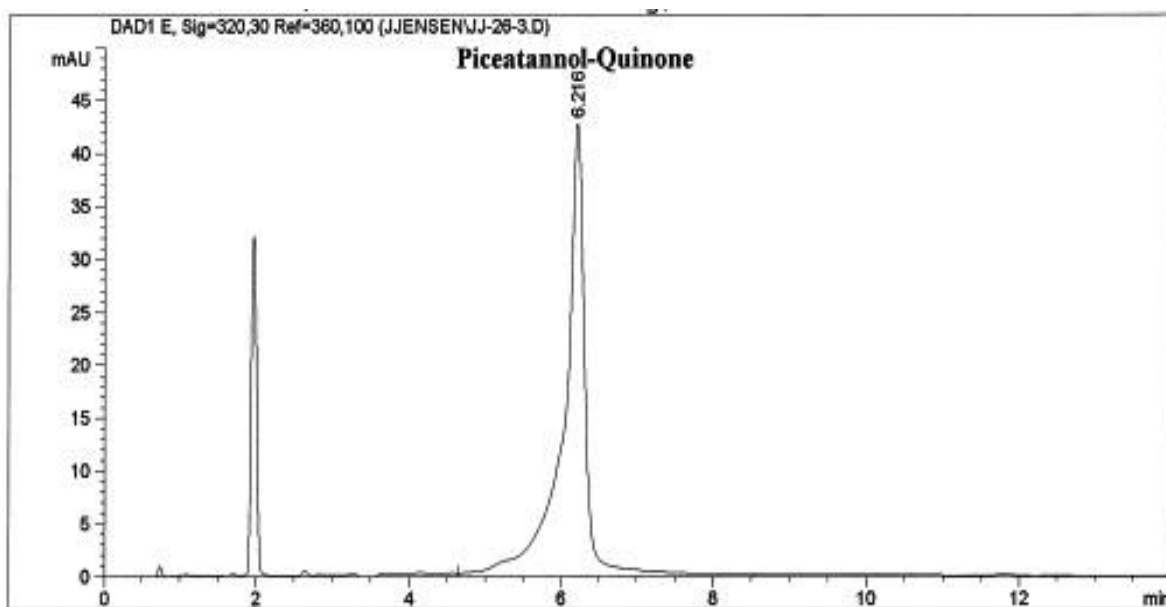


Figure 7. HPLC chromatogram of a *crude* mixture of piceatannol-*ortho*-quinone **8** (dissolved in dry acetone, 99.9%; column: Zorbax SB-C18 reversed phase; dimension: 4.6 x 150mm, 5-micron; flow rate: 1mL/min; injection volume = 1μL; run time = 14min; piceatannol-*o*-quinone **8**,  $t_r$  = 6.22min).

standardized HPLC protocol, retention time for piceatannol *ortho*-quinone **8** was found to be 6.22min (Figure 7). The separation between piceatannol **7** and piceatannol *ortho*-quinone **8** was less than a minute, but still sufficient for qualitative and quantitative identification of both compounds. Reproducibility of said HPLC separations was checked by repeating injections of all three compounds in an individual form, as well as in a mixture. Certain fluctuations in retention

times were observed without compromising our ability to analyze the product distribution in enzymatic reactions.

## **2.2. Enzymatic transformations of resveratrol induced by human enzymes**

Cytochrome CYP P450 enzymes are numerous in the human digestive tract, each responsible for metabolizing compounds like drugs, pesticides, toxins, or xenobiotics. Every enzyme is expressed in one or more organ systems and most of them are commercially available in the United States. Depicted in Figure 8 are human enzymes located in our alimentary canal along with their relative expressions.<sup>15b</sup> Out of those shown, twelve enzymes were chosen for screening with resveratrol **1** as a substrate in order to probe their ability to carry out an *ortho*-hydroxylation reaction.

*Standardized enzymatic reaction protocol.* We selectively introduced an array of cytochrome P450 isozymes to an aqueous medium mainly comprised of deionized water, a neutral buffer, nicotinamide adenine dinucleotide (NAD) reductase coenzymes, and a prepared stock solution, resveratrol in DMSO. This enzymatic mixture underwent incubation for 1 hour at 37 °C, then an equivalent volume of acetonitrile was added to each reaction vial (in triplicate) to denature the enzyme. The mixtures were placed on ice for 30 minutes, then centrifuged for 20 minutes. The filtered supernatant served as the crude sample and was analyzed on the same day by HPLC.

In some instances, we chose to “spike” crude samples with the authentic sample of piceatannol **7** in order to confirm its presence in crude samples. In other instances, we prepared so-called “pumped” samples by evacuating crude mixtures under reduced pressure for 14 hours,

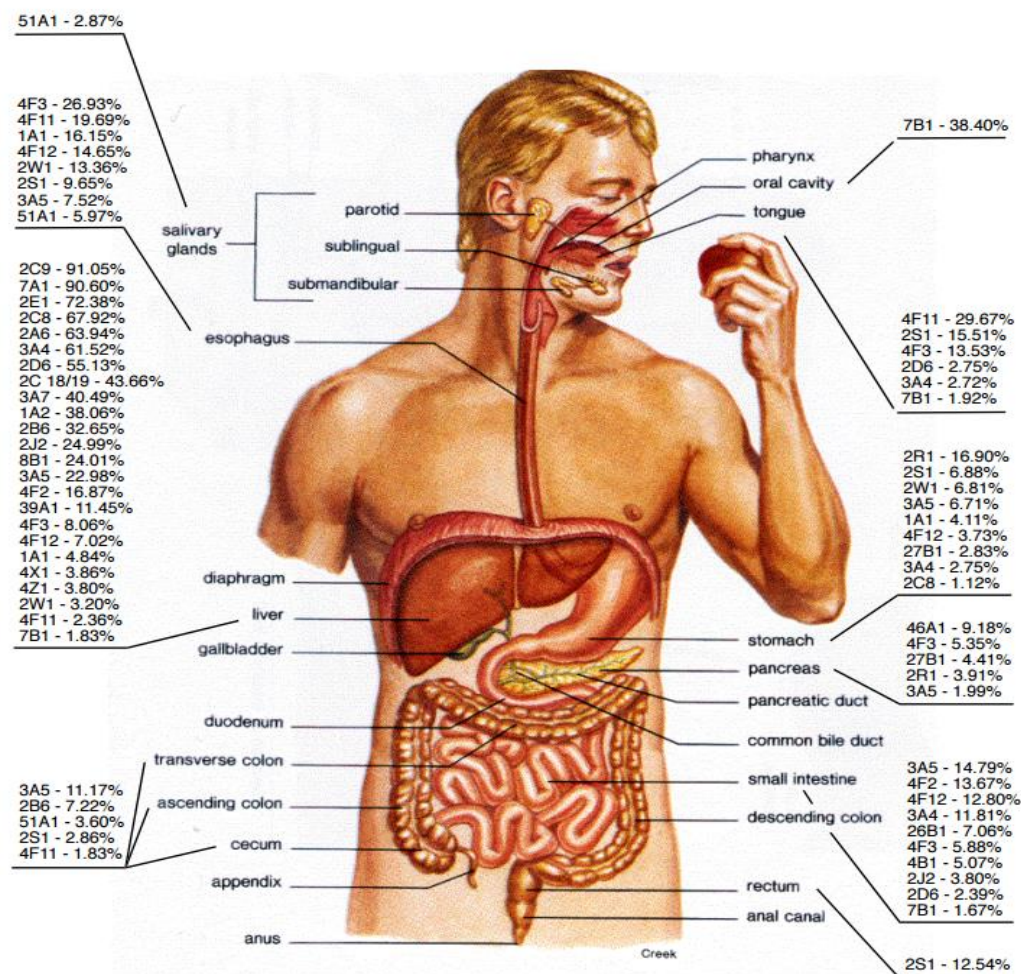


Figure 8. Alimentary CYP450 human enzymes and their allocated, multi-organ expressions. Courtesy of Dr. Gagik Melikyan, *Guilty Until Proven Innocent: Antioxidants, Foods, Supplements, and Cosmetics*.<sup>15b</sup>

then re-dissolving them in a small volume of acetonitrile and deionized water mixture (300μL; 1 : 3). This composition was optimized – empirically – to dissolve piceatannol **7**, not resveratrol **1** in order to allow for detection of minute quantities of the former in the presence of much larger concentrations of the starting material. A noteworthy point to mention here is that enzymatic reactions require certain components in order to initiate the reaction. If a catalyst, reductase cofactor NADPH, or the substrate were absent in the enzymatic mixture, these reactions would

simply not occur. We conducted a set of control experiments with the omission of one or more enzymatic components in order to confirm their functionality in enzymatic processes.

***Special handling protocol and storage conditions for cytochrome P450 enzymes.*** The main concerns about enzymatic handling were to minimize freeze-thaw cycles (to preserve catalytic activity), to minimize time-temperature abuse, and prevent cross-contamination. Upon obtaining a minute quantity of each enzyme from a micro syringe, delicate mixing techniques to ensure homogeneity were applied by means of light, consecutive finger-tapping (x10) against the reaction vial, and for some enzymes, where a precipitate was visually present, the use of swirling and mixing with a sterile, syringe tip. Possible end products, namely *ortho*-quinones that may result from secondary enzymatic transformations are known to be light-, heat-, and oxygen-sensitive, and special care was used to minimize these effects by aluminum “sheeting” and environmental light reduction. All enzymes, crude, spiked, and pumped samples were stored securely in designated vials that were wrapped tightly with parafilm and stored upright in clearly labeled storage bins under deep freezer conditions (-82 °C).

### ***Screening of CYP2C19 with resveratrol 1.***

Enzyme CYP2C19 is primarily expressed in the liver and is involved in the metabolism of at least 10 percent of widely prescribed drugs, such as Plavix, an anticoagulant (Figure 9). The CYP2C19 enzyme chemically modifies Plavix into its active form in order for the drug to function. The active form of the drug curtails a receptor protein, P2RY12 which is located on platelet surfaces. During blood aggregation, P2RY12 assists platelets to conglomerate to form a clot in order to attenuate blood loss and isolate damaged vessels.<sup>16a</sup> The CYP2C19 enzyme is

also involved in polyunsaturated fatty acid (PUFA) oxidation and arachidonic acid (AA) metabolism.<sup>16b</sup>

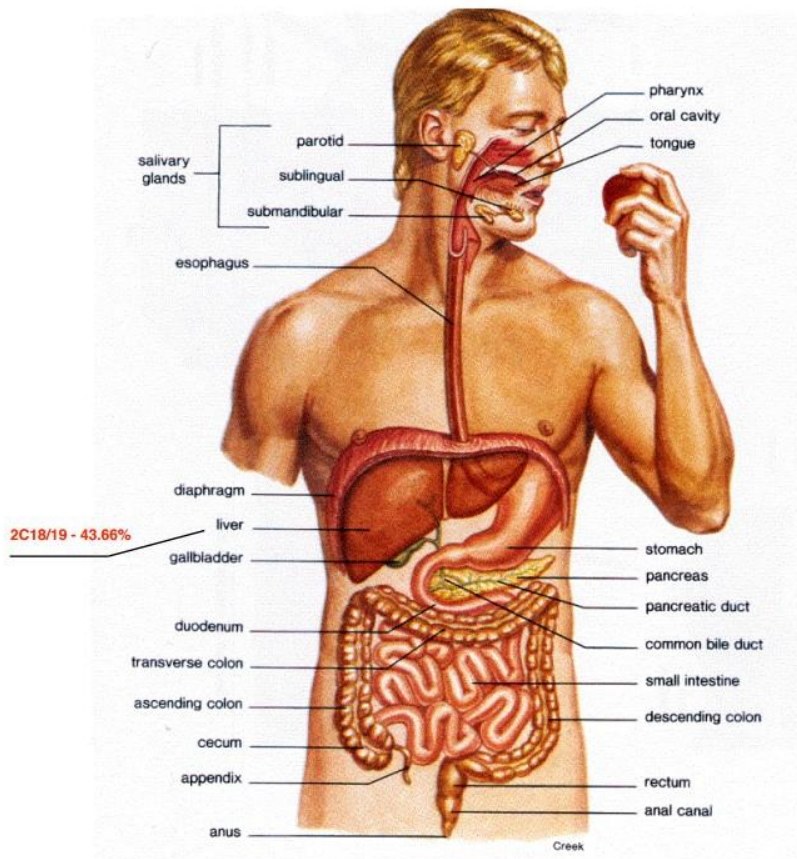


Figure 9. CYP2C19 mapping diagram of enzymatic expression in human organ systems.

An enzymatic reaction with resveratrol **1** was carried out according to the standard protocol, and the crude mixture, upon denaturing the CYP2C19 enzyme with acetonitrile, was analyzed by HPLC (Figure 10). No piceatannol **7** was detected; a low-intensity peak at ~3.5min can be ignored since the HPLC analysis of crude enzymatic mixtures frequently contain peaks with the retention times lower than 4min, representing most likely denatured enzymes. To check the retention of piceatannol **7** in this particular chemical environment, the crude mixture was spiked with an authentic sample and analyzed by HPLC (Figure 11). The observed retention time of 4.57min was consistent with model studies (Figure 5). In contrast to gas chromatography (GC),

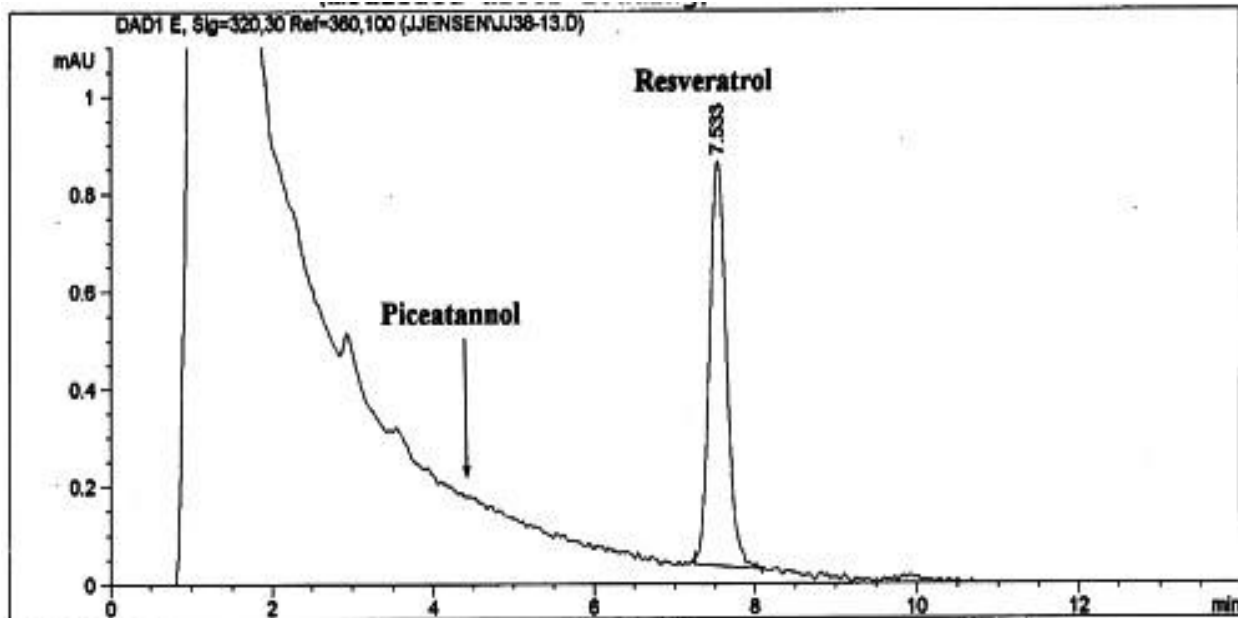


Figure 10. HPLC chromatogram of a crude mixture of resveratrol **1** + CYP2C19 enzymatic reaction (acetonitrile : deionized H<sub>2</sub>O, 1 : 1, v/v; column: Zorbax SB-C18 reversed phase; dimension: 4.6 x 150mm, 5-micron; flow rate: 1mL/min; injection volume = 30μL; run time = 14min; no piceatannol present; resveratrol  $t_r$  = 7.53min).

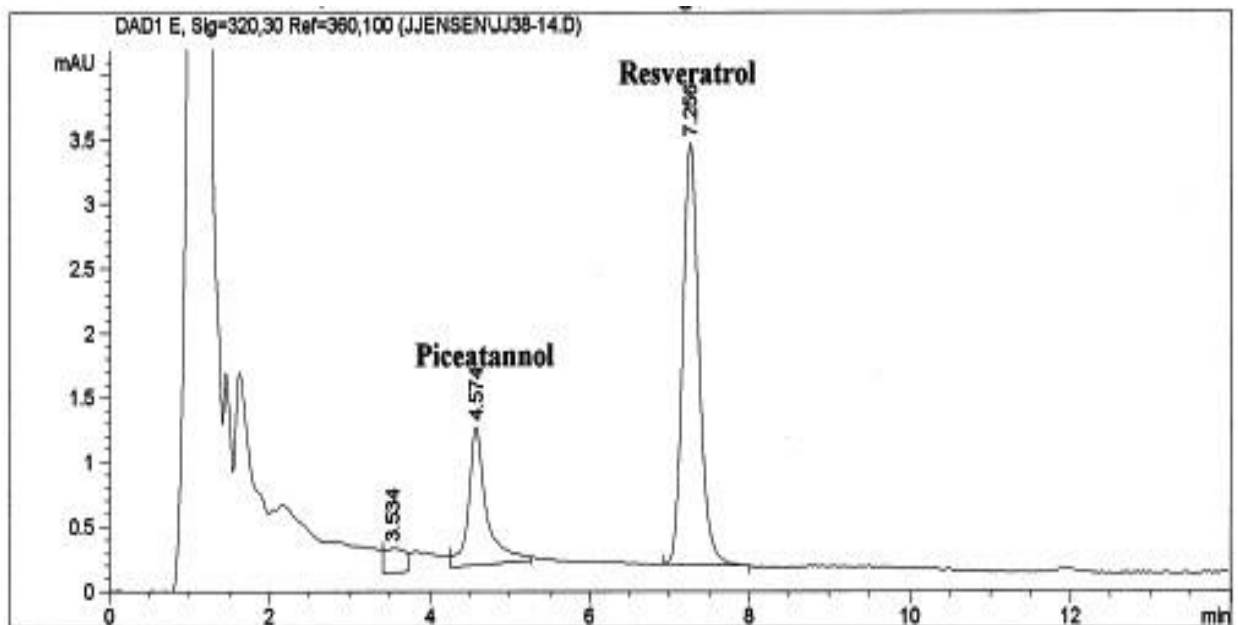


Figure 11. HPLC chromatogram of a crude mixture of resveratrol **1** + CYP2C19 enzymatic reaction spiked with piceatannol **7** / 2 drops (acetonitrile : deionized H<sub>2</sub>O, 1 : 1, v/v; column: Zorbax SB-C18 reversed phase; dimension: 4.6 x 150mm, 5-micron; flow rate: 1mL/min; injection volume = 30μL; run time = 14min; piceatannol  $t_r$  = 4.57min, resveratrol  $t_r$  = 7.26min).

in HPLC analyses retention times are more susceptible to fluctuations caused by other chemical components present in the enzymatic mixture. In this particular case, both resveratrol **1** and piceatannol **7** exhibited somewhat lower retention times, 7.26min vs 8.80min for the former, and 4.57min vs 5.85min for the latter. It is noteworthy, that despite a faster elution, critical separation of ~3min between both components is still preserved allowing for a reliable qualitative identification.

The fact that no conversion was observed indicates a mismatch between resveratrol **1** and CYP2C19 enzyme. For any substrate to be functionalized by an enzyme, certain steric, electronic, conformational, and coordination requirements must be met. An organic molecule needs to enter an enzyme cavity, to coordinate, usually via hydrogen bonds, with select functions on the enzyme wall, and then to undergo a multistep chemical transformation resulting in different synthetic outcomes, i. e. hydroxylation, hydrogenation, oxidation, aromatization, reduction, decarboxylation, and cyclization. Within this project, screening of resveratrol **1** with other CYP450 enzymes revealed cases of mismatch when no hydroxylation product was detected, and those of an excellent match when a sizable fraction of the starting material underwent conversion to piceatannol **7**, a product of site-selective aromatic hydroxylation.

### ***Screening of CYP2D6 with resveratrol 1.***

Enzyme CYP2D6 is involved in processing and elimination of about 25% of xenobiotics by altering functional groups usually by dealkylation, demethylation, or hydroxylation reactions.<sup>17a</sup> CYP2D6 is mostly expressed in the liver with lesser presence in a mouth cavity and small intestines (Figure 12). Pharmacologically, enzyme CYP2D6 is involved in the metabolism of Bufuralol (blood pressure medication) by hydroxylation<sup>17b</sup> and opioid codeine metabolism by O-



demethylation.<sup>17c</sup> It is worthy to mention that CYP2D6 expression is dependent on genetic variations, ethnicity, and individual CYP2D6 metabolic orientation whereas some people expedite drug elimination due to high CYP2D6 expression (ultra-rapid metabolizers), while others are poor (low CYP2D6) metabolizers. The negative effects are a decrease in a drug's action in fast metabolizers versus toxicity in slow metabolizers.<sup>17d</sup>

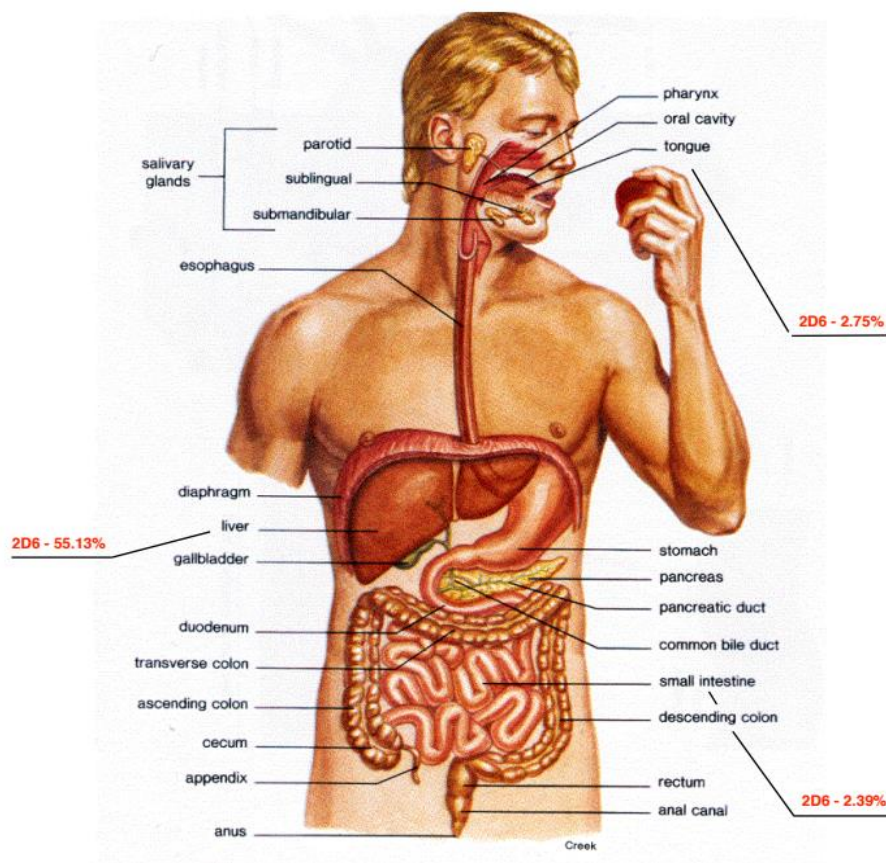


Figure 12. CYP2D6 mapping diagram of enzymatic expression in human organ systems.

An enzymatic reaction with resveratrol **1** was carried out according to the standard protocol, and the crude mixture, upon denaturing the CYP2D6 enzyme with acetonitrile, was analyzed by HPLC (Figure 13). No piceatannol **7** was detected after careful screening of the HPLC chromatogram. We speculated that had piceatannol **7** been present in this sample, it might have

eluted out at approximately 5 minutes. Hence, we spiked the crude mixture with an authentic sample of piceatannol **7** with a resultant signal intensity appearing at 5.52 min (Figure 14). A target 3-minute peak separation between both compounds was maintained with retention times (piceatannol **7** 5.52min; resveratrol **1** 8.57min) being quite close to those established in preliminary model studies (Figure 5: piceatannol **7** 5.85min; resveratrol **1** 8.80min). By peak intensity, piceatannol **7** was approximately half that of resveratrol **1** and exhibited mild shouldering (broadening on one side of peak base), but overall the “spiking” experiment was reliable in determining that no hydroxylation reaction took place in the course of the enzymatic treatment. The fact that CYP2D6 enzyme is known to carry out hydroxylation of p-tyramine to dopamine<sup>17a</sup> does not mean that the said oxidation reaction would occur with any phenolic compound. The matching substrate must effectively fit into the enzyme pocket and coordinate

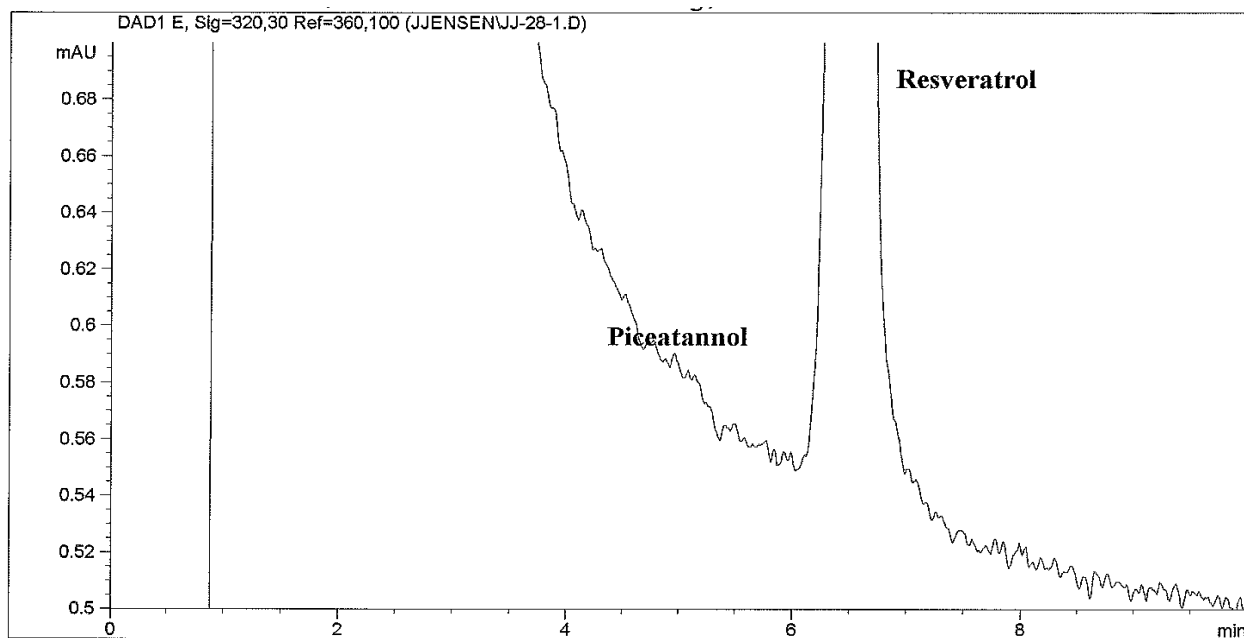


Figure 13. HPLC chromatogram of a crude mixture of resveratrol **1** + CYP2D6 enzymatic reaction (acetonitrile : deionized H<sub>2</sub>O, 1 : 1, v/v; column: Zorbax SB-C18 reversed phase; dimension: 4.6 x 150mm, 5-micron; flow rate: 1mL/min; injection volume = 30μL; run time = 10min; resveratrol, *t<sub>r</sub>* 6.53min; no piceatannol present).

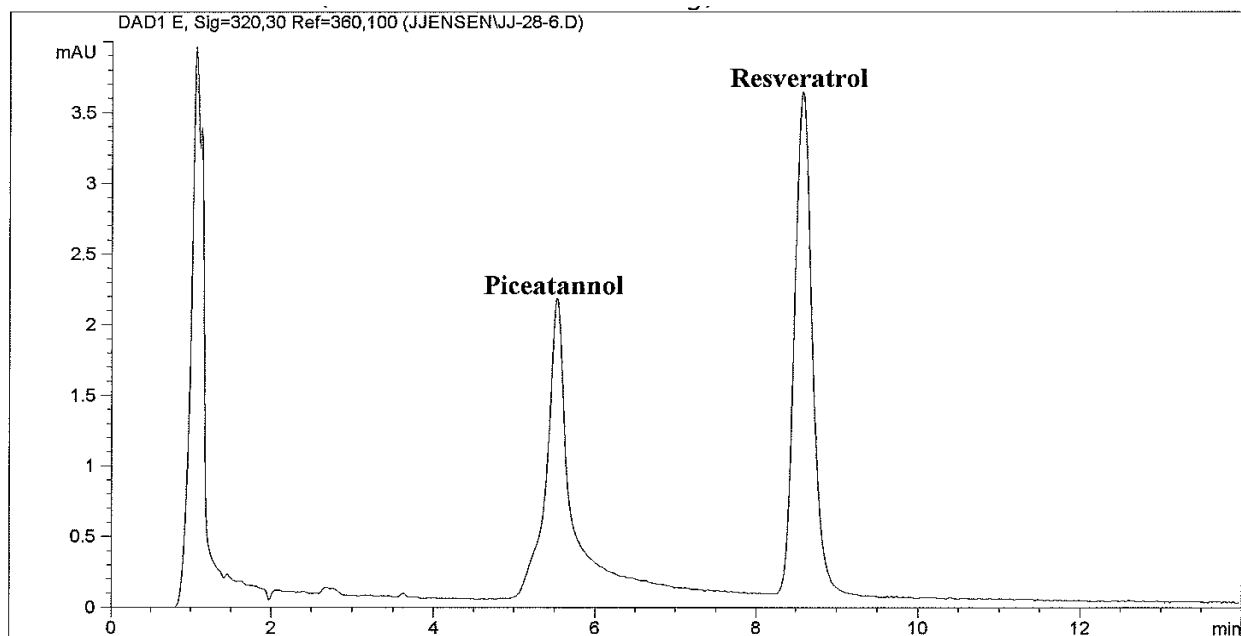


Figure 14. HPLC chromatogram of a crude mixture of resveratrol **1** + CYP2D6 enzymatic reaction spiked with piceatannol **7** / 10 drops (acetonitrile : deionized H<sub>2</sub>O, 1 : 3, v/v; column: Zorbax SB-C18 reversed phase; dimension: 4.6 x 150mm, 5-micron; flow rate: 1mL/min; injection volume = 5μL; run time = 12min; piceatannol  $t_r$  = 5.52min, resveratrol  $t_r$  = 8.57min).

with “the right” amino acids, thus triggering the enzymatic machinery. Resveratrol is quite different – geometrically, functionally, topologically – from p-tyramine and Bufuralol, two substrates to undergo hydroxylation with CYP2D6 enzyme. This might be the reason why the formation of piceatannol **7** was not observed by us in a CYP2D6-induced enzymatic reaction.

### ***Screening of CYP3A5 with resveratrol 1.***

Enzyme CYP3A5 is expressed in the liver, small intestine, transverse/ascending colon, cecum, and stomach (in descending order) (Figure 15). The CYP3A subfamilies are well-known heme-thiolate monooxygenases and play a crucial role in the NADPH-driven electron transport pathway in the liver. Fatty acids, steroids, and xenobiotics are all oxidized by CYP3A5, despite not having structural similarities.<sup>18a</sup> CYP3A5 is also involved in testosterone metabolism by 6β-hydroxylation<sup>18b</sup> and participates in dimerization reactions.<sup>18c</sup> This subfamily is one of the most

resourceful of all the metabolic systems in drug clearance, eliminating 37% of 200 frequently ordered drugs in the U.S.<sup>18d</sup>

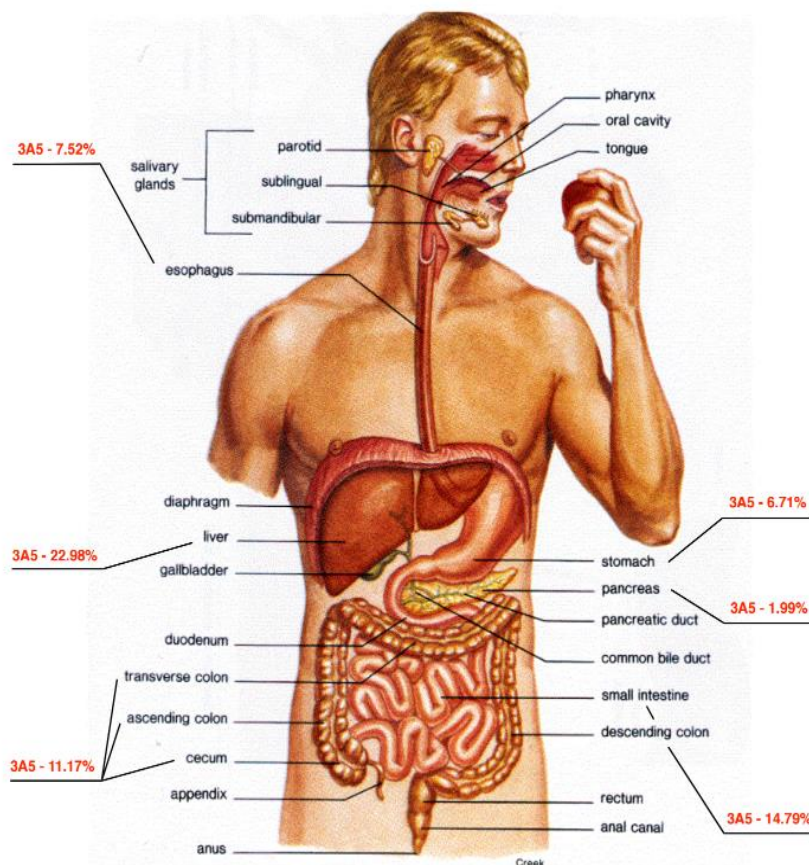


Figure 15. CYP3A5 mapping diagram of enzymatic expression in human organ systems.

An enzymatic reaction with resveratrol **1** was carried out according to the standardized protocol, and the crude mixture, upon denaturing the CYP3A5 enzyme with acetonitrile, was analyzed by HPLC under standard conditions (Figure 16). An arrow shown where piceatannol **7** peak would likely appear, making CYP3A5 the third enzyme, along with CYP2C19 and CYP2D6, that did not catalyze *ortho*-hydroxylation reaction, thus leaving resveratrol **1** intact. To further ensure the absence of piceatannol **7** in the reaction mixture, the spiking with an authentic sample was applied. The process has proven to be quite delicate, since given the nanomolar

amounts of substrates used, it is quite easy to over-“titrate” the crude mixture, delivering amounts of piceatannol **7** much larger than that of requisite resveratrol **1**. Preliminary analysis of the test sample concentration coupled with the precise delivery of the authentic sample was practiced many times over in order to master the “spiking” procedure. This technique was by far one of the most challenging parts of the project, since over-“titrating,” at times, ruined the whole enzymatic reaction. The reaction time observed for resveratrol **1** (6.75min; Figure 16) was much lower than the reference numbers in model studies (8.80min, Figure 5; 8.91min, Figure 4), reflecting an impact of multiple components present in the crude enzymatic mixture. In the “spiked” sample (Figure 17), piceatannol **7** and resveratrol **1** were observed at 4.33 and 7.08min, respectively.

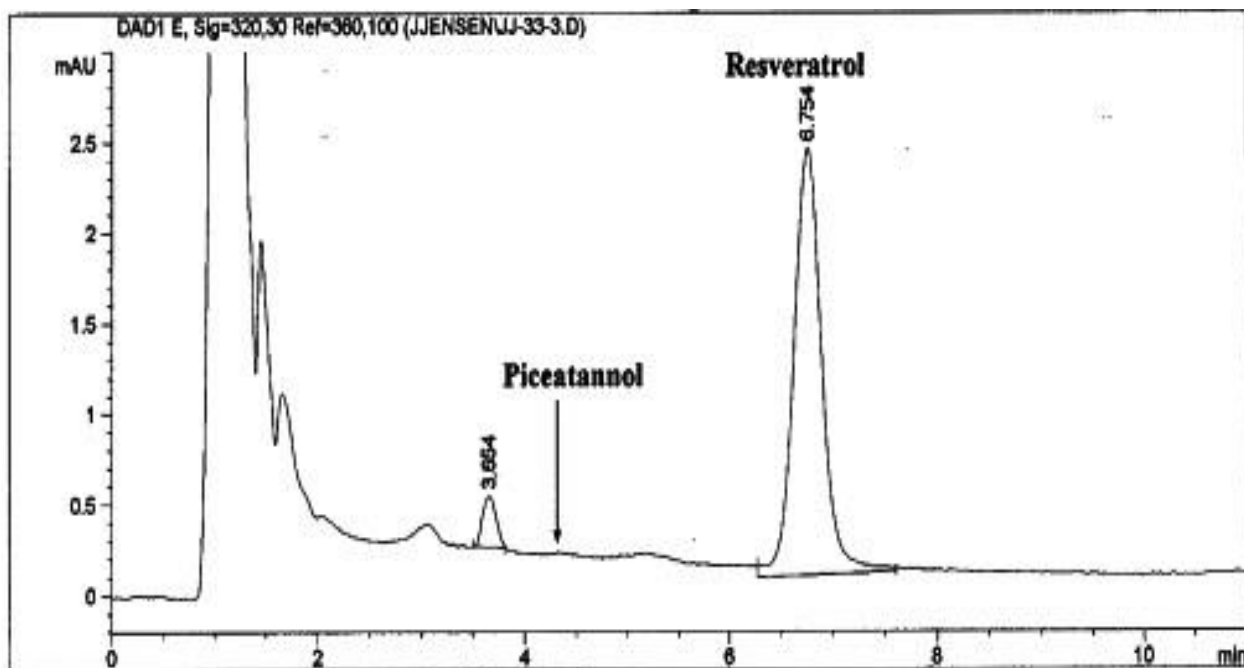


Figure 16. HPLC chromatogram of a crude mixture of resveratrol **1** + CYP3A5 enzymatic reaction (acetonitrile : deionized H<sub>2</sub>O, 1 : 3, v/v; column: Zorbax SB-C18 reversed phase; dimension: 4.6 x 150mm, 5-micron; flow rate: 1mL/min; injection volume = 30μL; run time = 14min; no piceatannol **7** present; resveratrol **1**  $t_r$  = 6.75min).

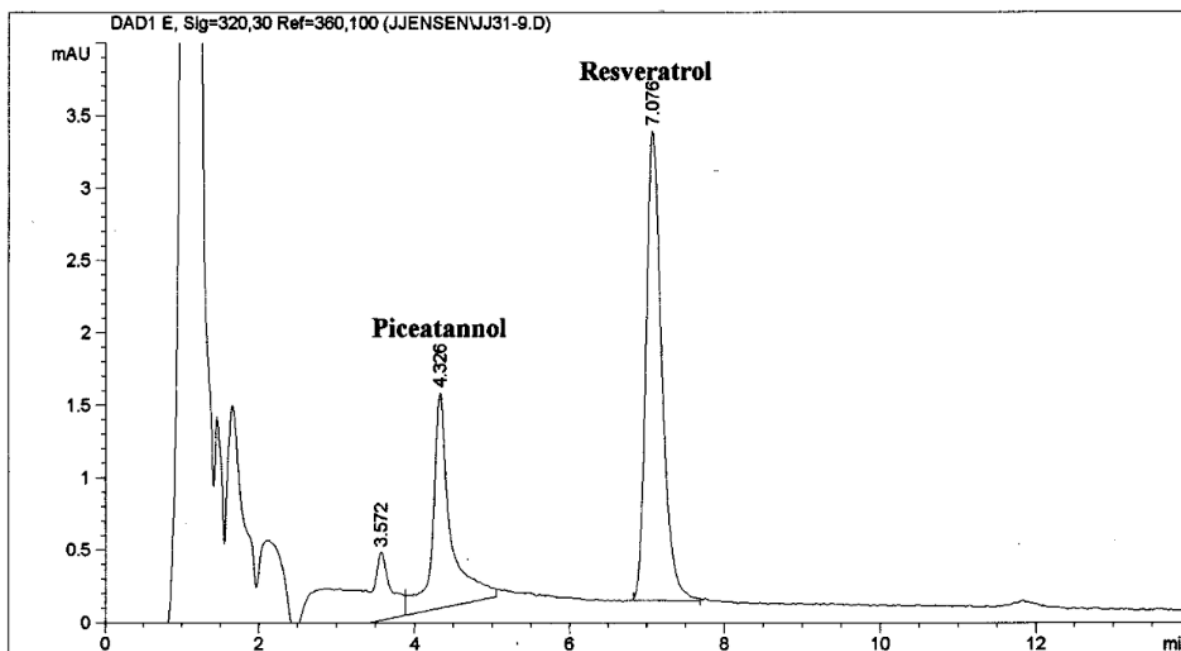


Figure 17. HPLC chromatogram of a crude mixture of resveratrol **1** + CYP3A5 enzymatic reaction spiked with piceatannol **7**/2 drops (acetonitrile : deionized H<sub>2</sub>O, 1 : 1, v/v; column: Zorbax SB-C18 reversed phase; dimension: 4.6 x 150mm, 5-micron; flow rate: 1mL/min; injection volume = 30μL; run time = 14min; piceatannol **7**  $t_r$  = 4.33min, resveratrol **1**  $t_r$  = 7.08min).

### ***Screening of CYP4F3A with resveratrol 1.***

Enzyme CYP4F3A is primarily expressed in the esophagus, tongue, and liver, as well as similarly expressed in the pancreas and small intestine (in descending order; Figure 18). Chemically, CYP4F3A is involved in PUFA (AA) metabolism,<sup>19a</sup> very long-chain fatty acid (VLCFA) metabolism by  $\omega$ -oxidation,<sup>19b</sup> and facilitates  $\omega$ -hydroxylation in leukotriene B<sub>4</sub> synthesis (inflammatory marker).<sup>19c</sup> These monooxygenases are also responsible for lipid synthesis (cholesterol, FA, and steroid) and drug metabolism.<sup>19d</sup>

An enzymatic reaction with resveratrol **1** was carried out according to the standardized protocol, and the crude mixture, upon denaturing the CYP4F3A enzyme with acetonitrile, was analyzed by HPLC to indicate, for the first time, the presence of minute amounts (1%) of piceatannol **7** (PIC : RV, 1 : 99; Figure 19). To confirm that piceatannol **7** is in fact present, the

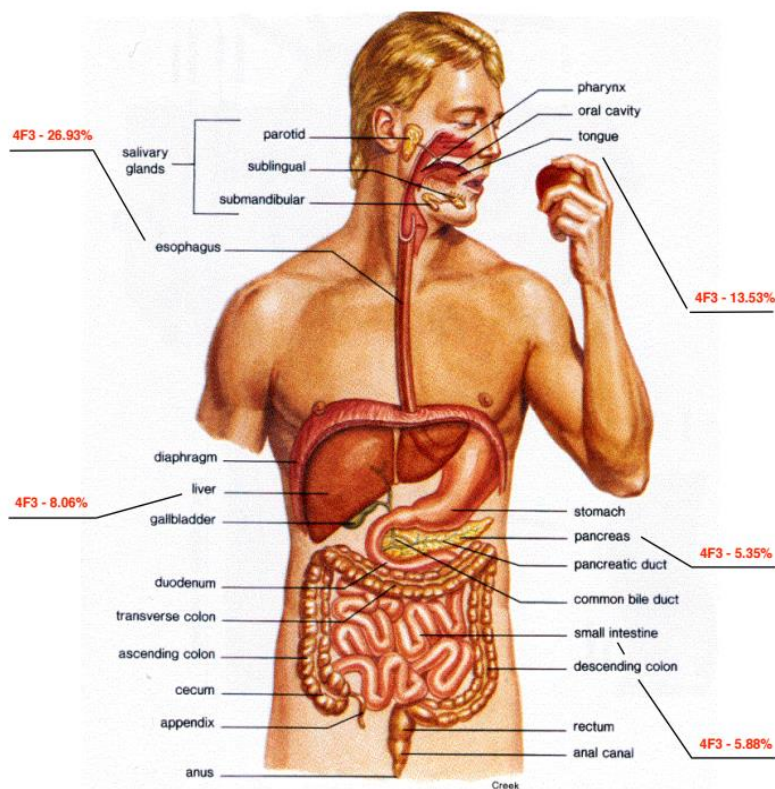


Figure 18. CYP4F3A mapping diagram of enzymatic expression in various organ systems.

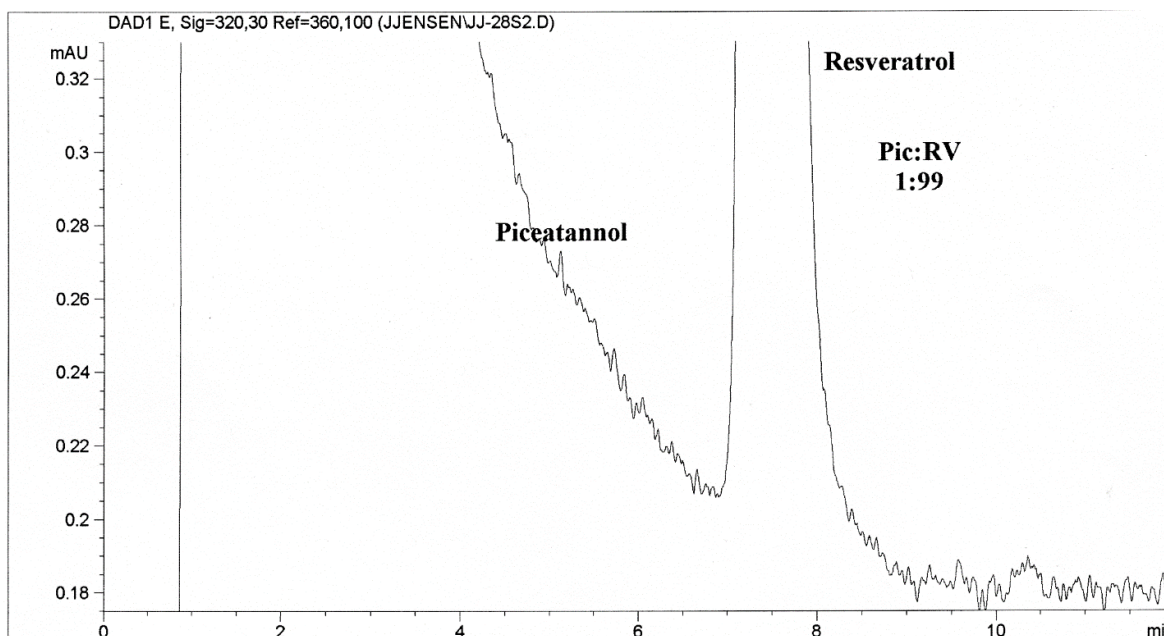


Figure 19. HPLC chromatogram of a crude mixture of resveratrol **1** + CYP4F3A enzymatic reaction (acetonitrile : deionized H<sub>2</sub>O, 1 : 1, v/v; column: Zorbax SB-C18 reversed phase; dimension: 4.6 x 150mm, 5-micron; flow rate: 1mL/min; injection volume = 30μL; run time = 12min; piceatannol **7**  $t_r$  = 5.13min, resveratrol **1**  $t_r$  = 7.55min).



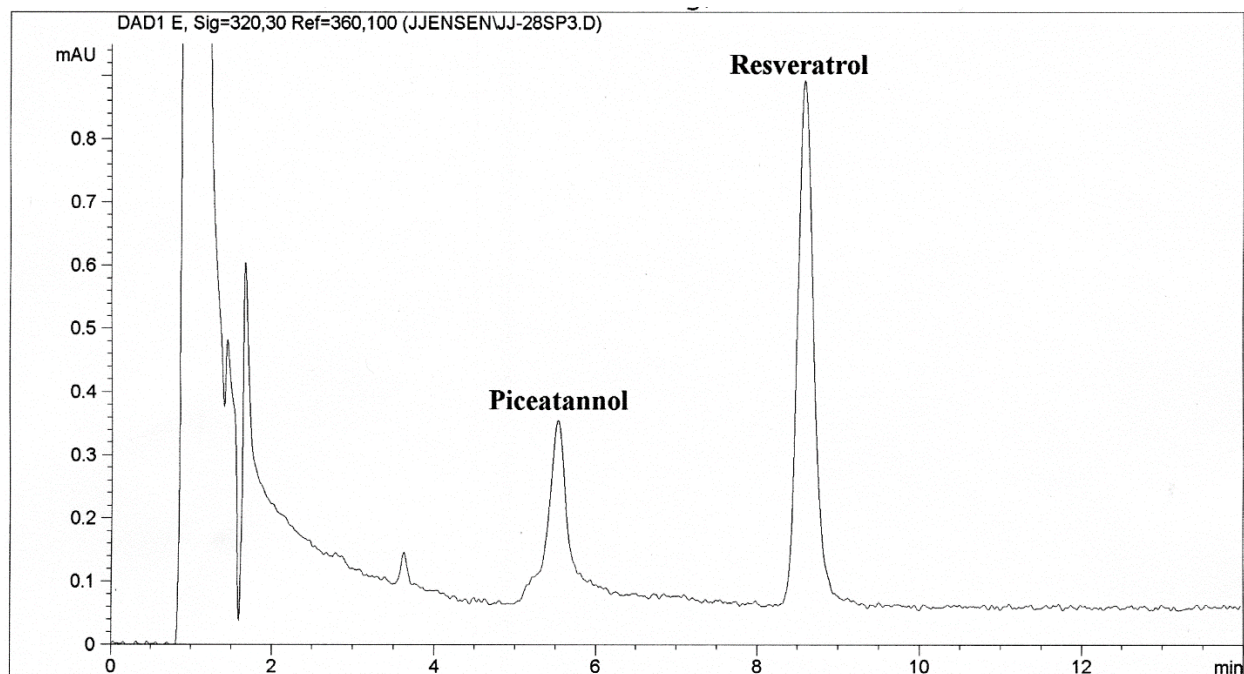


Figure 20. HPLC chromatogram of a crude mixture of resveratrol **1** + CYP4F3A enzymatic reaction spiked with piceatannol **7** / 2 drops (acetonitrile : deionized H<sub>2</sub>O, 1 : 1, v/v; column: Zorbax SB-C18 reversed phase; dimension: 4.6 x 150mm, 5-micron; flow rate: 1mL/min; injection volume = 5μL; piceatannol **7**  $t_r$  = 5.53min, resveratrol **1**  $t_r$  = 8.59min).

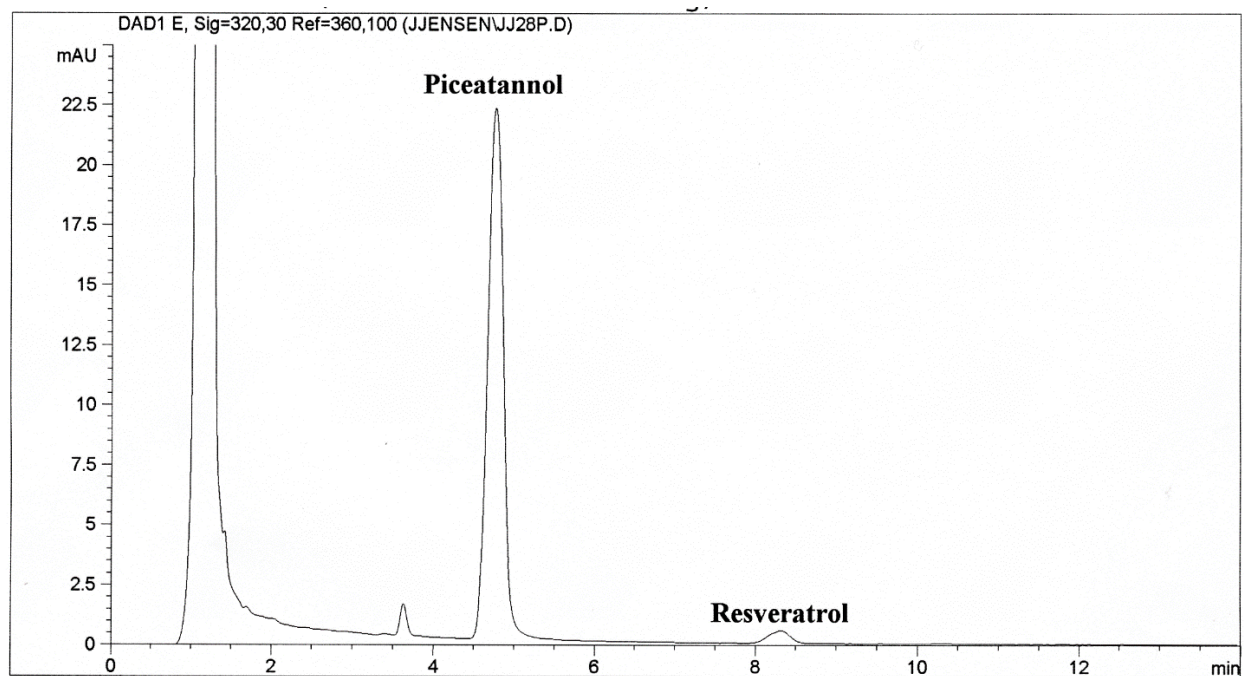


Figure 21. HPLC chromatogram of a crude mixture of resveratrol **1** + CYP4F3A enzymatic reaction: "pumped" sample (acetonitrile : deionized H<sub>2</sub>O, 1 : 3, v/v); column: Zorbax SB-C18 reversed phase; dimension: 4.6 x 150mm, 5-micron; flow rate: 1mL/min; injection volume = 30μL; run time = 14min; piceatannol **7**  $t_r$  = 4.77min, resveratrol **1**  $t_r$  = 8.32min).



crude mixture was spiked with two drops of an authentic sample. The elution profile demonstrated heightened signal intensity at 5.53min with only a 0.4-minute signal shift to the right showing an ideal 3-minute peak separation between requisite resveratrol **1** (8.59min) and piceatannol **7** (5.53min; Figure 20).

For low-conversion biotransformations, we also developed an amplification technique that allows for an increase in the concentration of piceatannol **7** in an analyte due to the differences in solubility between resveratrol **1** and its hydroxylated metabolite. Thus, 1 mL aliquot of the crude sample was evaporated to dryness (14hrs) under a reduced pressure (Schlenk line vacuum), treated with an empirically optimized mixture of acetonitrile : deionized water (1 : 3; 300  $\mu$ L), and stirred by hand using an inverted melting point capillary tube to dissolve any remaining visible solids. The HPLC elution profile demonstrated the heightened peak intensity of piceatannol **7** (4.77min) and dramatically reduced peak of resveratrol **1** (8.32min; Figure 21). This experiment affirmed resveratrol's biotransformation into piceatannol **7** catalyzed by CYP4F3A, and the successful peak amplification of the metabolic derivative.

### ***Screening of CYP2E1 with resveratrol 1.***

CYP2E1 is expressed primarily in the liver (Figure 22) and involved in some 4% of known P450-mediated drug oxidations.<sup>20a</sup> It carries out the  $\omega$ -hydroxylation of endogenous fatty acid such as arachidonic acid, and epoxidation of eicosatetraenoic acids,<sup>20b</sup> as well as bioactivates common anesthetics, including acetaminophen, halothane, enflurane, and isoflurane.<sup>20c</sup> Biosynthesis of CYP2E1 is induced by a variety of small organic molecules such as benzene,<sup>20c</sup> toluene,<sup>20c</sup> acetone,<sup>20c</sup> ethanol, and tobacco.<sup>20d</sup> Ironically, CYP2E1 is responsible for hepatotoxicity of drugs and can generate reactive oxygen species (ROS) resulting in lipid

peroxidation, DNA and RNA oxidation.<sup>20e</sup> Another important reaction that CYP2E1 is involved in is the transformation of ethanol to acetaldehyde to acetate (alcohol metabolism), where it metabolizes with alcohol and aldehyde dehydrogenases.<sup>20f</sup>

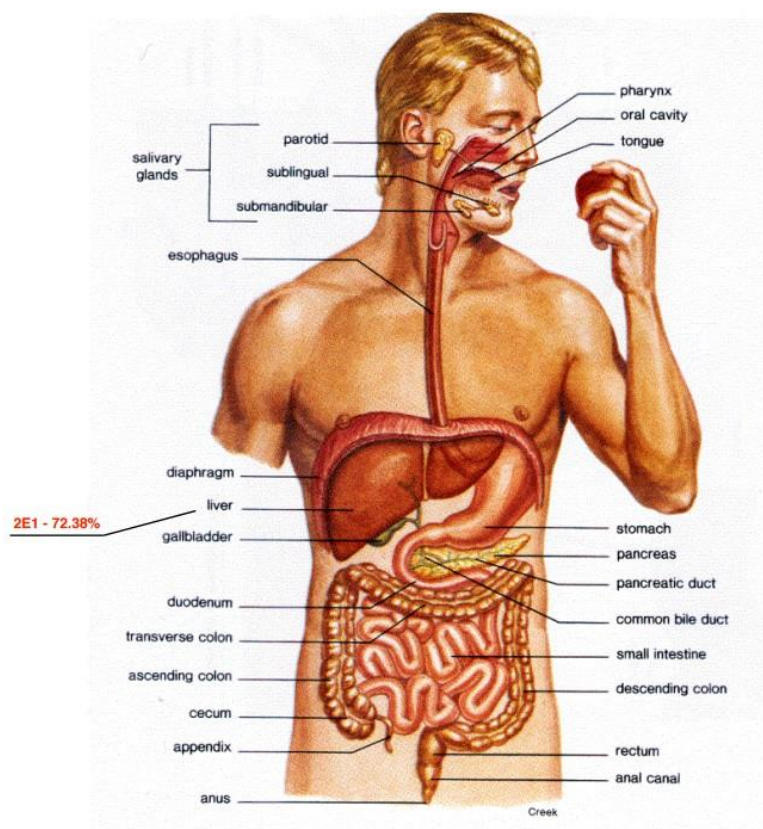


Figure 22. CYP2E1 mapping diagram of enzymatic expression in human organ systems.

An enzymatic reaction with resveratrol **1** was carried out according to the standardized protocol, and the crude mixture, upon denaturing the CYP2E1 enzyme with acetonitrile, was analyzed by HPLC to indicate the presence of small quantities (2%) of the hydroxylation metabolite, piceatannol **7** (PIC : RV, 2 : 98; Figure 23). To confirm its presence, the crude mixture was spiked with an authentic sample of piceatannol **7**; also, the amplification technique was used to further confirm the formation of resveratrol-derived metabolic product. The low conversion thus observed allows us to predict that CYP2E1 most probably would play a minimal

role in metabolizing resveratrol that can be introduced into the human body either as a component in red wine, or as a supplement.

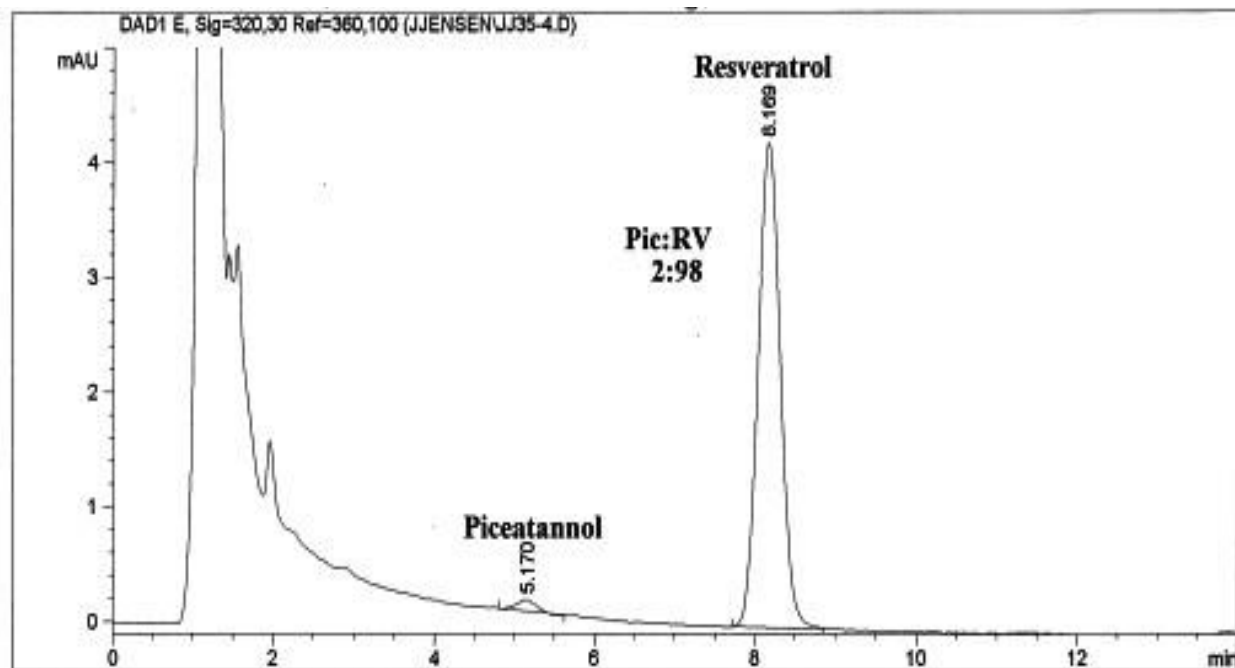


Figure 23. HPLC chromatogram of a crude mixture of resveratrol **1** + CYP2E1 enzymatic reaction (acetonitrile : deionized H<sub>2</sub>O, 1 : 1, v/v; column: Zorbax SB-C18 reversed phase; dimension: 4.6 x 150mm, 5-micron; flow rate: 1mL/min; injection volume = 30μL; run time = 14min; piceatannol **7**  $t_r$  = 5.17min, resveratrol **1**  $t_r$  = 8.17min).

### ***Screening of CYP2C18 with resveratrol 1.***

Enzyme CYP2C18 is primarily expressed in the liver and is involved in drug and pesticide metabolism (Figure 24).<sup>21</sup> This enzyme possesses an epoxygenase activity, allowing it to sequester very long chain fatty acids (VLCFA) at their double bonds, yielding respective epoxides. Other metabolic activities include the conversion of arachidonic acid (AA) to epoxyeicosatrienoic acid (EET), linoleic acid to vernolic and coronaric acids (both toxic products that have been shown to cause multi-organ failure and respiratory complications in animals),<sup>21b</sup> docosohexaenoic acid to epoxydocosapentaenoic acids (EDP's), and lastly, eicosapentaenoic acid to a number of epoxyeicosatetraenoic acids (EEQ's).<sup>21c-e</sup>

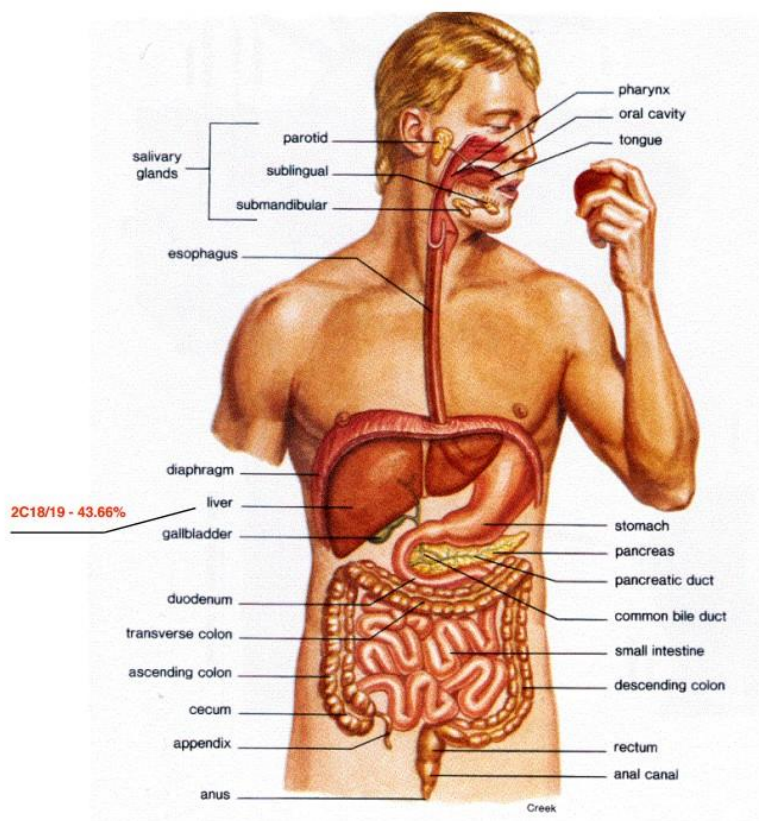


Figure 24. CYP2C18 mapping diagram of enzymatic expression in human organ systems.

An enzymatic reaction with resveratrol **1** was carried out according to the standardized protocol, and the crude mixture, upon denaturing the CYP2C18 enzyme with acetonitrile, was analyzed by HPLC to detect, for the first time, a high degree of metabolic hydroxylation (Figure 25). The ratio of resveratrol **1** to piceatannol **7** was equal to 5 : 95 with end-products maintaining a 3-min separation gap, albeit under more expedient elution times (piceatannol  $t_r$  = 4.14min, resveratrol  $t_r$  = 7.12min; control samples: Figure 5 piceatannol  $t_r$  = 5.85min, resveratrol  $t_r$  = 8.80min). Peak widths for both products were wider than usual and may be attributed to fluctuations in mobile phase composition or possible column overload from previous sample injections. Such a high conversion of resveratrol **1** to piceatannol **7** introduced by CYP2C18 enzyme could hardly be predicted based on its metabolic profile. Two major types of catalytic

transformations reported for this enzyme have been an epoxidation of the double bond<sup>21</sup> and hydroxylation in a saturated carbon chain or allylic position, both involving  $sp^3$ -hybridized carbon atoms.<sup>21</sup> Conversion of resveratrol **1** to piceatannol **7** includes an incorporation of a hydroxyl group at  $sp^2$ -hybridized aromatic carbon, the reaction which is quite different – kinetically, thermodynamically, mechanistically – from the prior art. It is conceivable that within the CYP2C18 enzyme, resveratrol **1** was able to activate coordination sites which are different from those participating in epoxidation and hydroxylation reactions, as well as triggered the participation of amino acids that tend to remain dormant with previously studied xenobiotics.

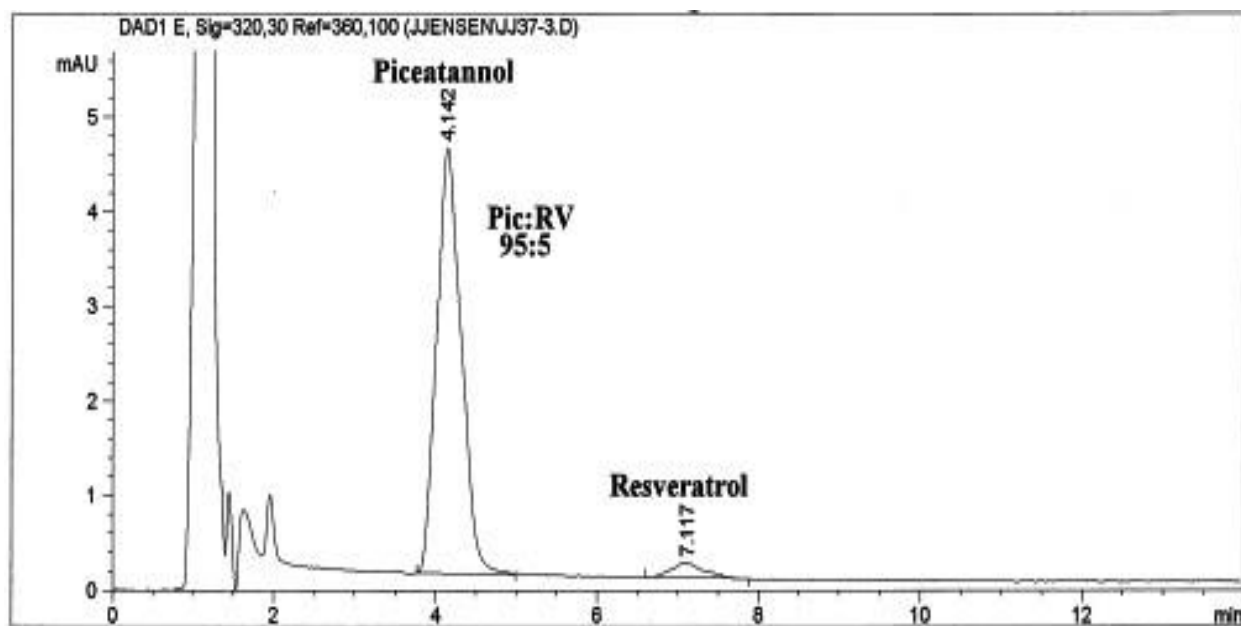


Figure 25. HPLC chromatogram of a crude mixture of resveratrol **1** + CYP2C18 enzymatic reaction (acetonitrile : deionized H<sub>2</sub>O, 1 : 1, v/v; column: Zorbax SB-C18 reversed phase; dimension: 4.6 x 150mm, 5-micron; flow rate: 1mL/min; injection volume = 30μL; run time = 14min; piceatannol **7**  $t_r$  = 4.14min, resveratrol **1**  $t_r$  = 7.12min).

#### ***Screening of CYP3A4 with resveratrol 1.***

Enzyme CYP3A4 is primarily expressed in the liver and small intestine, as well as in stomach and mouth cavity (in descending order; Figure 26). It is involved in hormone

metabolism by 6 $\beta$ -hydroxylation,<sup>22a</sup> vitamin A oxidation,<sup>22b</sup> epoxidation of arachidonic acid,<sup>22c</sup> and breakdown of drugs such as Repaglinide (antidiabetic).<sup>22d</sup> This subfamily is responsible for processing nearly half of the common drugs consumed today such as acetaminophen (NSAID) and erythromycin (antibiotic). This enzyme is unique since it not only contributes to detoxification of xenobiotics, it also can bioactivate drugs to form respective active forms as a result of an enzyme-induced metabolic reaction. Thus, blockbuster drug, tamoxifen, for breast cancer treatment,<sup>22e</sup> is activated by an aromatic hydroxylation reaction which is of immediate relevance to resveratrol-to-piceatannol conversion. The CYP3A4-induced oxidation converts tamoxifen to 4-hydroxytamoxifen, a pharmacologically active compound with antiestrogenic properties.<sup>22e</sup>

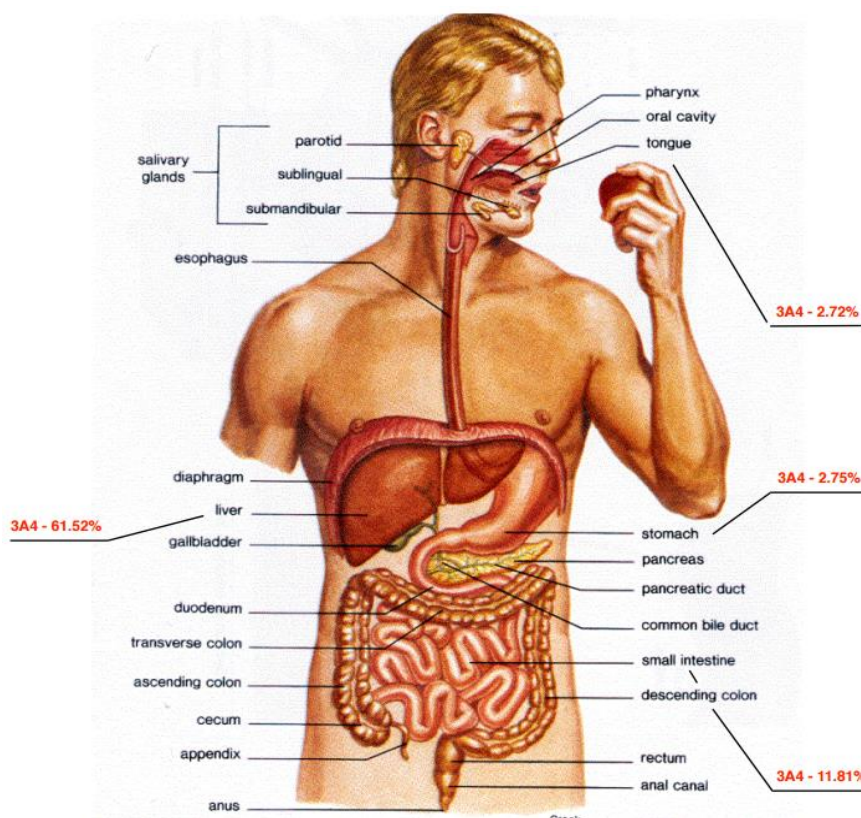


Figure 26. CYP3A4 mapping diagram of enzymatic expression in human organ systems.

An enzymatic reaction with resveratrol **1** was carried out according to the standardized protocol, and the crude mixture, upon denaturing the CYP3A4 enzyme with acetonitrile, was analyzed by HPLC to detect, for the second time, a high degree of metabolic hydroxylation (Figure 27). The ratio of resveratrol **1** to piceatannol **7** was equal to 4 : 96. High rates of conversion are indicative of how well this enzyme can metabolize resveratrol **1** to piceatannol **7**, a pro-carcinogen, with the heightened potential to further oxidize to piceatannol-derived *ortho*-quinone, a suspect carcinogen. The chromatogram depicted a near 4-minute peak separation between requisite substrate and its metabolite (resveratrol **1**  $t_r$  = 8.96min; piceatannol **7**  $t_r$  = 5.16min). The latter represented by a tall symmetrical peak has a retention time very close to that observed in model studies (Figure 5: piceatannol **7**  $t_r$  = 5.85min). It is noteworthy that CYP3A4 enzyme has a low *substrate specificity* that allows for a large number of chemical compounds,

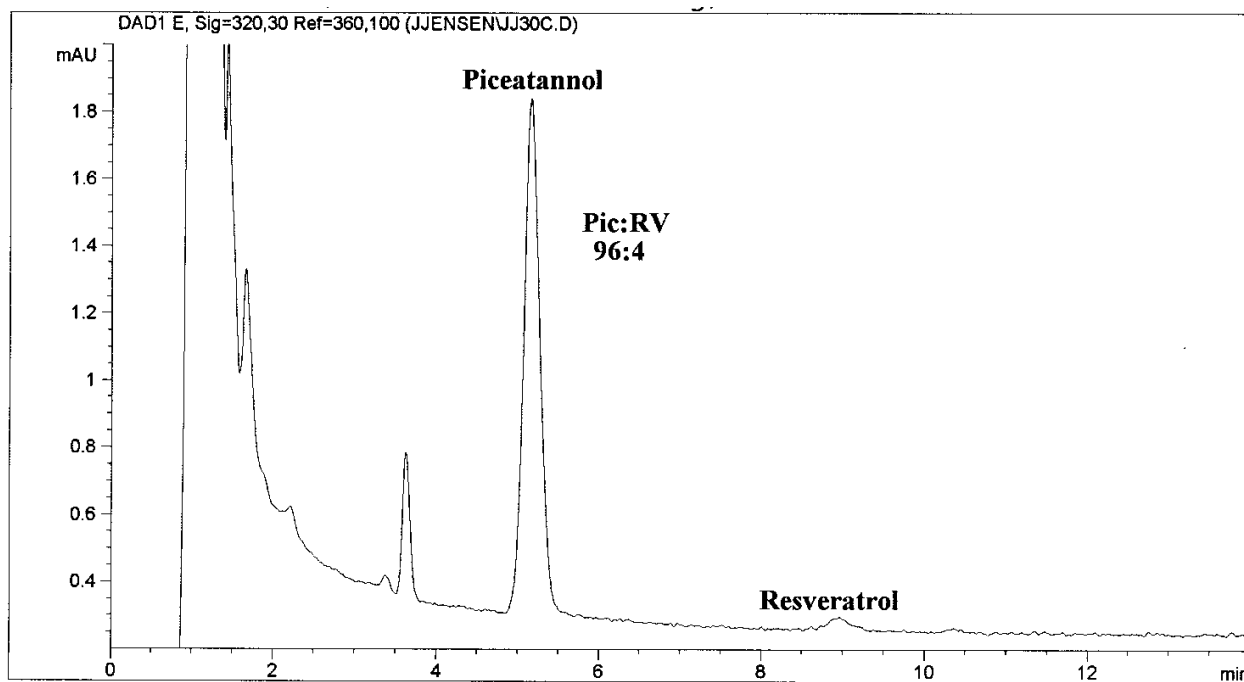


Figure 27. HPLC chromatogram of a crude mixture of resveratrol **1** + CYP3A4 enzymatic reaction (acetonitrile : deionized H<sub>2</sub>O, 1 : 1, v/v; column: Zorbax SB-C18 reversed phase; dimension: 4.6 x 150mm, 5-micron; flow rate: 1mL/min; injection volume = 30μL; run time = 14min; piceatannol **7**  $t_r$  = 5.16min, resveratrol **1**  $t_r$  = 8.96min).

natural products, and drugs to act as substrates and undergo chemical modifications.<sup>22f</sup> Besides this, a variety of chemical compounds, either synthetic or natural, are known to act as CYP3A4 inhibitors, or inducers,<sup>22f</sup> further attesting to its remarkable ability to “accommodate” diverse organic molecules. The hydroxylation reaction we discovered with CYP3A4 enzyme is chemically analogous to previously reported activation of tamoxifen<sup>22e</sup> and a multitude of other drugs that contain aromatic nuclei in their carbon framework.

### ***Screening of CYP1A1 with resveratrol 1.***

Enzyme CYP1A1 is expressed primarily in the esophagus and has low expression rates in the liver and stomach (Figure 28). It participates in a number of metabolic reactions: O-dealkylation of 7-ethoxyresorufin to its respective metabolite, resorufin,<sup>23a</sup> PUFA metabolism,<sup>19a</sup> and flavonoid metabolism by O-demethylation.<sup>23b</sup> Also CYP1A1 plays a critical role in Phase I metabolism of polycyclic aromatic hydrocarbons (PAH), a known class of carcinogens.<sup>23c</sup> Thus, benzo(a)pyrene is oxidized by CYP1A1 to benzo(a)pyrene-7,8-dihydrodiol-9,10-epoxide,<sup>23c</sup> a proven carcinogen that is capable of reacting with DNA bases and causing a DNA strand cleavage. The epoxidation reaction is most relevant to this project, since aromatic nuclei in PAH act as a reaction site receiving an oxygen atom via an iron-induced organometallic reaction.

An enzymatic reaction with resveratrol **1** was carried out according to the standardized protocol, and the crude mixture, upon denaturing the CYP1A1 enzyme with acetonitrile, was analyzed by HPLC to discover another case of highly efficient metabolic hydroxylation (Figure 29; resveratrol **1** : piceatannol **7**, 3 : 97). The chromatogram had an excellent peak symmetry and a 3-minute peak separation between substrate and metabolite (piceatannol **7**  $t_r$  = 4.05min,



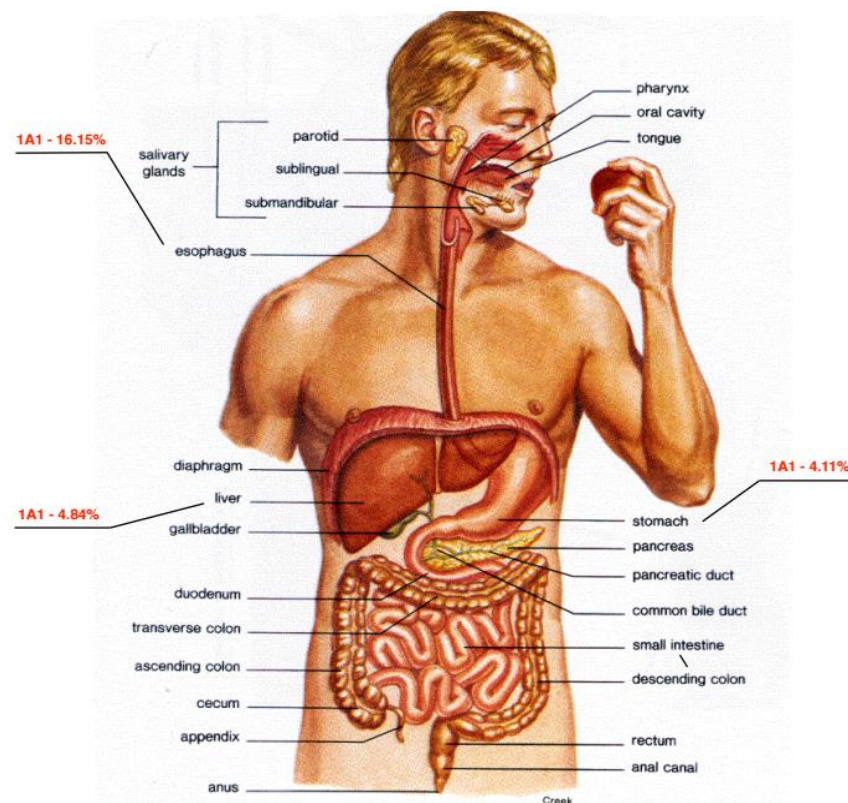


Figure 28. CYP1A1 mapping diagram of enzymatic expression in human organ systems.

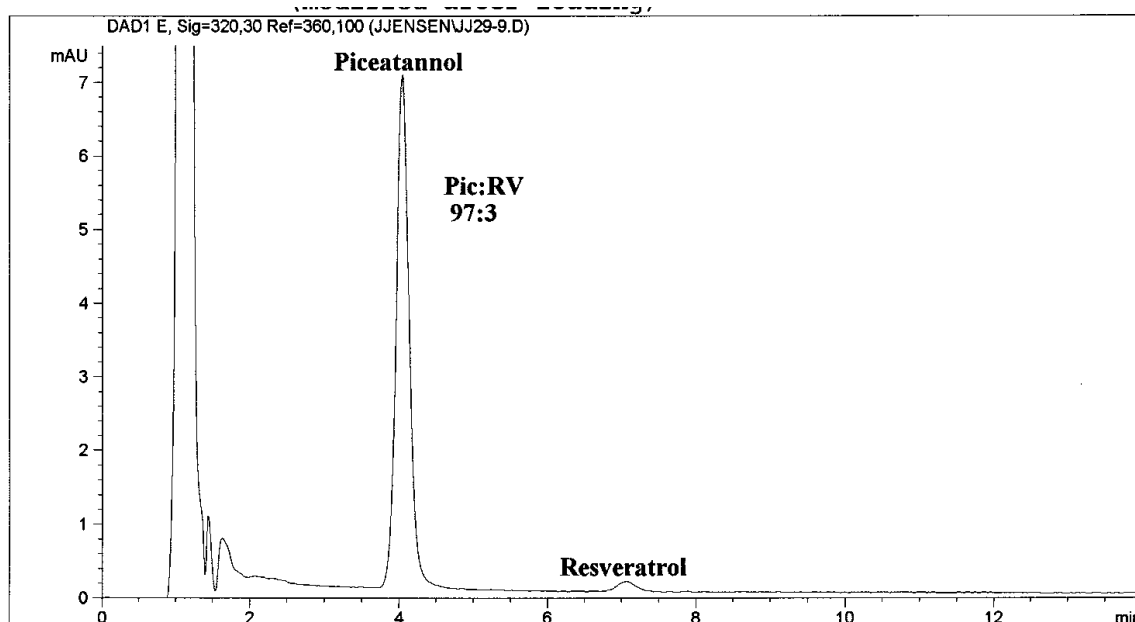


Figure 29. HPLC chromatogram of a crude mixture of resveratrol **1** + CYP1A1 enzymatic reaction (acetonitrile : deionized H<sub>2</sub>O, 1 : 1, v/v; column: Zorbax SB-C18 reversed phase; dimension: 4.6 x 150mm, 5-micron; flow rate: 1mL/min; injection volume = 30μL; run time = 14min; piceatannol **7**  $t_r$  = 4.05min, resveratrol **1**  $t_r$  = 7.07min).

resveratrol **1**  $t_r = 7.07\text{min}$ ). The retention times observed are the lowest among a series of enzymatic reactions studied, and might be caused by the presence of chemical components derived from denatured enzyme, by aging column, or by fluctuating column pressure. Most importantly, certain variations in retention times are derived from the very nature of high-pressure liquid chromatography, and due to availability of both authentic samples, do not compromise the reliability of qualitative identification of compounds involved.

### ***Screening of CYP2A6 with resveratrol 1.***

Enzyme CYP2A6 is expressed primarily in the liver (Figure 30) and is responsible for nicotine metabolism by means of a two-step reaction that involves the C-oxidation of nicotine to cotinine (carbonylation reaction), followed by a 3'-hydroxylation to the end-product, *trans*-3'-hydroxycotinine (hydroxylation at  $\text{sp}^3$ -hybridized carbon, alpha to a keto function).<sup>24a</sup> Most relevant to this project is the documented ability of CYP2A6 to carry out an aromatic hydroxylation in different topological and functional settings. Thus, polychlorinated biphenyls (PCBs) undergo an enzymatic 4'-hydroxylation at the aromatic nuclei and were banned as an environmental pollutant in 1979 by U.S. Congress.<sup>24b</sup> The CYP2A6 enzyme also catalyzes the 7-hydroxylation of coumarin; the oxidation process is of high efficacy, to the extent that formation of 7-hydroxycoumarine is used as a probe for mapping, or discovery, of CYP2A6 enzyme in human organs and tissues.<sup>24c</sup> Overall, the enzyme exhibits a remarkably wide substrate selectivity, metabolizing a number of drugs, carcinogens, and natural and synthetic toxins.<sup>24c</sup> Besides this, a large variety of chemical structures can act as CYP2A6 enzyme inhibitors or inducers.<sup>24c</sup> drugs (antiarrhythmic, calcium channel blockers, opioids, antifungal, anticonvulsants), natural extracts (flavonoids from grapefruit juice), aromatase inhibitors (letrozole), and barbiturates (amobarbital, pentobarbital).

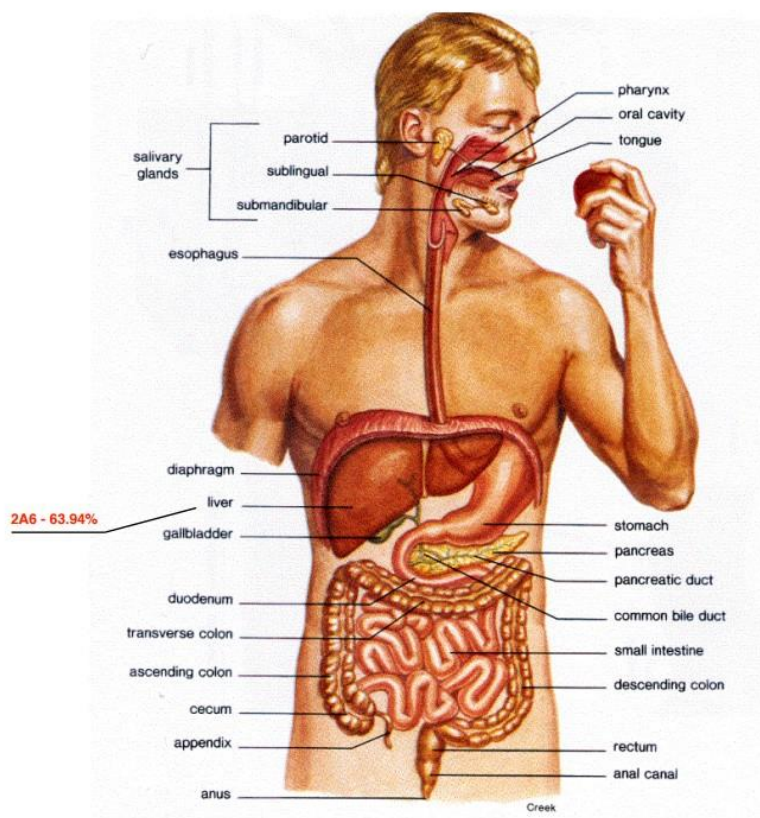


Figure 30. CYP2A6 mapping diagram of enzymatic expression in human organ systems.

An enzymatic reaction with resveratrol **1** was carried out according to the standardized protocol, and the crude mixture, upon denaturing the CYP2A6 enzyme with acetonitrile, was analyzed by HPLC to discover another case of highly efficient metabolic hydroxylation (Figure 31; resveratrol **1** : piceatannol **7**, 3 : 97). The certain fluctuation in retention times was observed (piceatannol  $t_r = 4.64\text{min}$ , resveratrol  $t_r = 8.10\text{min}$ ), albeit within the acceptable limits that still allow for qualitative identification of the metabolic product. Whenever in doubt, spiking with an authentic piceatannol **7** was routinely applied as additional proof that the metabolic conversion in question has in fact taken place. Functionally and conformationally, resveratrol **1** has similarities with CYP2A6 known substrates, in particular those with restricted rotations of aromatic rings due to either conjugation with double bonds (coumarins), or steric repulsion between aromatic

rings (biphenyls), or availability of positions 3'- and 4'- at aromatic nuclei to enzymatic hydroxylation reactions. Given the analogy and a demonstrated ability of CYP2A6 to interact with a wide spectrum of chemical compounds, either as substrates, or inhibitors, or inducers,<sup>24c</sup> it does not come as a surprise that resveratrol **1** also undergoes functionalization by incorporating a hydroxyl group in a 3'-position, ortho- to 4'-hydroxyl group.

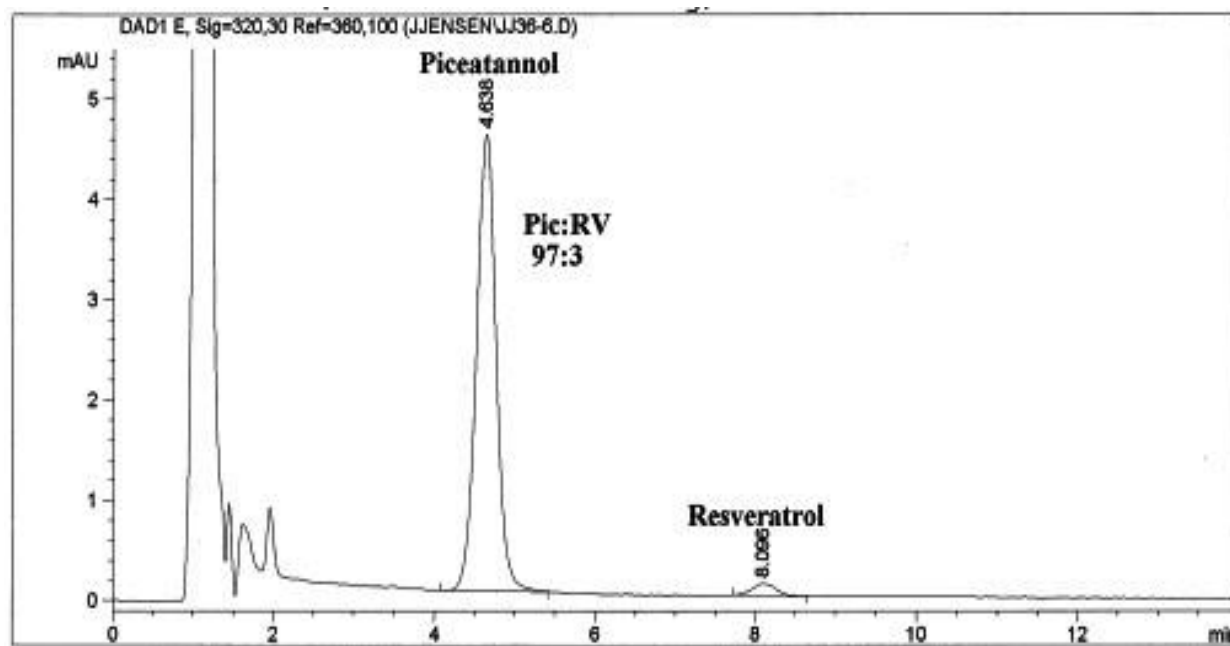


Figure 31. HPLC chromatogram of a crude mixture of resveratrol **1** + CYP2A6 enzymatic reaction (acetonitrile : deionized H<sub>2</sub>O, 1 : 1, v/v; column: Zorbax SB-C18 reversed phase; dimension: 4.6 x 150mm, 5-micron; flow rate: 1mL/min; injection volume = 30μL; run time = 14min; piceatannol **7**  $t_r$  = 4.64min, resveratrol **1**  $t_r$  = 8.10min).

#### *Screening of CYP2C9 with resveratrol **1**.*

Enzyme CYP2C9 is expressed mainly in the liver (Figure 32) and metabolizes some 100 therapeutic agents. Aromatic hydroxylation is reported for diclofenac, a widely prescribed nonsteroidal anti-inflammatory drug (NSAID).<sup>25a</sup> Warfarin (coumadin), a blood thinning drug, is also metabolized by CYP2C9, although by a different mechanism, i. e. vicinal hydroxylation at aromatic positions 6 and 7.<sup>25b</sup> Structurally, warfarin is analogous to resveratrol **1** containing two

aromatic rings opposite to each other, with the internal double bond providing for rigidity due its trans-configuration. Tetrahydrocannabinol (THC), the main psychoactive constituent of cannabis, is also a suitable substrate for CYP2C9 enzyme and forms an active metabolite (11-OH-THC) by allylic oxidation of its methyl group.<sup>25c</sup> Epoxidation is another metabolic reaction that can be induced by CYP2C9 enzyme. Thus, polyunsaturated fatty acids (PUFA), such as arachidonic acid can undergo multiple oxidations involving allylic triads that in turn convert PUFAs to biologically active end-products.<sup>25d, 21b</sup>

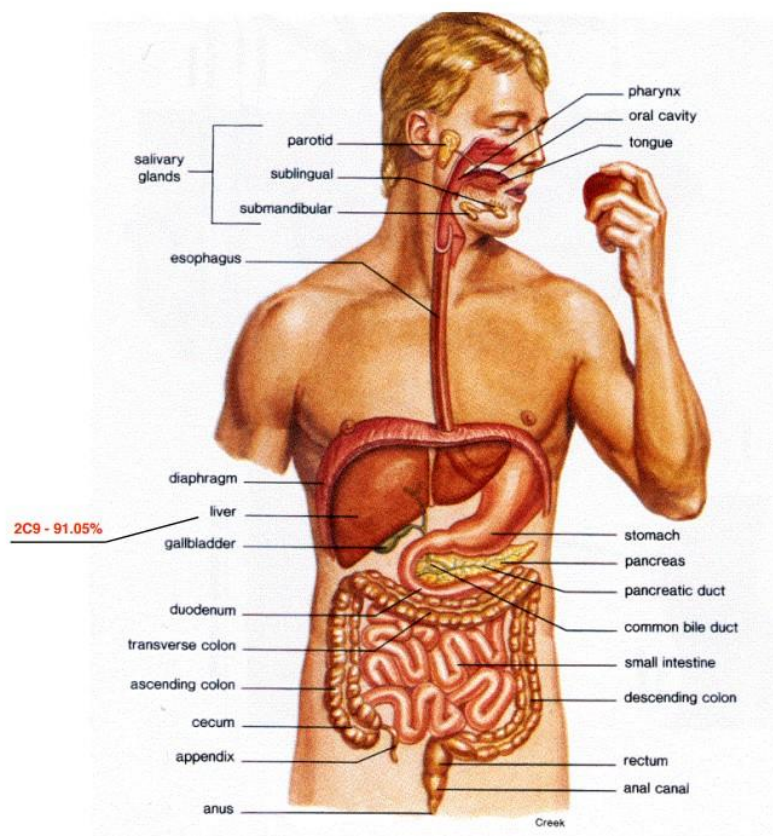


Figure 32. CYP2C9 mapping diagram of enzymatic expression in human organ systems.

An enzymatic reaction with resveratrol **1** was carried out according to the standardized protocol, and the crude mixture, upon denaturing the CYP2C9 enzyme with acetonitrile, was analyzed by HPLC to discover another case of an highly efficient metabolic hydroxylation

(Figure 33; resveratrol **1** : piceatannol **7**, 3 : 97). The retention times for both main components (piceatannol **7**  $t_r$  = 4.62min, resveratrol **1**  $t_r$  = 8.09min) were close to those observed with CYP2A6 enzyme (piceatannol **7**  $t_r$  = 4.64min, resveratrol **1**  $t_r$  = 8.10min). A 3.4-minute separation between enzymatic substrate and its metabolite was observed with exceptionally clean peak symmetry (Figure 33). Among the enzymes studied so far, CYP2C9 constitutes the third case within CYP2 family when hydroxylation was successfully effected (CYP2C18, CYP2A6, CYP2C9). In contrast, with CYP2C19, we were not able to detect even trace amounts of piceatannol **7** in the crude mixture, further underscoring the importance of intimate enzymatic make-up for enzyme's efficacy.

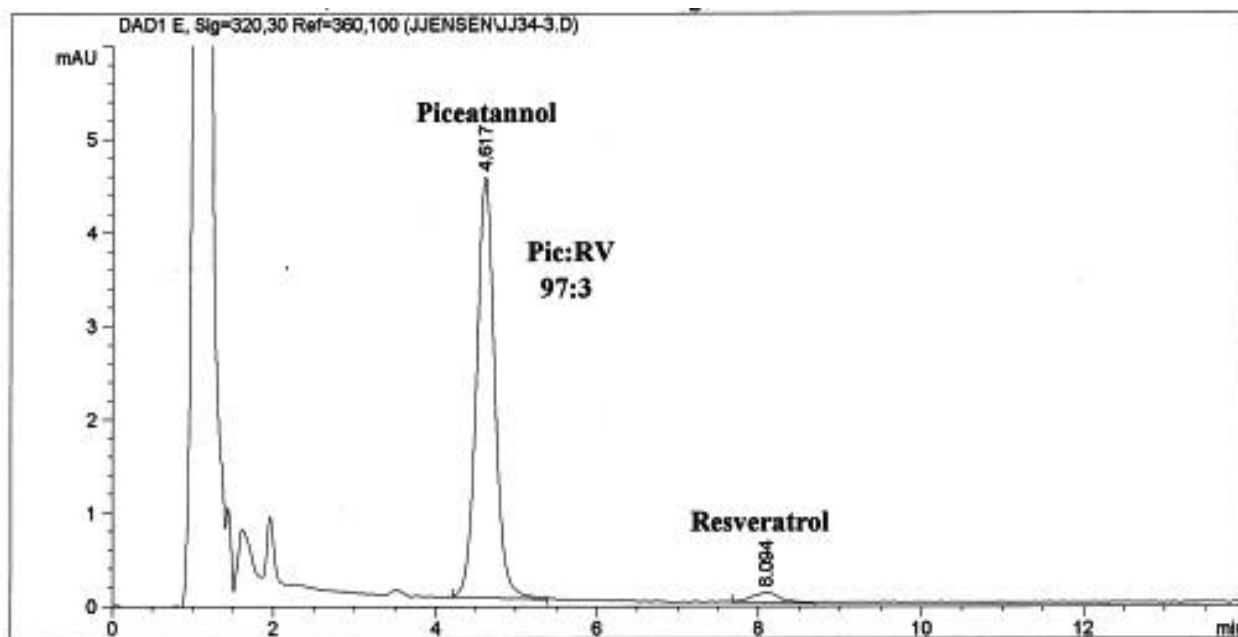


Figure 33. HPLC chromatogram of a crude mixture of resveratrol **1** + CYP2C9 enzymatic reaction (acetonitrile : deionized H<sub>2</sub>O, 1 : 1, v/v; column: Zorbax SB-C18 reversed phase; dimension: 4.6 x 150mm, 5-micron; flow rate: 1mL/min; injection volume = 30μL; run time = 14min; piceatannol **7**  $t_r$  = 4.62min, resveratrol **1**  $t_r$  = 8.09min).

#### ***Screening of CYP2C8 with resveratrol 1.***

Enzyme CYP2C8 expressed primarily in the liver and to a much lesser extent in stomach (Figure 34), is a participant of the “cytochrome P450 mixed-function oxidase system” and



recruited for xenobiotic metabolism. CYP2C8 exhibits epoxigenase activity whereby it processes long-chain PUFA's such as arachidonic acid (AA), eicosapentaenoic acid (EPA), docosahexaenoic acid (DHA), and linoleic acid (LA) into their respective epoxides.<sup>26</sup> CYP2C8 enzyme also metabolizes the type 2 diabetes mellitus (T2DM) drug, *repaglinide*, in a series of CYP-induced transformations such as aromatic hydroxylation (major metabolite), aromatic amination (minor metabolite), and hydroxylation of the isopropyl moiety (minor metabolite).<sup>22d</sup> The presence of two aromatic rings in repaglinide and enzymatic hydroxylation at one of them makes this reaction quite relevant to resveratrol-to-piceatannol conversion, increasing chances for a successful enzymatic hydroxylation, or related oxidation reaction.

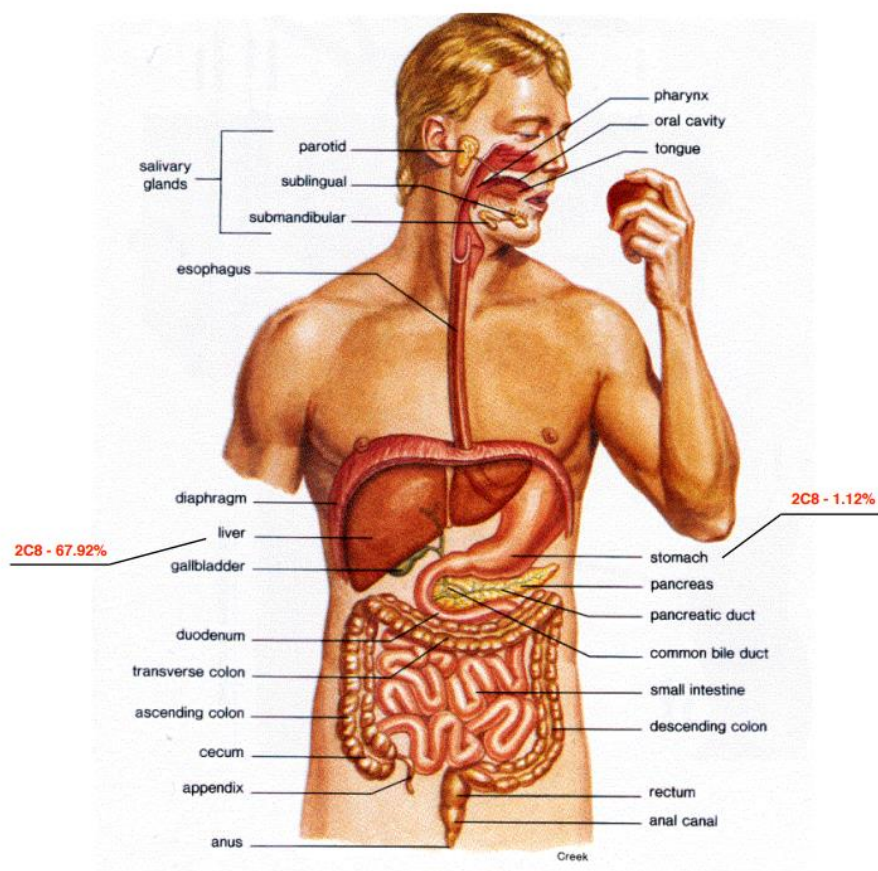


Figure 34. CYP2C8 mapping diagram of enzymatic expression in human organ systems.

An enzymatic reaction with resveratrol **1** was carried out according to the standardized protocol, and the crude mixture, upon denaturing the CYP2C8 enzyme with acetonitrile, was analyzed by HPLC to present another case of an efficient metabolic hydroxylation (Figure 35; resveratrol **1** : piceatannol **7**, 2 : 98). The retention times were beginning to optimize to the authentic sample retention times we observed earlier, i. e. near 5min for piceatannol **7** and near 8min for resveratrol **1**. By degree of conversion and retention times for main components, this reaction is analogous to that of CYP2C9 (Figure 33), making it the fourth case of enzymes that belong to CYP2 family and demonstrate a high efficiency in aromatic hydroxylation reactions.

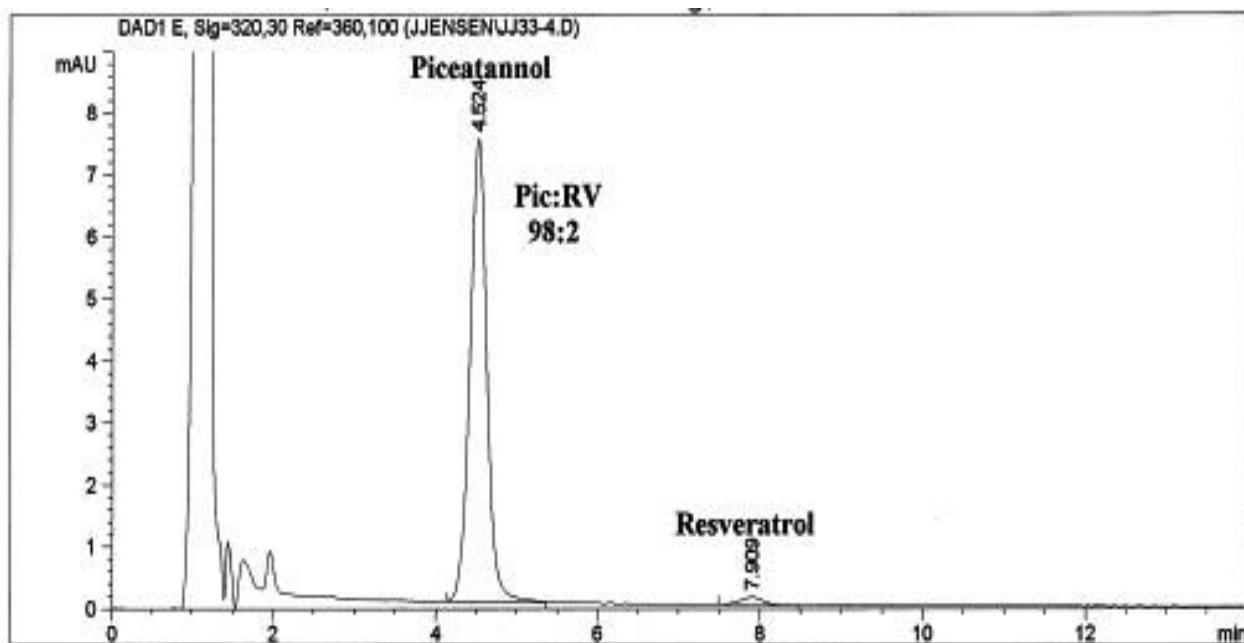


Figure 35. HPLC chromatogram of a crude mixture of resveratrol **1** + CYP2C8 enzymatic reaction (acetonitrile : deionized H<sub>2</sub>O, 1 : 3, v/v; column: Zorbax SB-C18 reversed phase; dimension: 4.6 x 150mm, 5-micron; flow rate: 1mL/min; injection volume = 30μL; run time = 14min; piceatannol **7**  $t_r$  = 4.52min, resveratrol **1**  $t_r$  = 7.91min).

#### ***Screening of CYP4F12 with resveratrol 1.***

Enzyme CYP4F12 is expressed in the esophagus, small intestine, and to a lesser extent, in the stomach (Figure 36) and implied in metabolism of antihistamine drugs, *Ebastine*, *Astemizole* and



*Terfenadine*.<sup>27a,b</sup> When expressed in yeast, this enzyme introduces a hydroxyl group in arachidonic acid and related polyunsaturated fatty acids (allylic oxidation), although its physiological significance has not been determined.<sup>27c</sup> Thus, CYP4F12 is recruited to process prostaglandin H2 (PGH2) and PGH1 to their designated 19-hydroxyl analogs in a reaction that may serve to reduce their activities.<sup>27c</sup> Epoxidation is another enzymatic pathway that was documented with CYP4F12 as an enzyme and omega-3 fatty acids acting as substrates. Some epoxides such as epoxydocosapentaenoic (EDP) acid and epoxyeicosatetraenoic (EEQ) acid exhibited a broad range of activities.<sup>27e,f</sup> In *in vitro* studies on human and animal tissues, as well as in various animal models these fatty acid-derived epoxides decreased hypertension, suppressed inflammation, inhibited angiogenesis, and positively impacted metastasis in breast and prostate cancer cell lines.<sup>27e,f</sup>

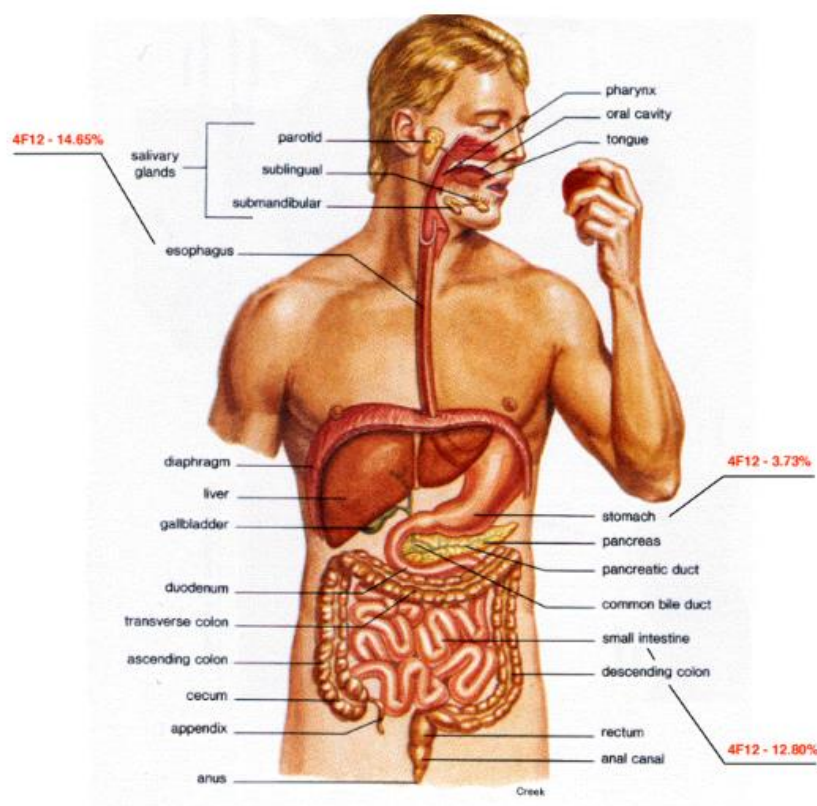


Figure 36. CYP4F12 mapping diagram of enzymatic expression in human organ systems.

An enzymatic reaction with resveratrol **1** was carried out according to the standardized protocol, and the crude mixture, upon denaturing the CYP4F12 enzyme with acetonitrile, was analyzed by HPLC to present another case of an efficient metabolic hydroxylation (Figure 37; resveratrol **1** : piceatannol **7**, 2 : 98; piceatannol **7**  $t_r$  = 4.65min, resveratrol **1**  $t_r$  = 8.05min). Although CYP4F12 enzyme is known to effect the epoxidation reaction as well, the crude mixture did not contain any metabolites, other than piceatannol **7**, that could represent the epoxide derived from an oxidation of the internal double bond connecting both aromatic nuclei. Thus, the metabolic profile of CYP4F12 follows the same, highly regioselective profile of other enzymes with an *ortho*-position of the aromatic ring being the only site of an oxidation reaction.

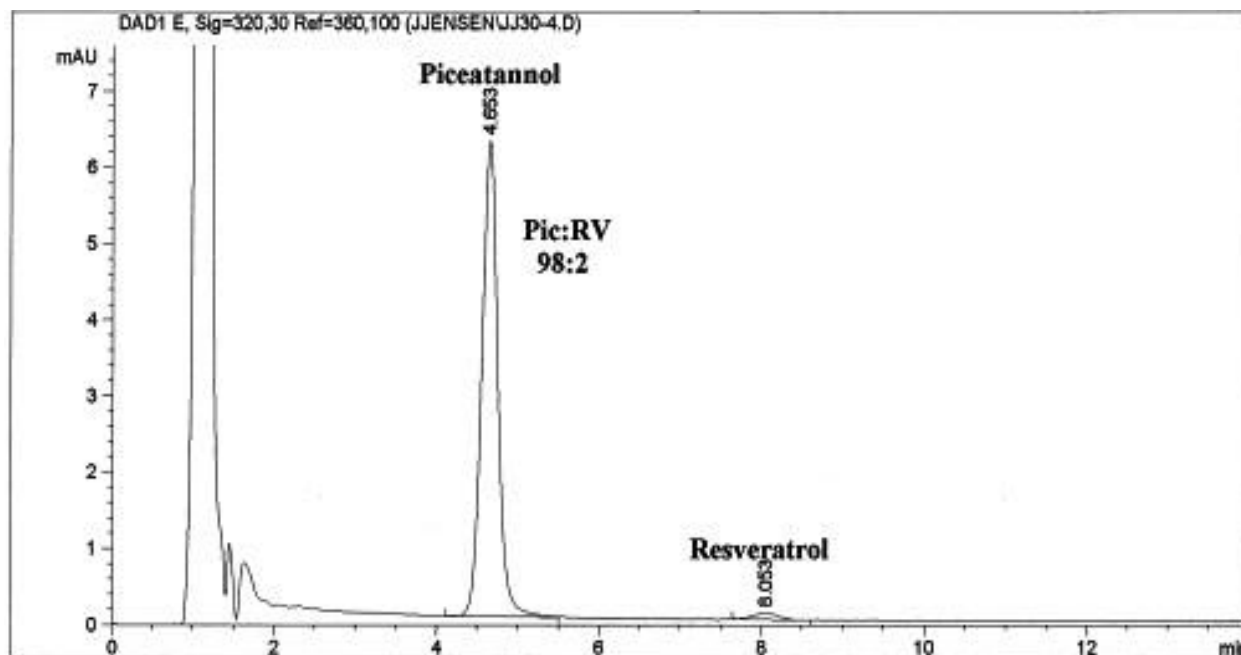


Figure 37. HPLC chromatogram of a crude mixture of resveratrol **1** + CYP4F12 enzymatic reaction (acetonitrile : deionized H<sub>2</sub>O, 1 : 1, v/v; column: Zorbax SB-C18 reversed phase; dimension: 4.6 x 150mm, 5-micron; flow rate: 1mL/min; injection volume = 30μL; run time = 14min; piceatannol **7**  $t_r$  = 4.65min, resveratrol **1**  $t_r$  = 8.05min).

The summary of enzymatic transformations of resveratrol **1** to piceatannol **7** is given in Table

1. A high degree of conversion was observed for seven CYP enzymes out of 12 studied in the

course of this project. Given the fact that piceatannol **7** belongs to the class of ortho-hydroquinones is a cause of concern from the standpoint of public health. Those active enzymes are located in different positions throughout the alimentary canal and can generate piceatannol **7** inside the human body, which in turn can oxidize to respective ortho-quinones, a known class of carcinogens.

Table 1. Metabolic transformations of resveratrol **1** by cytochrome P450 human enzymes.

<b>Substrate + Enzyme</b>	<b>Metabolic Conversion</b>	
Resveratrol + CYP2C19	No product	0%
Resveratrol + CYP2D6	No product	0%
Resveratrol + CYP3A5	No product	0%
Resveratrol + CYP4F3A	Piceatannol	1%
Resveratrol + CYP2E1	Piceatannol	2%
Resveratrol + CYP2C18	Piceatannol	95%
Resveratrol + CYP3A4	Piceatannol	96%
Resveratrol + CYP1A1	Piceatannol	97%
Resveratrol + CYP2A6	Piceatannol	97%
Resveratrol + CYP2C9	Piceatannol	97%
Resveratrol + CYP2C8	Piceatannol	98%
Resveratrol + CYP4F12	Piceatannol	98%

We consider these data to be preliminary. Additional experiments will be conducted in the future to accomplish the following: (1) to check the reproducibility of enzymatic conversions by

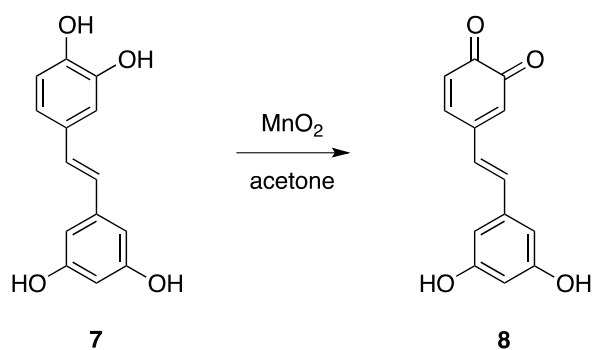
using enzymes from alternative commercial sources; (2) to develop an alternative method of HPLC analysis using gradient elution protocol; (3) to modify HPLC conditions in such a way so that a higher than 3-min separation can be achieved between the substrate and metabolite(s); (4) to use Liquid Chromatography–Mass Spectroscopy (LC-MS) method to analyze crude enzymatic mixtures so that the formation of piceatannol **7** would be independently confirmed by mass spectroscopic analysis; (5) to scale-up enzymatic reactions and isolate milligram quantities of metabolites on preparative HPLC column; and (6) to identify metabolites by using Nuclear Magnetic Resonance (NMR) spectroscopy. In the course of this project, the main impediment was the lack of reproducibility in different batches of commercial enzymes when ordered months or years apart, or when the same enzymes were provided by different vendors. Another problem was derived from the fact that enzyme producers are testing the quality of their products by not using HPLC, but a UV-vis method. Intrinsically, the latter does not have the same level of reliability as HPLC method when assessing model enzymatic reactions such as the formation of resorufin from O-ethyl resorufin or hydroxytestosterone from the parent hormone. The reason is that the UV-vis spectroscopy relies on broad absorption bands without actually “seeing” the individual components as chromatographic peaks. As a result, in contrast to HPLC, no qualitative or quantitative identification can be carried out for potential metabolites even if the authentic samples are available either from commercial sources, or through the independent synthesis.

### **2.3. Chemical transformation of piceatannol to piceatannol-*ortho*-quinone**

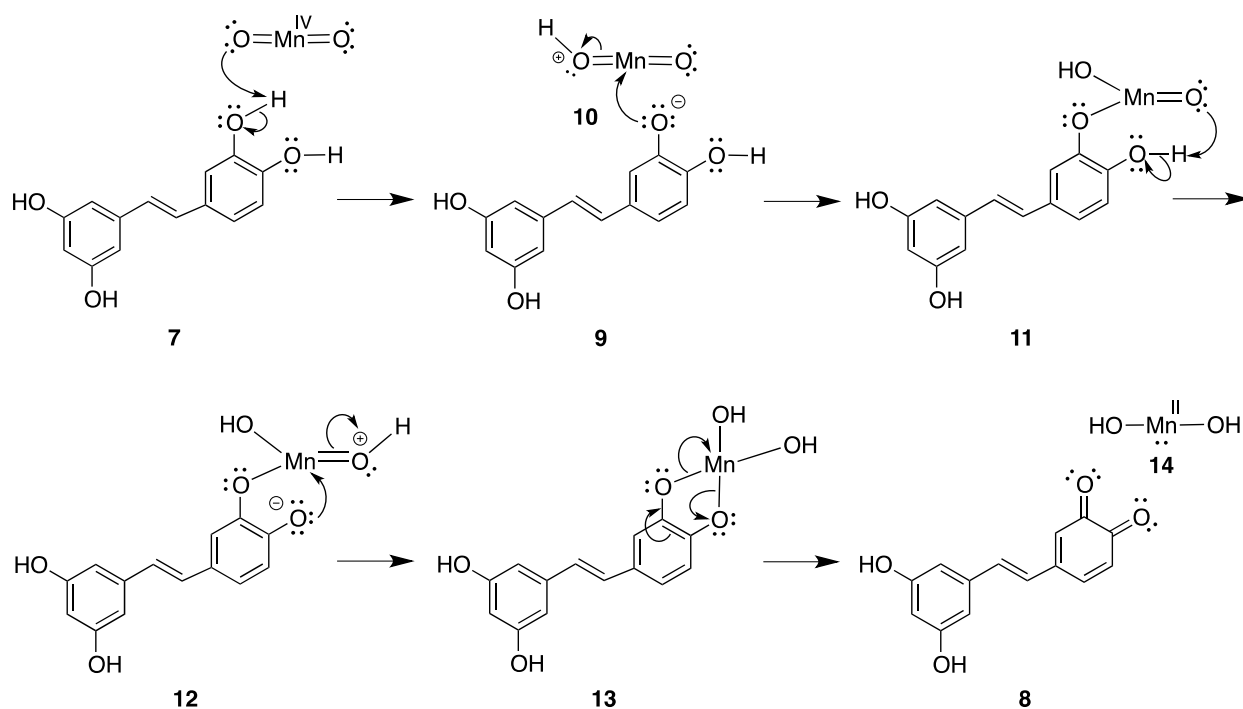
Enzymatic studies on the secondary oxidation of piceatannol **7** to its respective *ortho*-quinone **8** were preceded by an in-flask oxidation with manganese dioxide (Scheme 1). The goal

was to develop a protocol for oxidation, followed by the isolation and structural characterization of a target molecule. Having an authentic sample for *ortho*-quinone **8** would significantly facilitate its detection in the crude mixture of an enzymatic reaction. The experimental protocol involved treatment of piceatannol **7** with manganese dioxide in acetone under an empirically optimized molar ratio of 1 : 9. The reaction progress was monitored by HPLC (2h, 20°C) with an excess oxidant being removed by centrifugation, and the crude mixture being analyzed by NMR and MS spectroscopy. The protocol developed by us is analogous to previously reported oxidation of parent catechol to catechol-*ortho*-quinone by using silver(I) oxide or sodium periodate.<sup>28</sup> The formation of the product was confirmed by the pattern of hydrogen atoms drastically changing with respect to that in piceatannol **7**. Due to the formation of an *ortho*-quinone unit, neighboring hydrogens undergo a significant downfield shift, acquiring, by NMR, a typical appearance of  $\alpha,\beta$ -unsaturated ketones. The NMR  $^{13}\text{C}$  further confirmed the oxidation, since carbonyl groups in carbon spectroscopy are located in the far-left domain of the spectral window (C1, C2: 180.31, 180.99). Determining the molecular ion by mass spectroscopy proved to be extremely challenging. In LIFDI (Laser-Induced Field Desorption Ionization) analysis which is considered to be one of the mildest and most benign, no molecular ion was observed. An alternative ESI (Electron Spray Ionization) method also failed. And only spiking the sample with sodium ions in ESI analysis allowed us to observe the expected - albeit low intensity - molecular ion  $\text{MNa}^+$  265.0469 ( $\text{MNa}^+$  calculated - 265.0471). For comparison, piceatannol **7** exhibits a high intensity peak under analogous conditions.

The formation of quinone **8** occurs by a multistep mechanism according to which piceatannol **7** loses two hydrogen ions ( $\text{H}^+$ ) and two electrons, while  $\text{MnO}_2$  acquires the total of two hydrogen atoms (Scheme 2). The first step of the mechanism involves protonation of  $\text{MnO}_2$  with



Scheme 1.



Scheme 2.

catechol moiety, forming phenolate ion **9** and oxidant-derived protonated form **10** (Scheme 2). The subsequent addition of the phenolate ion **9**, as a nucleophile, to the electropositive metal ion completes an addition of a hydroxyl group across a manganese-oxygen double bond. The next step is an intramolecular addition across the second doubly-bonded metal-oxygen bond with hydrogen ion protonating Lewis base, followed by the cyclization step in bipolar intermediate

**12.** A five-membered metalla-cycle **13** undergoes cleavage, either by radical, or ionic mechanism, releasing *ortho*-quinone **8** and manganese(II) hydroxide **14** (Scheme 2).

*ortho*-Quinone **8**, a black solid, was found to be a relatively unstable compound: in solid form, it undergoes a partial decomposition even after 5min at room temperature (newly formed signals are visible in  $^1\text{H}$  NMR spectrum). The major decomposition occurs after 30min at room temperature, converting black solid into a partially purple substance. In acetone solution (red), *ortho*-quinone **8** is stable at  $-15^\circ\text{C}$  for 20 hours, or at  $-80^\circ\text{C}$  for 7 days. The purity can only be determined by NMR since the red color of the quinone solution instantaneously disappears when applied to silicagel. Development of TLC plate in acetone, as an eluent, did not show any mobile organic spots indicating a rapid, and complete decomposition.

The HPLC analyses were carried out under the standard conditions that we developed for resveratrol **1** and piceatannol **7** (Figure 5), as well as for piceatannol-*ortho*-quinone **8** (Figure 7). The former was used as an internal standard and stability of quinone **8** at ambient temperatures was monitored by HPLC (Figure 38). After each  $10\mu\text{L}$  injection, the HPLC vial was placed in a  $21^\circ\text{C}$  water bath that was shielded with aluminum foil in order to minimize light exposure. The HPLC vial was sealed with a septum, with a syringe tip inserted to provide access to oxygen. Under standard conditions, *ortho*-quinone **8** eluted at 6.1-6.3min and its concentrations were calculated with respect to resveratrol peak, assuming the reference compound was stable under reaction conditions. Sampling was carried out at 0h, 18h, 26h, 42h, 67h, 91h, 116h, 141h, and 165h lapsed times (Figure 39-47). Quinone **8** became nearly non-detectable at 141h (Figure 46) that was considered to be the end of the spontaneous decomposition reaction (Figure 38).

In the course of HPLC monitoring we discovered that with gradual decrease in quinone **8** concentration, that of piceatannol **7** steadily increases (Figure 38-47). At the beginning of the

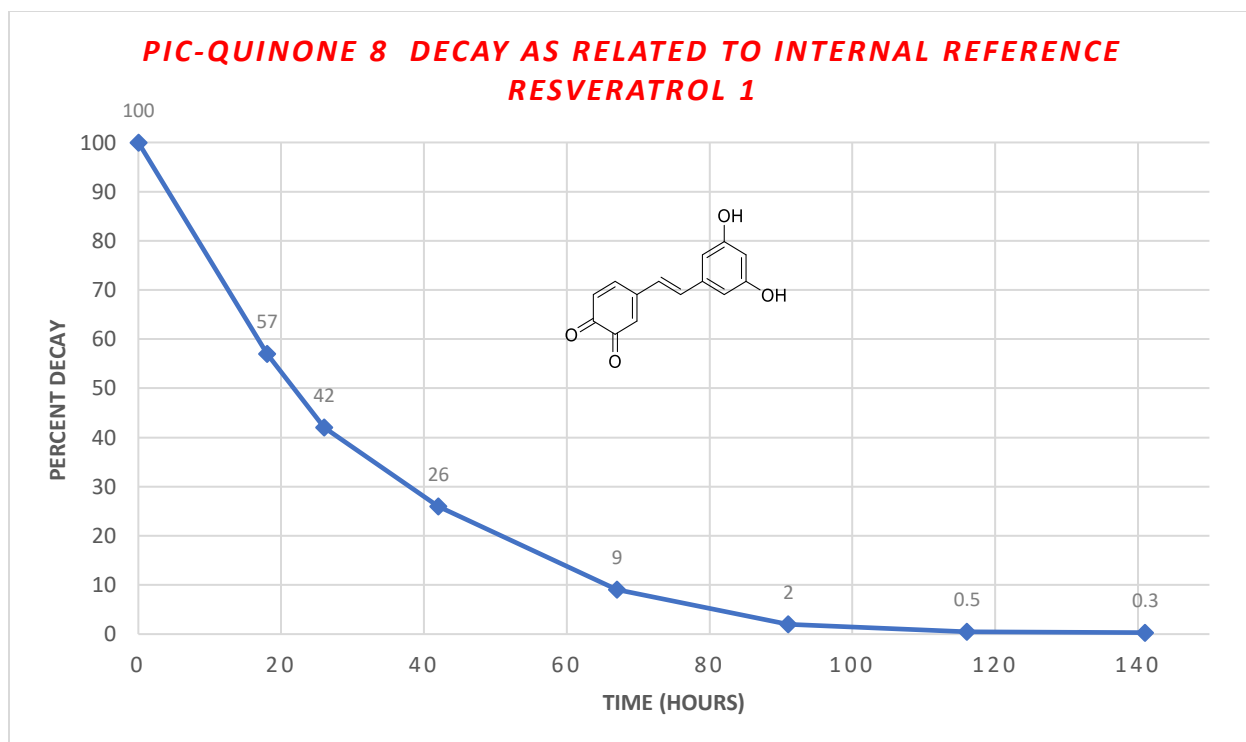


Figure 38. Progression of Pic-Q 8 decay with resveratrol 1 as an internal reference.

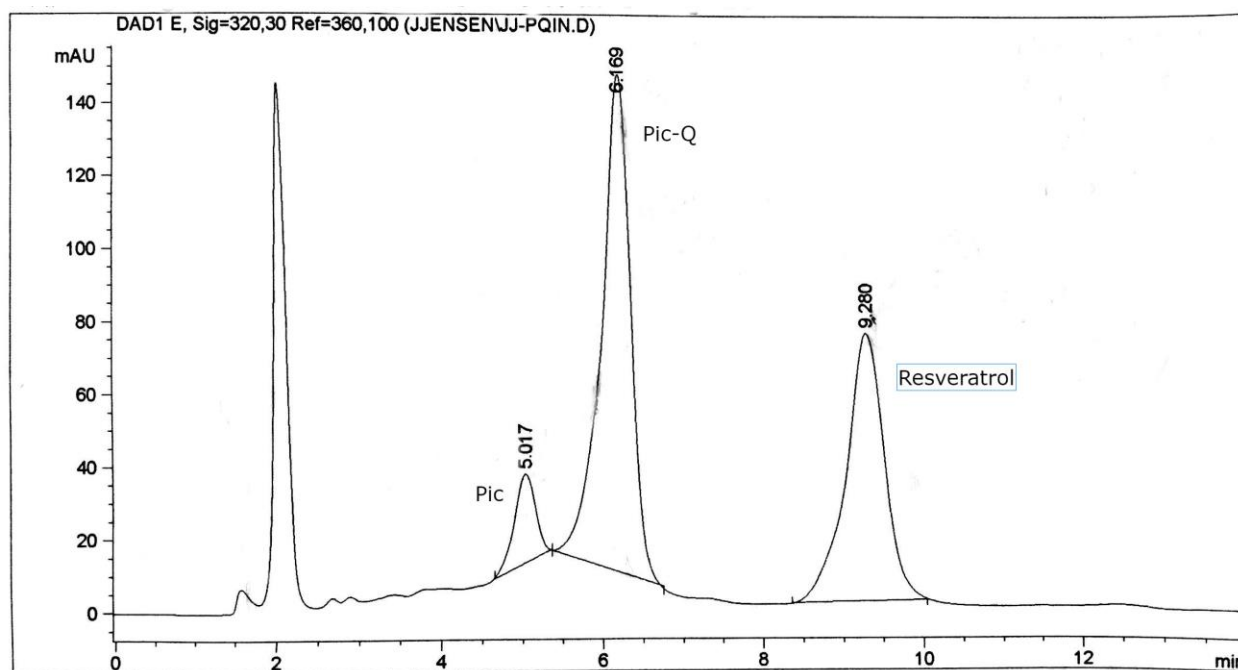


Figure 39. HPLC monitoring of spontaneous degradation of Pic-Q 8 with resveratrol 1 as an internal reference; lapsed time: 0 hours.



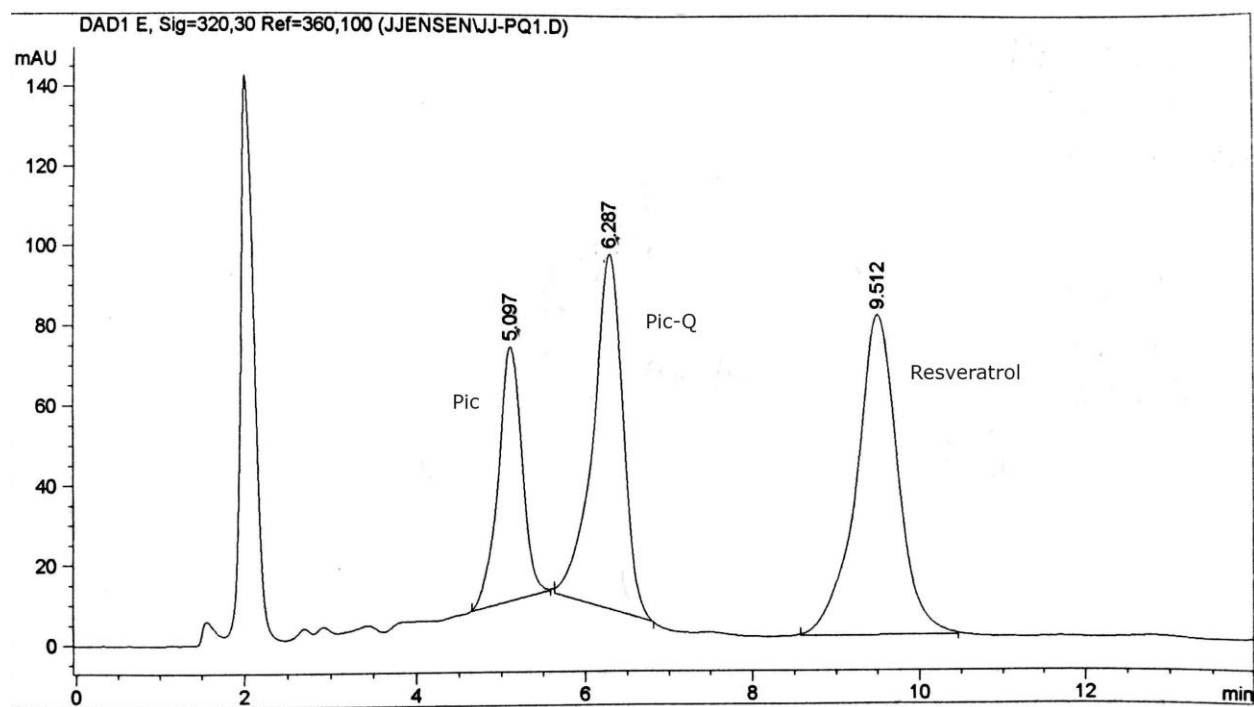


Figure 40. HPLC monitoring of spontaneous degradation of Pic-Q 8 with resveratrol 1 as an internal reference; *lapsed time: 18 hours.*

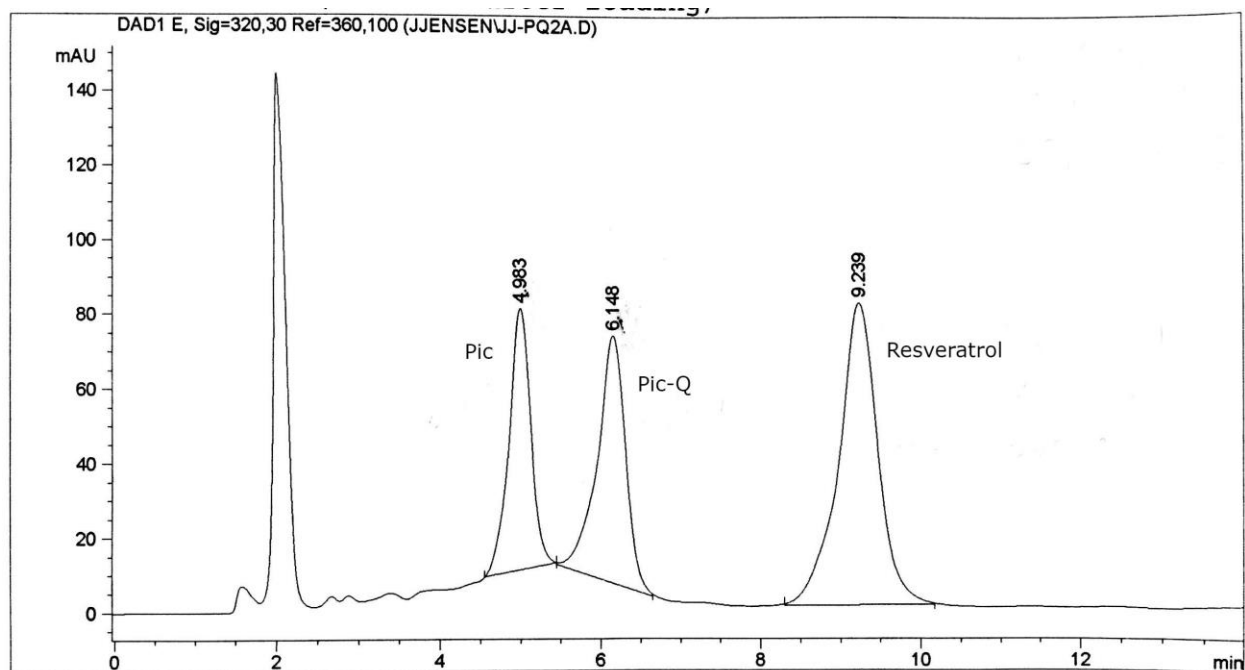


Figure 41. HPLC monitoring of spontaneous degradation of Pic-Q 8 with resveratrol 1 as an internal reference; *lapsed time: 26 hours.*

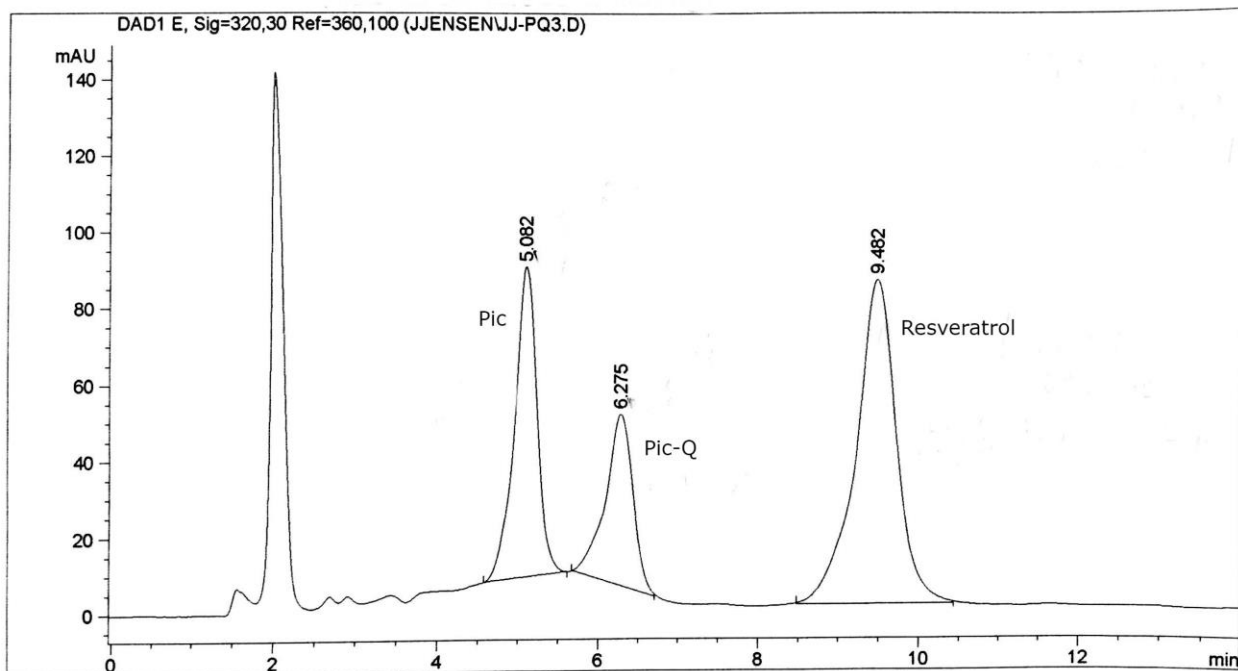


Figure 42. HPLC monitoring of spontaneous degradation of Pic-Q 8 with resveratrol 1 as an internal reference; *lapsed time: 42 hours.*

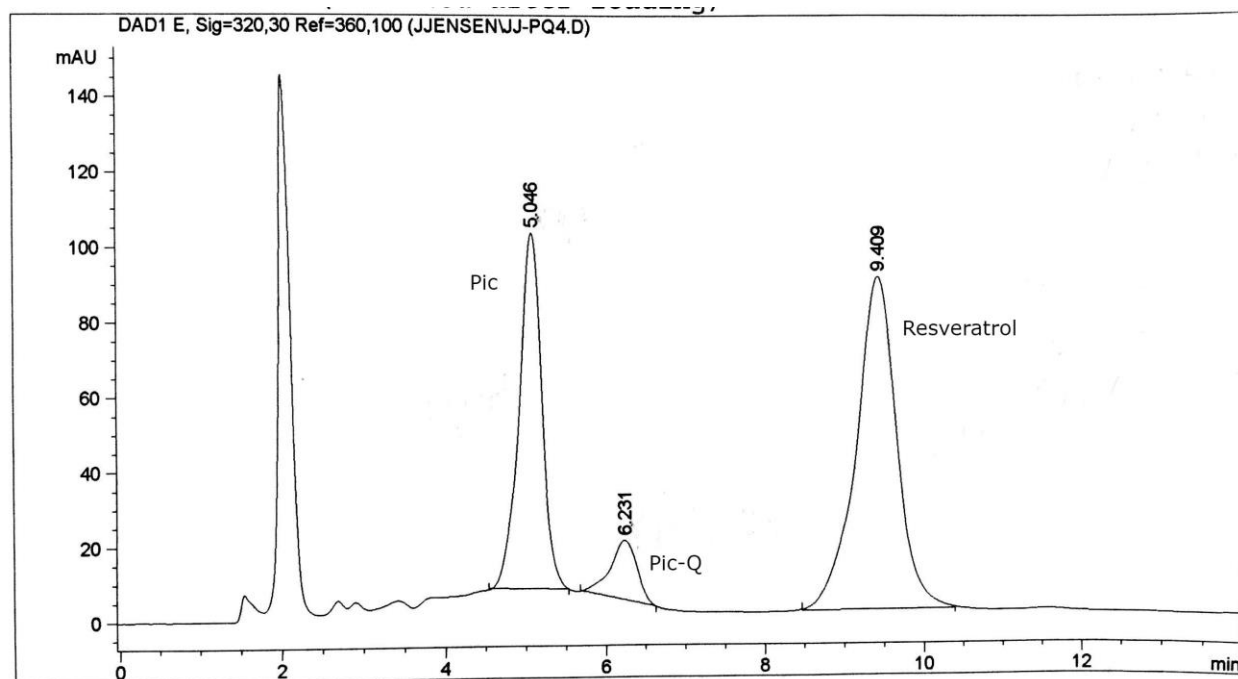


Figure 43. HPLC monitoring of spontaneous degradation of Pic-Q 8 with resveratrol 1 as an internal reference; *lapsed time: 67 hours.*

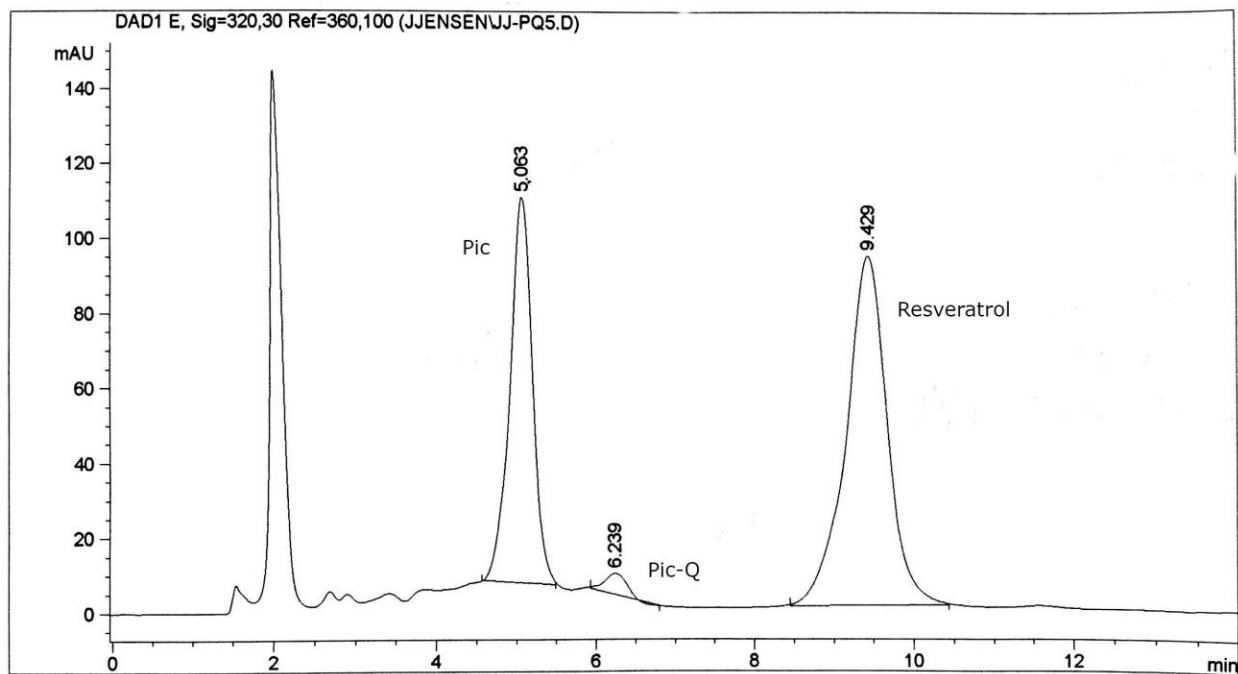


Figure 44. HPLC monitoring of spontaneous degradation of Pic-Q 8 with resveratrol 1 as an internal reference; *lapsed time: 91 hours*.

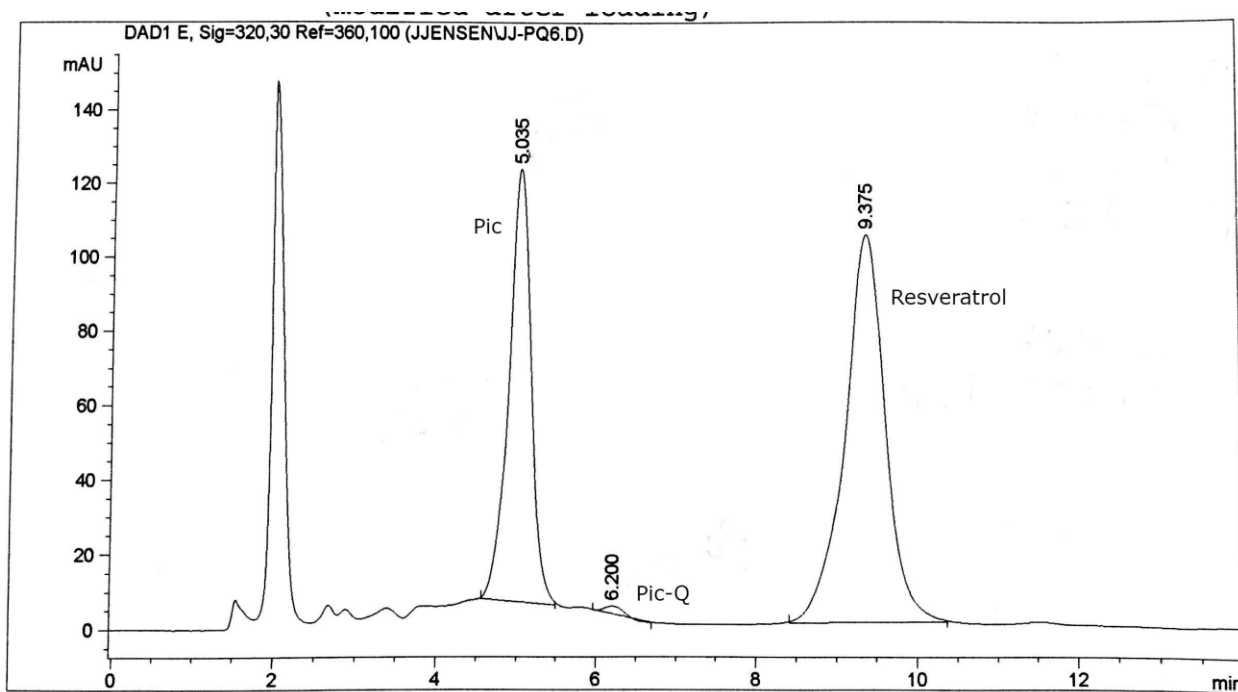


Figure 45. HPLC monitoring of spontaneous degradation of Pic-Q 8 with resveratrol 1 as an internal reference; *lapsed time: 116 hours*.

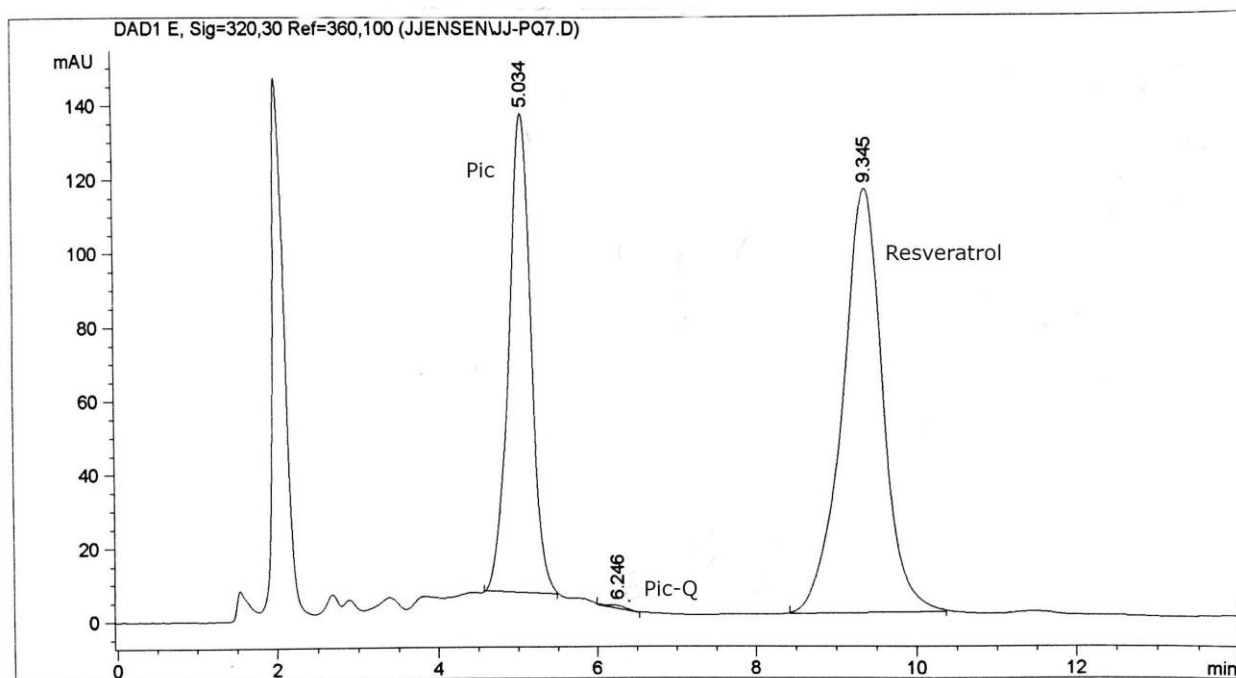


Figure 46. HPLC monitoring of spontaneous degradation of Pic-Q 8 with resveratrol 1 as an internal reference; *lapsed time: 141 hours.*

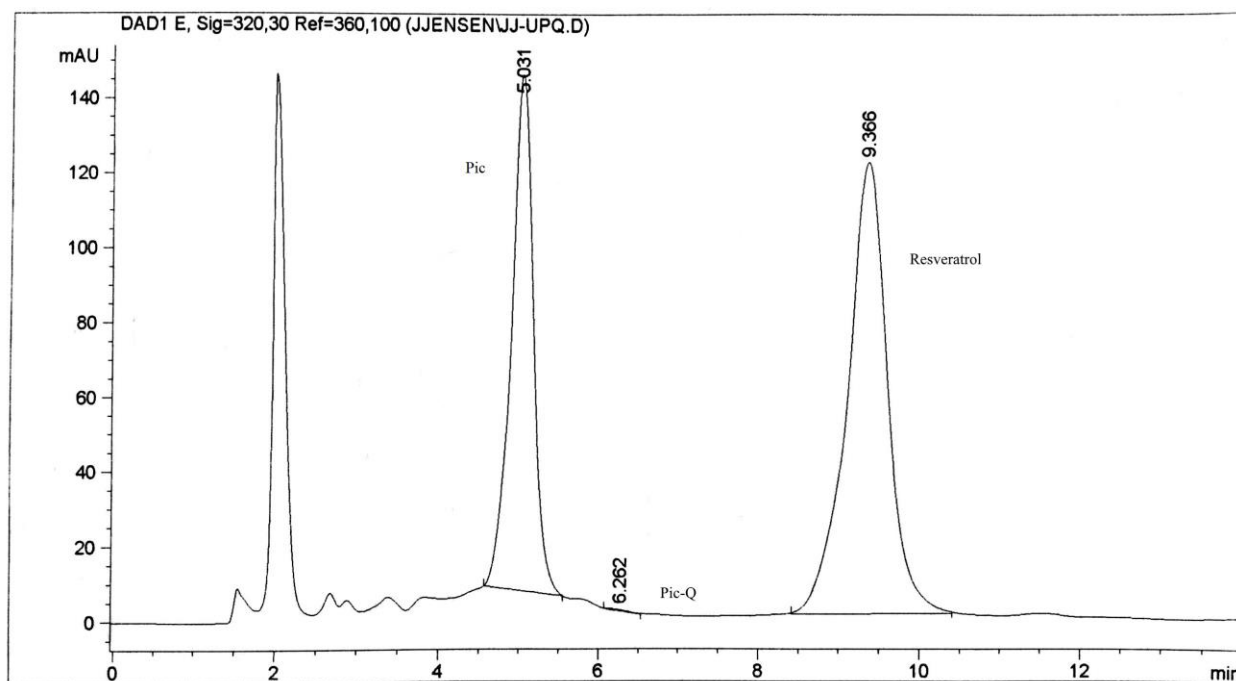


Figure 47. HPLC monitoring of spontaneous degradation of Pic-Q 8 with resveratrol 1 as an internal reference; *lapsed time: 165 hours.*

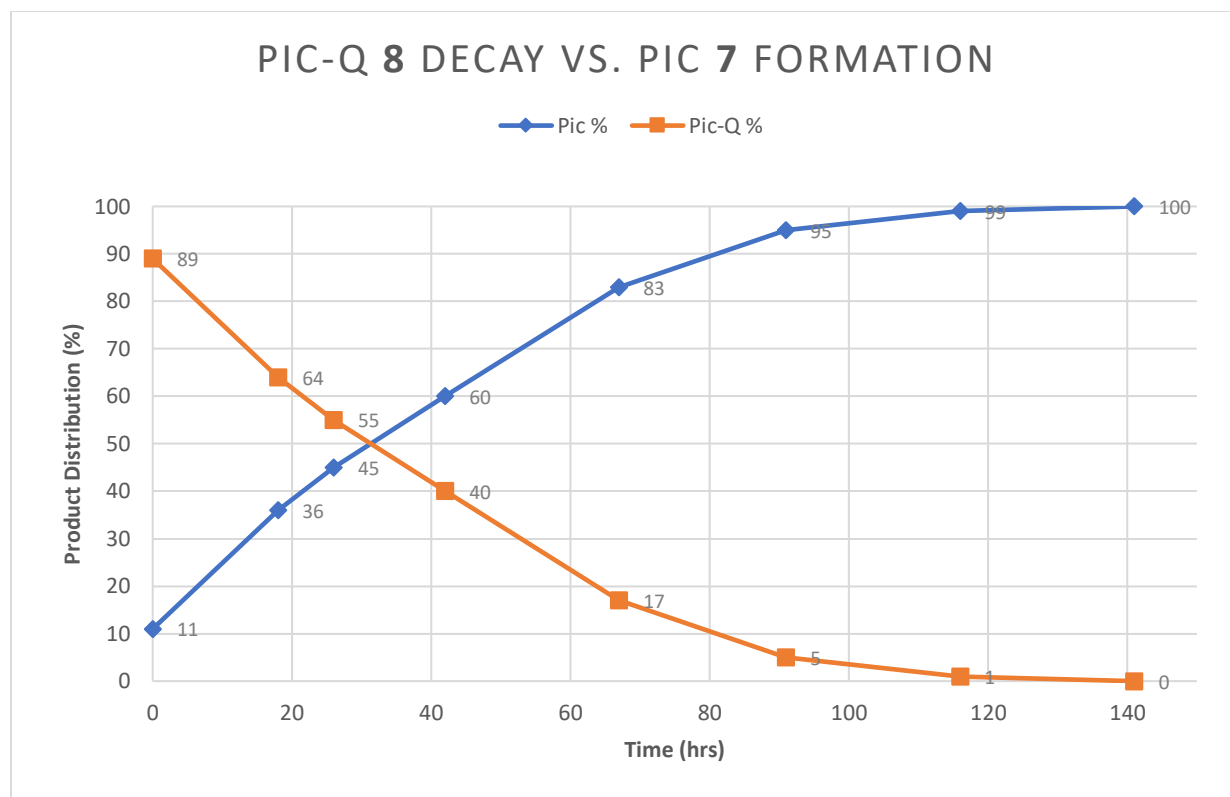
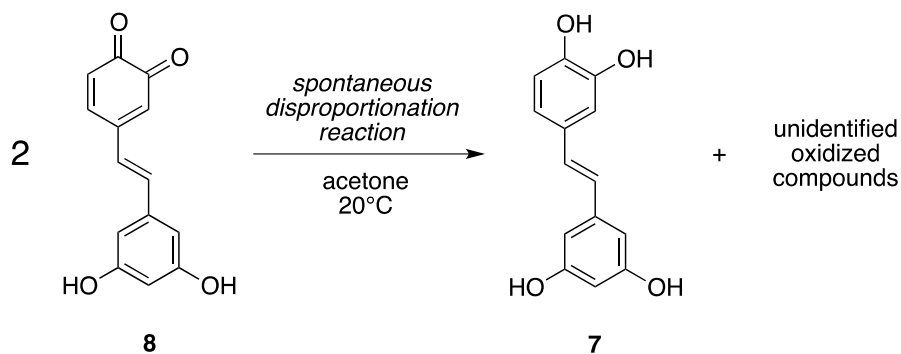


Figure 48. Spontaneous disproportionation of Pic-Q 8 converting to Pic 7 over time span of 141 hours.

experiment (Figure 39), piceatannol 7 concentration was minimal (10%), while at 141h lapsed time, conversion of *ortho*-quinone 8 to piceatannol 7 was complete (Figures 46, 48). In other words, “decay” of *ortho*-quinone 8 is not a decomposition *per se*, but spontaneous disproportionation requiring two molecules, with one of them undergoing reduction to piceatannol 7 and the other one forming oxidized product, or products (Scheme 3). Careful examination of the crude mixture by means of TLC and NMR indicated that more than one oxidized products are formed, and their structural characterization can only be completed upon scaling up the experiment, and isolation of polar compounds in a homogeneous form. The disproportionation reaction profile, and its kinetics, remained the same even in the absence of resveratrol 1, as an internal standard. Literature search revealed that there is only one case of

disproportionation reported for *ortho*-quinones.<sup>29</sup> Carnosic acid quinone converts to four hydroquinones – carnosic acid, 7-O-methylrosmanol, carnosol, and rosmanol – when heated in methanol at 60°C for 2h, or in acetonitrile/water at 37°C for 5h. Among *ortho*-hydroquinones, most relevant to our finding is carnosic acid which was used as substrate in iron(III)-mediated oxidation to the respective *ortho*-quinone.<sup>29</sup>



Scheme 3.

## 2.4. Enzymatic transformation of piceatannol to piceatannol-*ortho*-quinone

### *Screening of CYP1A1 with piceatannol 7.*

As indicated in the section on RV metabolism with CYP1A1, this enzyme is expressed primarily in the esophagus and has much low expression rates in the liver and stomach (for convenience, Figure 28 is repeated below). It is known to participate in a number of oxidative reactions, such as O-dealkylation of 7-ethoxyresorufin,<sup>23a</sup> allylic hydroxylation of polyunsaturated fatty acids (PUFA),<sup>19a</sup> O-demethylation in flavonoids,<sup>23b</sup> and epoxidation of polycyclic aromatic hydrocarbons (PAH), such as benzo(a)pyrene.<sup>23c</sup> With resveratrol **1** as a substrate, with CYP1A1 we observed a high degree of conversion to *ortho*-hydroxylated piceatannol **7** (Figure 29). It was of utmost importance to find out if the latter, when independently exposed to CYP1A1, could undergo a secondary oxidation to piceatannol-*ortho*-quinone **8** (Scheme 1). The availability of the authentic sample synthesized from piceatannol **7**

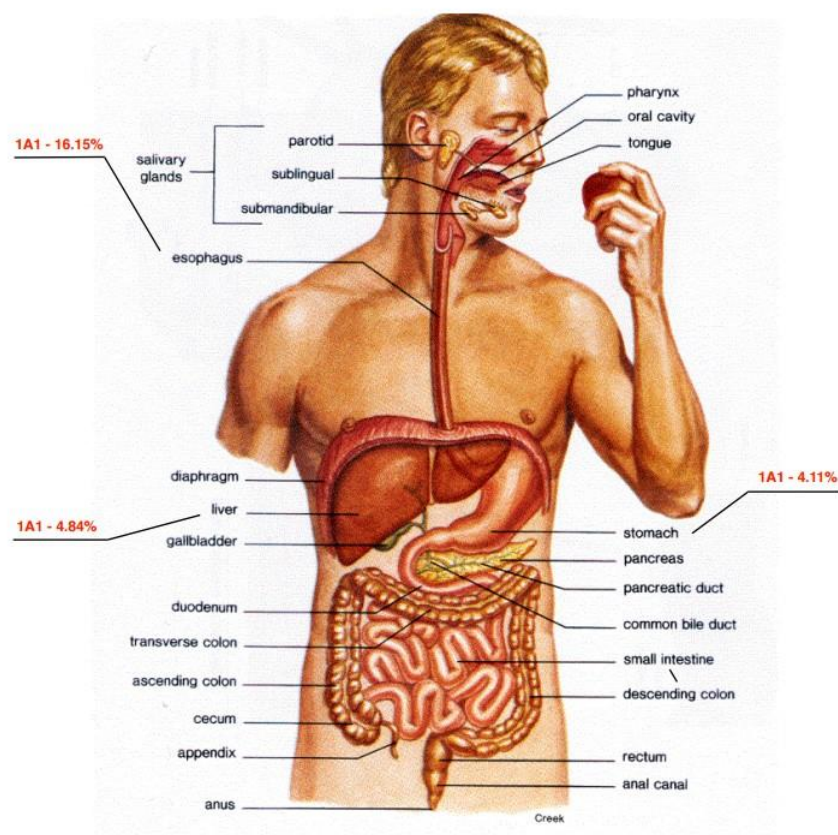


Figure 28. CYP1A1 mapping diagram of enzymatic expression in human organ systems.

by chemical means (subchapter 2.3) significantly facilitated screening and detection of target compound in the crude product. Enzymatic reaction with piceatannol **7** was carried out according to the standardized protocol, and the crude mixture, upon denaturing the CYP1A1 enzyme with acetonitrile, was analyzed by HPLC (Figure 49). Along with piceatannol **7** ( $t_r = 4.30\text{min}$ ), the formation *ortho*-quinone **8** was observed ( $t_r = 6.35\text{min}$ ) with the ratio of Pic : Pic-Q equal to 17 : 83 (Figure 49). The observed retention time ( $t_r = 6.35\text{min}$ ) is fully consistent with prior HPLC analyses of an authentic sample [Figures 39-47:  $t_r = 6.15\text{-}6.29\text{min}$ ;  $t_r$  (average) =  $6.23\text{min}$ ], allowing with a great deal of certainty to conclude that CYP1A1 enzyme successfully converted piceatannol **7** to *ortho*-quinone **8**. The said reaction has significant practical ramifications since we established that first, resveratrol **1**, being introduced as a supplement, or a red wine

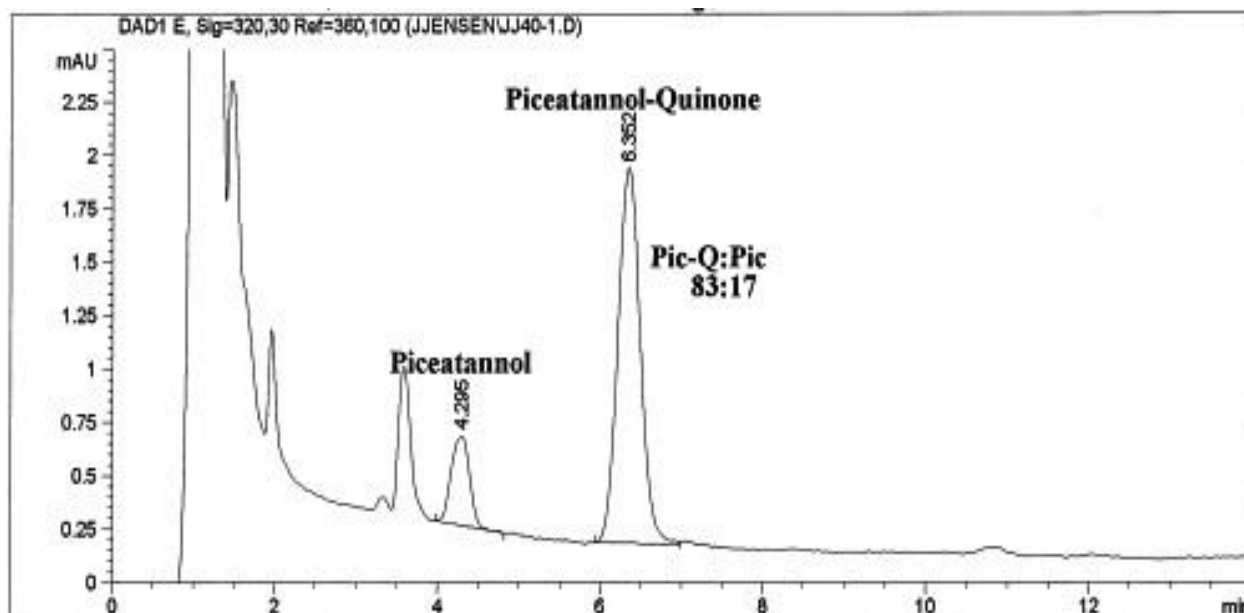


Figure 49. HPLC chromatogram of a crude mixture of piceatannol **7** + CYP1A1 enzymatic reaction (acetonitrile : deionized H<sub>2</sub>O, 1 : 1, v/v; column: Zorbax SB-C18 reversed phase; dimension: 4.6 x 150mm, 5-micron; flow rate: 1mL/min; injection volume = 30μL; run time = 14min; piceatannol-*ortho*-quinone **8** *t<sub>r</sub>* = 6.35min, piceatannol **7** *t<sub>r</sub>* = 4.30min).

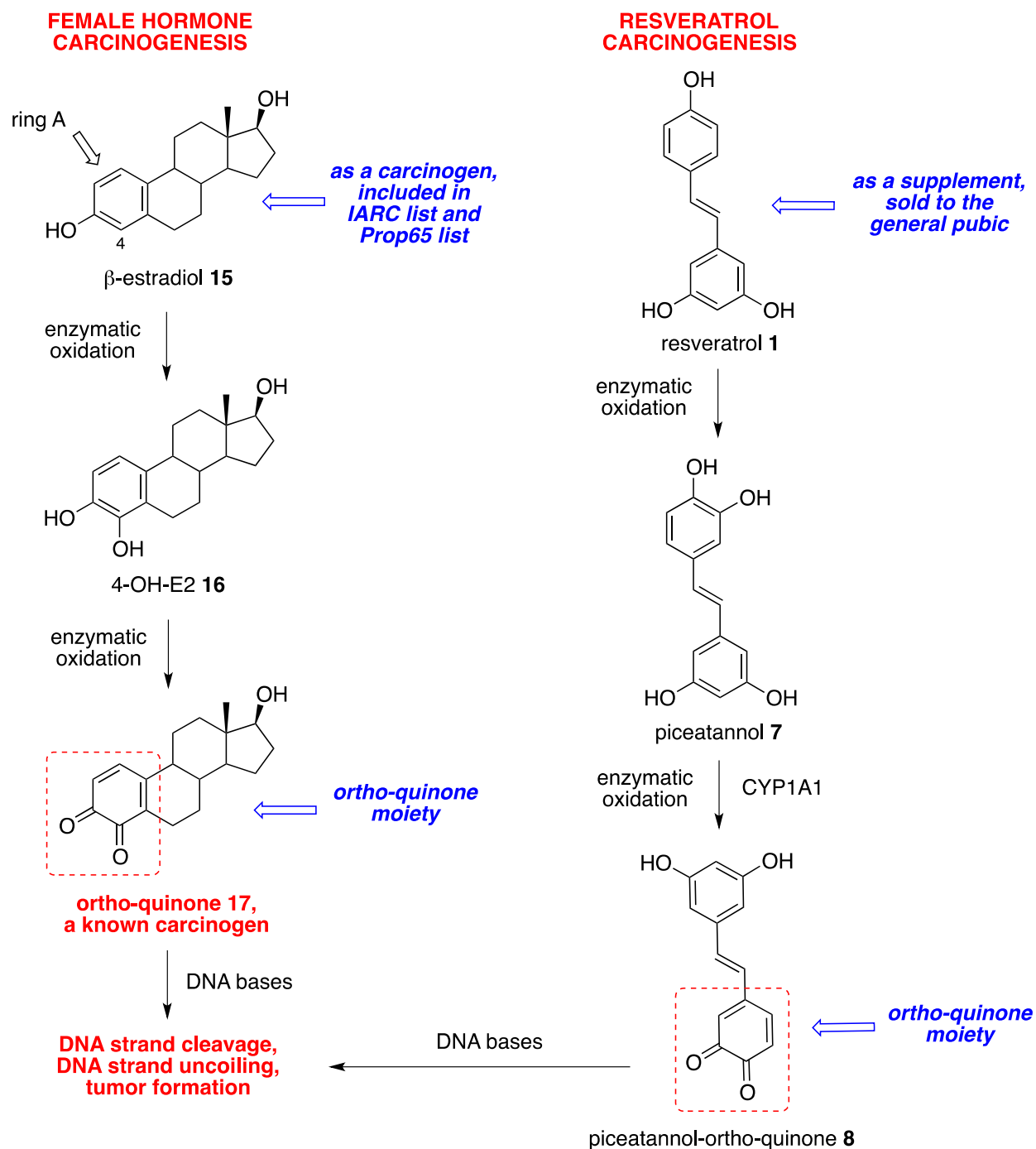
component, into the human body can be oxidized to piceatannol **7** by a multitude of enzymes (Table 1), and second, the latter can undergo a “deeper” oxidation to *ortho*-quinone **8**, a representative of the class of known carcinogens.<sup>29</sup> Although only CYP1A1 enzyme located in esophagus, liver, and stomach, was tested so far, it is conceivable that some other CYP enzymes (Table 1) will also be able to induce the same conversion, thus generating the carcinogenic compound all over the human body, at the sites where CYP enzymes are known to be expressed (Figure 8).

## 2.5. Conclusion

In the course of this study we established that cytochrome P450 enzymes are capable of converting resveratrol to its *ortho*-hydroxylated derivative, piceatannol, and piceatannol to its carcinogenic derivative, piceatannol *ortho*-quinone. Among 12 commercially available enzyme



preparations, seven of them *ortho*-hydroxylated resveratrol with high conversion rates: (CYP2C18, 95%; CYP3A4, 96%; CYP1A1, 97%; CYP2A6, 97%; CYP2C9, 97%; CYP2C8; 98%; CYP4F12, 98%). Enzyme CYP1A1 was able to convert piceatannol to its oxidized form, piceatannol *ortho*-quinone that belongs to the class of organic carcinogens, *ortho*-quinones. Feasibility of piceatannol oxidation to the respective *ortho*-quinone is corroborated by its chemical oxidation with manganese dioxide and full structural characterization by totality of analytical methods. Stability studies on piceatannol *ortho*-quinone indicated that while its decomposition is rapid at room temperature in a solid form, or in contact with chromatographic sorbents, in a solution, at ambient temperatures, this potential carcinogen survives for 141 hours, or almost 6 days. These experimental data suggest that consumption of resveratrol from dietary sources (wine, peanuts, berries), or through RV supplementation, represents a clear danger to public health. Given the abundance of cytochrome P450 enzymes in the human body, and their demonstrated ability to effect the resveratrol-*to*-piceatannol-*to*-piceatannol-*ortho*-quinone chemical sequence, it is conceivable that the same enzymatic transformations can also occur inside the human body, in multiple locations (Scheme 4). *Ortho*-quinones thus formed can potentially survive *in vivo* for days, and trigger tumor formation due to a well-known ability of *ortho*-quinones to react with DNA bases and render them biologically dysfunctional. The mechanism of carcinogenesis suggested for resveratrol is analogous to that established for  $\beta$ -estradiol **15** (Scheme 4): CYP-induced *ortho*-hydroxylation in ring A produces 4-hydroxy derivative **16**, which in turn is enzymatically oxidized to *ortho*-quinone **17**. The latter is demonstrated to be carcinogenic to humans, was introduced into the list of carcinogens compiled by the International Agency for Research on Cancer (IARC), and represents the main reason why the hormone-replacement therapy (HRT) was strongly discredited, and re-evaluated for treatment



Scheme 4.

of post-menopausal symptoms. This newly acquired knowledge on resveratrol enzymatics should be made available to the general public who is exposed to unrelenting advertisements on

resveratrol and its supplements (mega-dose range, 1.0-2.5 grams per pill). Longitudinal, randomized studies are needed to further investigate possible detrimental effects of plant-based isolates upon human ingestion. In contrast to resveratrol supplements, its dietary sources may exhibit a far less deleterious impact due to having a much lower potency. In the long run, the uncontrollable intake of resveratrol may contribute to proliferation of various cancers, potentially becoming the next public health disaster. The relevance of the research presented herein solicits broad dissemination to assist individuals, families, and communities about the dangers of uncharted resveratrol use. Medical practitioners (doctors and nutritionists) are urged to utilize their healthcare platforms to educate patient populations about the inevitable consequences that resveratrol supplementation may present. Otherwise, the societal health impact could be *on par* with asbestos, diethylstilbestrol (DES), thalidomide, bis-phenol A (BPA), or hexavalent chromium exposure.

### III. EXPERIMENTAL

All manipulations of air-sensitive materials were carried out in flame-dried Schlenk-type glassware on a dual-manifold Schlenk line interfaced to a vacuum line. Argon and nitrogen (Airgas, ultrahigh purity) were dried by passing through a Drierite tube (Hammond). All reagents were purchased from TCI, Sigma-Aldrich, and Acros and used as received. NMR solvents were supplied by Cambridge Isotope Laboratories.  $^1\text{H}$  and  $^{13}\text{C}$  NMR spectra were recorded on Bruker DRX-400 ( $^1\text{H}$ , 400MHz;  $^{13}\text{C}$ , 100MHz) spectrometer. Chemical shifts were referenced to internal solvent resonances and are reported relative to tetramethylsilane. Spin-spin coupling constants ( $J$ ) are given in hertz. Analytical and preparative TLC analysis (PTLC) were conducted on Silica gel 60 F<sub>254</sub> (EM Science; aluminum sheets) and Silica Gel 60 PF<sub>254</sub> (EM Science; w/gypsum; 20 x 20 cm), respectively. Eluents are ether (E), petroleum ether (PE), and pentane (P). Mass spectra were run at the Regional Center on Mass-Spectroscopy, UC Riverside, Riverside, CA (FAB, ZAB-SE; CI-NH<sub>3</sub>, 7070EHF; Micromass; TOF Agilent 6210 LCTOF instrument with a Multimode source).

## Preparation for Enzymatic Reactions

**DI water** was generated on Millipore Super-Q Water System and stored in designated, oven-sterile, amber bottle (replaced every 2 weeks).

**Phosphate buffer** (0.5M potassium phosphate, pH 7.4, 500mL, #451201) was purchased from Corning Life Sciences / Discovery Labware Inc. and replaced every two years.

**NADPH regenerating system (Solution A, 5mL; cat # 451220)** was purchased from Corning Life Sciences / Discovery Labware Inc. and stored at -82°C. *Handling:* before each enzymatic reaction, solution A was placed into wet ice bucket for 1h 30min. and then into water bath (20°C) for 5min. The container was swirled gently by hand and used immediately by removing the needed volume with Hamilton syringe and transferring it into the reaction vial.

**NADPH regenerating system (Solution B, 1mL; cat # 451200)** was purchased from Corning Life Sciences / Discovery Labware Inc. and stored at -82°C. *Handling:* before each enzymatic reaction, solution B was placed into wet ice bucket for 1h 30min. and then into water bath (20°C) for 1min. The container was swirled gently by hand and used immediately by removing the needed volume with Hamilton syringe and transferring it into the reaction vial.

**Human Enzyme CYP1B1 + Reductase (0.5nmol; cat # 456220)** was purchased from Corning Life Sciences / Discovery Labware Inc. and stored at -82°C. *Handling:* the enzyme vial was placed into wet ice bucket for 1h, then into water bath (20°C) for 1min, tapped with finger 10 times, and used immediately by removing the needed volume with Hamilton syringe and transferring it into pre-warmed (37°C) reaction vials containing all enzymatic reaction components (substrate, solutions A/B, phosphate buffer, and DI water). Total thaw times may vary slightly among enzymes due to varying volumes and composition.

**Preparation of resveratrol stock solution in DMSO (1mM).** Resveratrol (4.6mg, 0.02mmol; TCI cat # R0071; stored at 0°C) was added into a 25mL round-bottom flask (upon addition, pumped & filled, 3x) and dissolved in DMSO (20mL; Sigma-Aldrich; cat #276855; DMSO bottle was pumped & filled three times by using an air-free Schlenk-line hose which was evacuated under reduced pressure prior to the transfer of the solvent) forming a colorless solution which was stored at room temperature (20°C/septum/parafilm).

**Preparation of piceatannol stock solution in DMSO (1mM).** Piceatannol (2.3mg, 0.01mmol; TCI cat # P1928; stored at 0°C) was added into a 25mL round-bottom flask (upon addition, pumped & filled, 3x) and dissolved in DMSO (10mL; Sigma-Aldrich; cat #276855; DMSO bottle was pumped & filled three times by using an air-free Schlenk-line hose which was evacuated under reduced pressure prior to the transfer of the solvent) forming a colorless solution which was stored in room temperature (20°C/septum/parafilm). The integrity (decomposition rate) of resveratrol and piceatannol were checked visually (colorization from colorless to clear yellow solution) and by HPLC analysis.

**General procedure for enzymatic reactions of resveratrol 1 with Cytochrome P-450 human enzymes (*Protocol A*).** DI water (710μL), phosphate buffer (0.5M; 200μL), NADPH solution A (50μL), NADPH solution B (10μL), and stock solution of resveratrol **1** (10μL; 1mM DMSO) were consecutively added into a 2.0-mL clear, homo-polymer, graduated microtube “reaction vial” with hinged lid (Axygen Scientific; cat #311-10-051). The reaction vial was capped, inverted twice, locked into a floating microtube rack, and submerged two-thirds deep into a pre-heated oil bath (37°C) for 5 min. The rack was raised, the reaction vial was wiped with a Kim wipe, transferred to a stationary stand, and enzyme solution (20μL) was added dropwise

using a Hamilton syringe. The reaction vial was inverted twice, placed into a floating microtube rack, immersed into an oil bath (37°C), and kept in dark (foil-tented) for 60 min. The rack was raised, the reaction vial was wiped with a Kim wipe, and brought to room temperature (~5min). The mixture was diluted with acetonitrile (1mL; UN1648, HPLC grade, Acros) and homogenized by drawing up into an oven-sterile Pasteur pipette and releasing it with moderate pressure into the reaction vial (x10). The reaction vial was kept on wet ice for 30 min fully submerged (in dark), centrifuged (Galaxy Mini Centrifuge; model C1413; 6,000 rpm) for 20 min (in dark), and the supernatant (~2mL) was transferred with a sterile Pasteur pipette into a foil-covered 5-dram vial. All enzymatic experiments were conducted in triplicates and the total volume of combined supernatants was equal to ~6mL. The crude mixture was filtered into a 9-mL glass storage vial with screw cap by using a 5-mL glass syringe (Popper and Sons) equipped with a regenerated cellulose syringe filter (0.45µm, 15mm; Agilent Technologies, cat #5190-5109). The filtered crude mixture was homogenized by drawing up into an oven-sterile Pasteur pipette and releasing it with moderate pressure into the reaction vial (x10). A fraction (~150µL) was transferred with a sterile Pasteur pipette to an HPLC vial containing an insert with polymer feet (Agilent Technologies, cat #5783-2088). The remaining crude mixture was covered with foil, insulated with parafilm, and stored at -82°C.

The crude mixture was analyzed by high performance liquid chromatography (HPLC) on the reverse-phase, stable bond column (Zorbax SB-C18; 4.6 x 150mm, 5-micron, high purity silica, 80Å) using acetonitrile and deionized water (1 : 3, v/v) as a mobile phase (flow rate - 1mL/min; injection volume 30µL). Wavelength absorbance parameters were set to  $\lambda = 320\text{nm}$  and  $\lambda_{\text{ref}} = 360\text{nm}$  and 100nm. The Hewlett Packard 1100 series HPLC chromatograph equipped with degasser (G1322A), quaternary pump (G1311A), auto-sampler (G1313A, housing 100 sample

vials), and diode array (wavelength) detector (G1315A) configured with *HP ChemStation* software for LC and LC/MS systems was used to analyze crude enzymatic products. Reaction metabolites were detected at high sensitivities, quantified by manual or auto- integration, and qualitatively identified with known compounds based on their retention times.

**Metabolite concentration technique (*Protocol B*).** The crude mixture (1mL aliquot) was evaporated to dryness under reduced pressure (Schlenk line, 20°C, 14h, in dark) and extracted with a mixture of acetonitrile – DI water (1 : 3, v/v; 300µL) by manually stirring with an inverted melting point capillary tube (1min). The solution was allowed to rest for 5min at 20°C and then transferred with a micropipette (Eppendorf Reference, 200µL) with a preset volume (150µL) to a foil-covered, HPLC vial containing an insert with polymer feet. *This protocol allows for dissolution of minute quantities of the metabolites, while leaving most of the resveratrol 1 undissolved, thus increasing the concentration of enzymatic products and facilitating their detection and identification by HPLC.*

**“Spiking” technique (*Protocol C*).** Prepared samples that underwent enzymatic transformations with respective substrates, resveratrol **1** or piceatannol **7**, were spiked to confirm that the predicted metabolites were formed. Successful spiking of a sample allowed for a low concentration, prominent peak signal strength and accurate retention times with respect to optimized conditions of authentic samples. The technique requires the use of a Pasteur pipette with a hand bulb to deliver a fresh, authentic sample, drop-wise into an HPLC inset of an existing sample in order to increase the peak intensity of the end product in question.



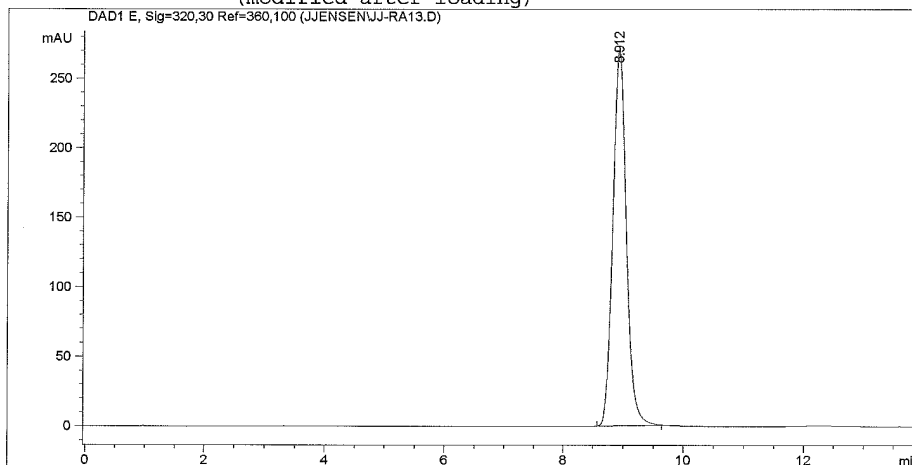
## HPLC analysis of an authentic sample of resveratrol 1.

Commercially available resveratrol 1 (4.6mg) was dissolved in the mixture of acetonitrile :  
deionized H<sub>2</sub>O, 1 : 3 (v/v, 20mL).

Data File C:\HPCHEM\1\DATA\JJENSEN\JJ-RA13.D Sample Name: JJ-RA13

5.12.16 JJ-RA13 (RV Authentic sample 1:3), Isocratic si  
ngle bottle delivery 1:3 AcN:Di-H<sub>2</sub>O mobile phase, 1.0 m  
L/min. flowrate  
Sample Name:RV in 1:3 5.12.16

```
=====
Injection Date   : 5/12/2016 6:01:34 PM
Sample Name      : JJ-RA13                      Vial :    1
Acq. Operator    : JJ                          Inj Volume : 5 ul
Method           : C:\HPCHEM\1\METHODS\SAMCAP1.M
Last changed     : 5/12/2016 5:56:37 PM by JJ
                  (modified after loading)
```



### Area Percent Report

```
=====
Sorted By      :      Signal
Multiplier     :      1.0000
Dilution       :      1.0000
Sample Amount  :      1.00000 [ng/ul]   (not used in calc.)
```

Signal 1: DAD1 E, Sig=320,30 Ref=360,100

Peak #	RetTime [min]	Type	Width [min]	Area [mAU*s]	Height [mAU]	Area %
1	8.912	BB	0.2388	4233.91992	270.15555	100.0000

Totals : 4233.91992 270.15555

Results obtained with enhanced integrator!

Instrument 1 5/12/2016 6:15:43 PM JJ

Page 1 of 1

## HPLC analysis of an authentic sample of resveratrol 1.

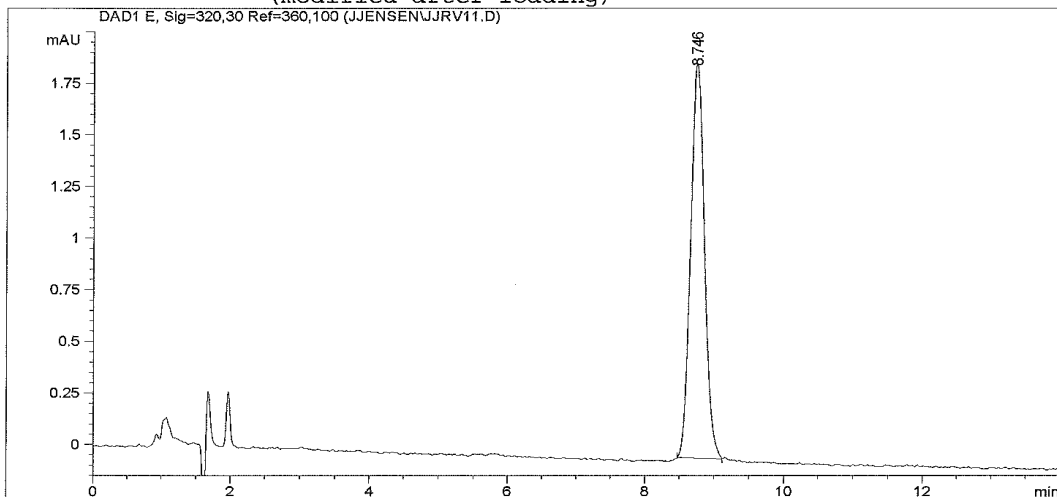
Commercially available resveratrol 1 (unspecified amount) was added to 6mL acetonitrile : deionized H<sub>2</sub>O, 1 : 1. This ratio mimicked the solvent composition of the enzymatic reaction mixture ( $t_r = 8.75\text{min}$ ).

Data File C:\HPCHEM\1\DATA\JJENSEN\JJRV11.D

Sample Name: JJRV11

3.4.16, JJRV11, Isocratic-single bottle 1:3 AcN:Di-H<sub>2</sub>O  
mobile phase, 1.0 mL/min.  
Sample name:RV in 1:1 AcN:Di-H<sub>2</sub>O 3.4.16

```
=====
Injection Date   : 3/4/2016 2:07:18 PM
Sample Name      : JJRV11                      Vial :    1
Acq. Operator    : JJ                          Inj Volume : 5 ul
Acq. Method      : C:\HPCHEM\1\METHODS\SAMCAP1.M
Last changed     : 3/4/2016 2:06:24 PM by JJ
                  (modified after loading)
Analysis Method  : C:\HPCHEM\1\METHODS\SAMCAP1.M
Last changed     : 5/16/2016 5:06:45 PM by JJ
                  (modified after loading)
=====
```



### Area Percent Report

```
=====
Sorted By      :      Signal
Multiplier     :      1.0000
Dilution       :      1.0000
Sample Amount  :      1.00000 [ng/ul]   (not used in calc.)
=====
```

Signal 1: DAD1 E, Sig=320,30 Ref=360,100

Peak #	RetTime [min]	Type	Width [min]	Area [mAU*s]	Height [mAU]	Area %
1	8.746	PB	0.2175	26.48330	1.91321	100.0000

Instrument 1 5/16/2016 5:06:53 PM JJ

Page 1 of 2

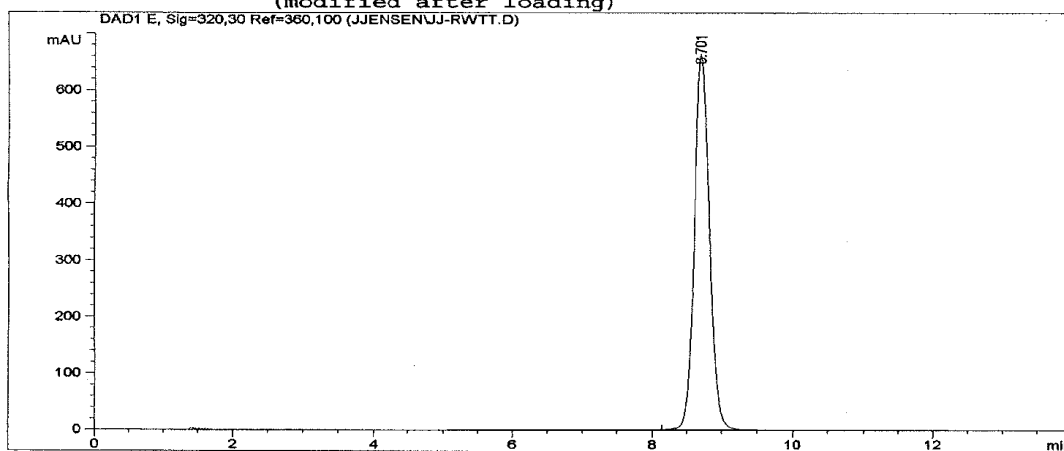
## HPLC analysis of an authentic sample of resveratrol 1.

Commercially available resveratrol 1 (4.6mg) was added to 10mL DMSO to prepare the stock solution used in enzymatic reactions ( $t_r = 8.70\text{min}$ ).

Data File C:\HPCHEM\1\DATA\JJENSEN\JJ-RWTT.D Sample Name: JJ-RWTT

2.26.16, RWTT (RV weekly test), Isocratic-single bottle  
1:3 AcN:Di-H2O mobile phase, 1.0 mL/min.  
Sample name:RV/DMSO Stock Prep 12.28.15

```
=====
Injection Date   : 2/26/2016 11:57:43 AM
Sample Name      : JJ-RWTT
Acq. Operator    : JJ
Vial             : 11
Inj Volume       : 10 ul
Acq. Method      : C:\HPCHEM\1\METHODS\SAMCAP1.M
Last changed     : 2/26/2016 11:56:46 AM by JJ
                  (modified after loading)
Analysis Method  : C:\HPCHEM\1\METHODS\SAMCAP1.M
Last changed     : 2/26/2016 12:23:45 PM by JJ
                  (modified after loading)
=====
```



### Area Percent Report

```
=====
Sorted By       : Signal
Multiplier      : 1.0000
Dilution        : 1.0000
Sample Amount   : 1.00000 [ng/ul] (not used in calc.)
=====
```

Signal 1: DAD1 E, Sig=320,30 Ref=360,100

Peak #	RetTime [min]	Type	Width [min]	Area [mAU*s]	Height [mAU]	Area %
1	8.701	BB	0.2355	1.00985e4	663.90521	100.0000

Instrument 1 2/26/2016 12:23:54 PM JJ

Page 1 of 2

## HPLC analysis of an authentic sample of piceatannol 7.

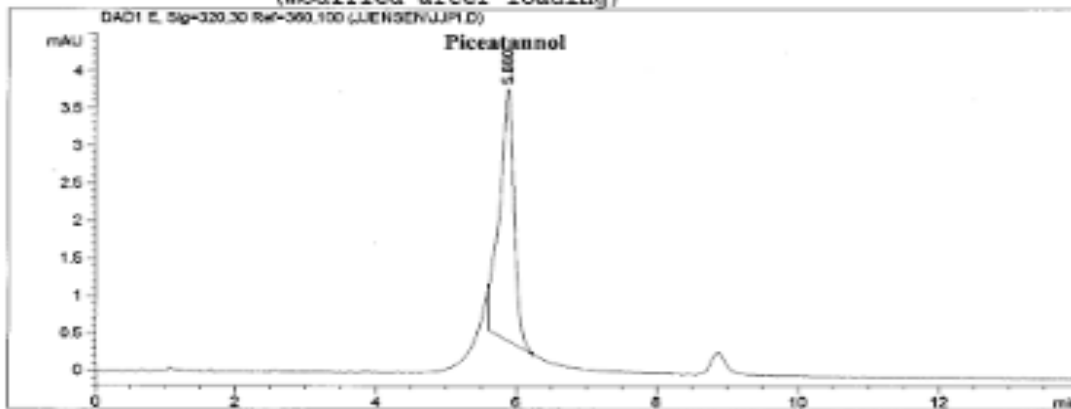
Commercially available piceatannol 7 (unspecified amount) was added to acetonitrile : deionized H<sub>2</sub>O, 1 : 3 (3mL). This ratio mimicked the solvent composition of the enzymatic reaction mixture ( $t_r = 5.88\text{min}$ ).

Data File C:\HPCHEM\1\DATA\JJPI\JJPI.D Sample Name: JJPI

3.3.16, JJPI, Pic crystal dissolved in Isocratic 1:3, Isocratic-single bottle 1:3 AcN:DI-H<sub>2</sub>O mobile phase, 1.0 mL/min.

Sample name: Pic in Isocratic 1:3 3.3.16

```
=====
Injection Date   : 3/3/2016 3:57:01 PM
Sample Name      : JJPI
Acq. Operator    : JJ
Vial             : 2
Inj Volume       : 5 ul
Acq. Method      : C:\HPCHEM\1\METHODS\SANCAPI1.M
Last changed     : 3/3/2016 3:56:26 PM by JJ
                  (modified after loading)
Analysis Method  : C:\HPCHEM\1\METHODS\SANCAPI1.M
Last changed     : 6/3/2016 3:20:48 PM by MP
                  (modified after loading)
=====
```



### Area Percent Report

```
=====
Sorted By       : Signal
Multiplier      : 1.0000
Dilution        : 1.0000
Sample Amount   : 1.00000 [ng/ul] (not used in calc.)
=====
```

Signal 1: DAD1 E, Sig=320.30 Ref=360.100

Peak #	RetTime [min]	Type	Width [min]	Area [mAU*s]	Height [mAU]	Area %
1	5.880	BB	0.2117	49.52981	3.36550	100.0000

Totals : 49.52981 3.36550

Results obtained with enhanced integrator!

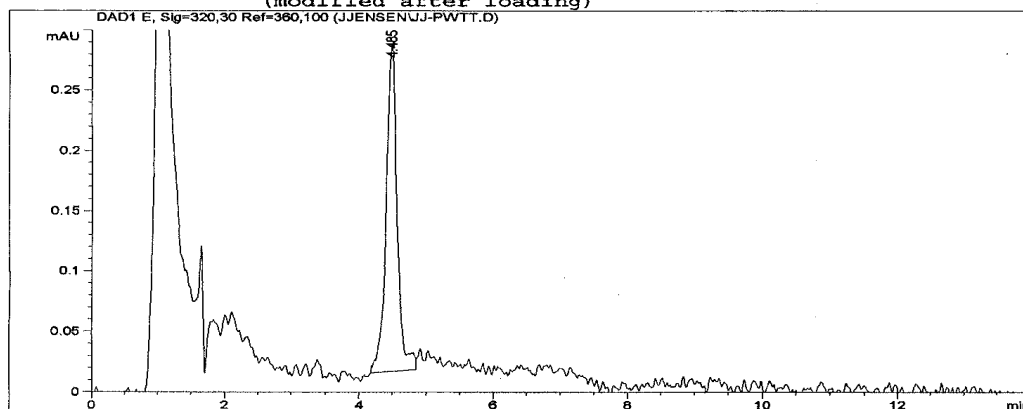
## HPLC analysis of an authentic sample of piceatannol 7.

Commercially available piceatannol **7** (unspecified amount) was added to 10mL acetonitrile : deionized H<sub>2</sub>O, 1 : 3 (v/v) which was analogous to the HPLC mobile phase.

ata File C:\HPCHEM\1\DATA\JJENSEN\JJ-PWTT.D Sample Name: JJ-PWTT  
4.11.16 JJ-PWTT, Isocratic single bottle delivery 1:3 A  
cN:Di-H2O mobile phase, 1.0 mL/min. flowrate  
Sample name: Pic in 1:3 AcN:di-H2O 3.11.16

=====

Injection Date	: 4/11/2016 2:30:00 PM	Vial	: 6
Sample Name	: JJ-PWTT	Inj Volume	: 2 ul
Acq. Operator	: JJ		
Acq. Method	: C:\HPCHEM\1\METHODS\SAMCAP1.M		
Last changed	: 4/11/2016 2:28:32 PM by JJ		
	(modified after loading)		
Analysis Method	: C:\HPCHEM\1\METHODS\SAMCAP1.M		
Last changed	: 4/11/2016 2:45:45 PM by JJ		
	(modified after loading)		



### Area Percent Report

=====

Sorted By	:	Signal
Multiplier	:	1.0000
Dilution	:	1.0000
Sample Amount	:	1.00000 [ng/ul] (not used in calc.)

Signal 1: DAD1 E, Sig=320,30 Ref=360,100

Peak #	RetTime [min]	Type	Width [min]	Area [mAU*s]	Height [mAU]	Area %
1	4.485	BV	0.1665	3.07860	2.71030e-1	100.0000

Totals : 3.07860 2.71030e-1

Instrument 1 4/11/2016 2:45:48 PM JJ

Page 1 of 2

## Authentic equimolar mixture of resveratrol 1 and piceatannol 7.

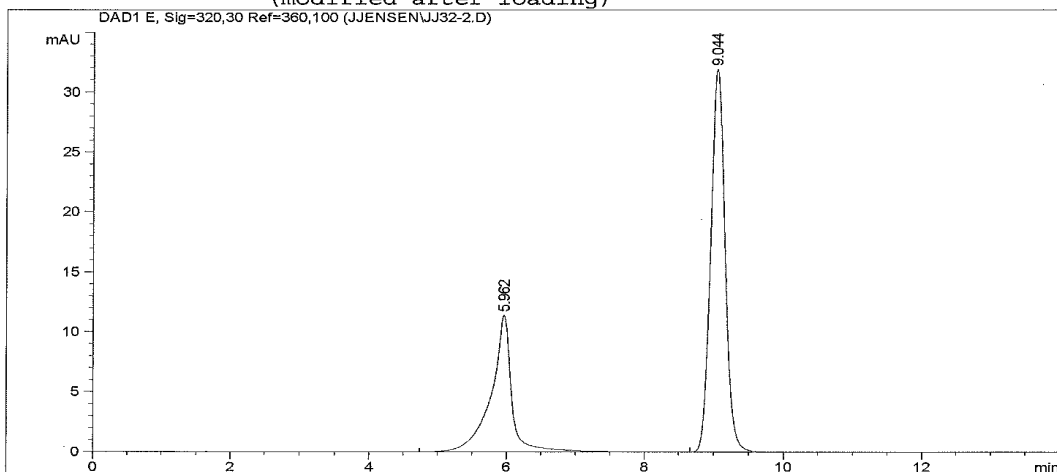
Commercially available piceatannol **7** (12.2mg) and resveratrol **1** (11.4mg) was added to 6mL acetonitrile : deionized H<sub>2</sub>O (1 : 1, v/v). This ratio mimicked the solvent composition of the enzymatic reaction mixture. Serial dilution (x10) of authentic, equimolar mixture of piceatannol and resveratrol.

Data File C:\HPCHEM\1\DATA\JJENSEN\JJ32-2.D

Sample Name: JJ32-2

3.18.16 JJ32-2, Pic/RV dissolved in 1:1 AcN:di-H2O, the  
n diluted 10X. (1mL original authentic Pic/RV mixture i  
n 1:1 plus 9 mL di-H2O), Isocratic-single bottle 1:3 Ac  
N:Di-H2O mobile phase, 1.0 mL/min. flowrate  
Sample name:JJ32 RV/Pic 1:1 dil 10X 3.18.16

```
=====
Injection Date   : 3/18/2016 4:05:03 PM
Sample Name      : JJ32-2
Acq. Operator    : JJ
Vial             : 1
Inj Volume       : 1 ul
Acq. Method      : C:\HPCHEM\1\METHODS\SAMCAP1.M
Last changed     : 3/18/2016 3:58:38 PM by JJ
                  (modified after loading)
Analysis Method  : C:\HPCHEM\1\METHODS\SAMCAP1.M
Last changed     : 5/15/2016 7:39:03 PM by JJ
                  (modified after loading)
=====
```



Area Percent Report

```
=====
Sorted By      : Signal
Multiplier     : 1.0000
Dilution       : 1.0000
Sample Amount  : 1.00000 [ng/ul] (not used in calc.)
=====
```

Instrument 1 5/15/2016 7:39:20 PM JJ

Page 1 of 2

Data File C:\HPCHEM\1\DATA\JJENSEN\JJ32-2.D

Sample Name: JJ32-2

Signal 1: DAD1 E, Sig=320,30 Ref=360,100

Peak #	RetTime [min]	Type	Width [min]	Area [mAU*s]	Height [mAU]	Area %
1	5.962	BB	0.2934	249.12219	11.47080	34.8410
2	9.044	BB	0.2219	465.90466	31.98529	65.1590

Totals : 715.02686 43.45609

Results obtained with enhanced integrator!

\*\*\* End of Report \*\*\*

## Authentic equimolar mixture of resveratrol 1 and piceatannol 7.

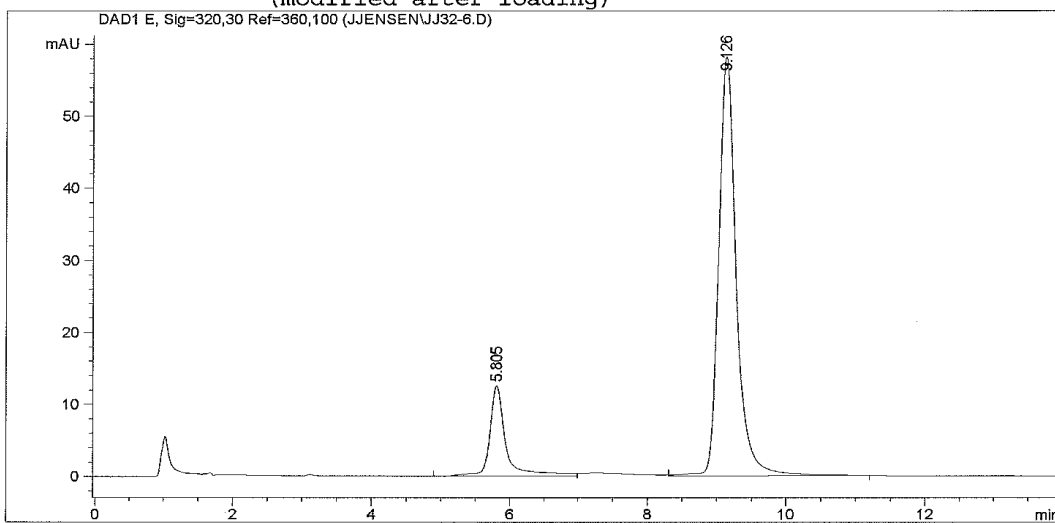
Authentic, diluted, equimolar mixture of piceatannol 7 and resveratrol 1 re-injected for reproducibility.

Data File C:\HPCHEM\1\DATA\JJENSEN\JJ32-6.D

Sample Name: JJ32-

5.6.16 JJ32-6, Isocratic single bottle delivery 1:3 AcN  
:Di-H2O mobile phase, 1.0 mL/min. flowrate  
Sample Name:JJ32 RV:Pic 1:1 5.6.16

```
=====
Injection Date   : 5/6/2016 9:32:15 PM
Sample Name      : JJ32-
Acq. Operator    : JJ
Vial             : 1
Inj Volume       : 3 ul
Acq. Method      : C:\HPCHEM\1\METHODS\SAMCAP1.M
Last changed     : 5/6/2016 9:28:26 PM by JJ
                  (modified after loading)
Analysis Method  : C:\HPCHEM\1\METHODS\SAMCAP1.M
Last changed     : 5/15/2016 7:33:28 PM by JJ
                  (modified after loading)
=====
```



### Area Percent Report

```
=====
Sorted By       : Signal
Multiplier      : 1.0000
Dilution        : 1.0000
Sample Amount   : 1.00000 [ng/ul] (not used in calc.)
=====
```

Signal 1: DAD1 E, Sig=320,30 Ref=360,100

Peak #	RetTime [min]	Type	Width [min]	Area [mAU*s]	Height [mAU]	Area %
1	5.805	PV	0.2392	205.21584	12.52197	16.6485
2	9.126	VB	0.2660	1027.41907	58.19283	83.3515

Totals : 1232.63490 70.71480

Instrument 1 5/15/2016 7:34:19 PM JJ

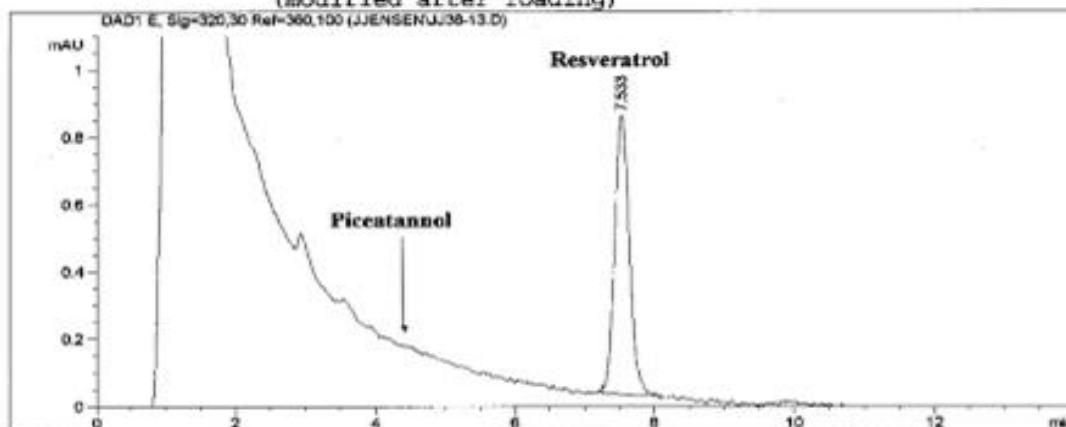
Page 1 of 2

**Interaction of resveratrol 1 with CYP2C19 enzyme.** According to protocol A, interaction of resveratrol 1 (10 $\mu$ L) and CYP2C19 enzyme (20 $\mu$ L) produced the crude mixture which, according to HPLC, contained no piceatannol 7 (0%; anticipated  $t_r$  = 4.57min; resveratrol 1,  $t_r$  = 7.53min).

Data File C:\HPCHEM\1\DATA\JJENSEN\JJ38-13.D Sample Name: JJ38-13

05.26.16 JJ38-13,Decompos. ck, Isocratic single bottle  
delivery 1:3 AcN:Di-H2O mobile phase, 1.0 mL/min. flow  
rate  
Sample Name:JJ-38 RV/2C19 NS 5.26.16

```
=====
Injection Date   : 5/26/2016 7:36:39 PM
Sample Name      : JJ38-13
Acq. Operator    : JJ
Vial             : 1
Inj Volume       : 30 ul
Acq. Method      : C:\HPCHEM\1\METHODS\SAMCAP1.M
Last changed     : 5/26/2016 7:17:37 PM by JJ
                  (modified after loading)
Analysis Method  : C:\HPCHEM\1\METHODS\SAMCAP1.M
Last changed     : 5/26/2016 9:22:47 PM by MP
                  (modified after loading)
=====
```



#### Area Percent Report

```
=====
Sorted By       : Signal
Multiplier      : 1.0000
Dilution        : 1.0000
Sample Amount    : 1.00000 [ng/ul] (not used in calc.)
=====
```

Signal 1: DAD1 E, Sig=320,30 Ref=360,100

Peak #	RetTime [min]	Type	Width [min]	Area [mAU*s]	Height [mAU]	Area %
1	7.533	BB	0.2263	12.25659	8.29990e-1	100.0000

Totals : 12.25659 8.29990e-1

Results obtained with enhanced integrator:

\*\*\* End of Report \*\*\*



**Interaction of resveratrol 1 with CYP2C19 enzyme:** crude mixture spiked with 2 drops of piceatannol 7 ( $t_r = 4.57\text{min}$ ; ; resveratrol 1,  $t_r = 7.26\text{min}$ ).

Data File C:\HPCHEM\1\DATA\JJENSEN\JJ38-14.D

Sample Name: JJ38-14

05.26.16 JJ38-14, Pic-spiked (2drops), Isocratic single  
bottle delivery 1:3 AcN:Di-H2O mobile phase, 1.0 mL/min  
n. flowrate  
Sample Name:JJ-38 RV/2C19 NS 5.26.16

Injection Date : 5/26/2016 8:19:07 PM

Sample Name : JJ38-14

Vial : 1

Acq. Operator : JJ

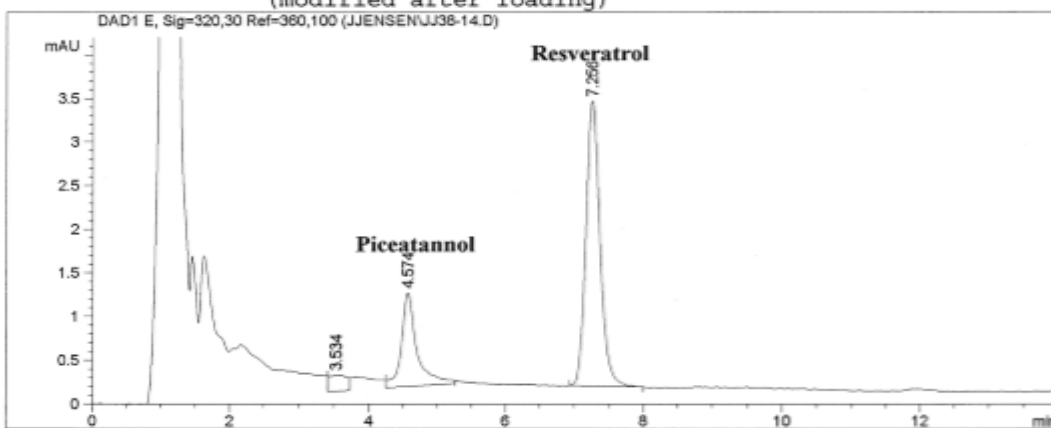
Inj Volume : 30 ul

Acq. Method : C:\HPCHEM\1\METHODS\SAMCAP1.M

Last changed : 5/26/2016 7:17:37 PM by JJ  
(modified after loading)

Analysis Method : C:\HPCHEM\1\METHODS\SAMCAP1.M

Last changed : 5/26/2016 8:42:54 PM by MP  
(modified after loading)



#### Area Percent Report

Sorted By : Signal  
Multiplier : 1.0000  
Dilution : 1.0000  
Sample Amount : 1.00000 [ng/ul] (not used in calc.)

Signal 1: DAD1 E, Sig=320,30 Ref=360,100

Peak #	RetTime [min]	Type	Width [min]	Area [mAU*s]	Height [mAU]	Area %
1	3.534	BV	0.2150	3.27548	1.88201e-1	4.9174
2	4.574	BB	0.2256	17.10897	1.07539	25.6855
3	7.256	BB	0.2151	46.22495	3.26732	69.3970

Totals : 66.60940 4.53091

Results obtained with enhanced integrator!

Instrument 1 5/26/2016 8:42:57 PM MP

Page 1 of 1

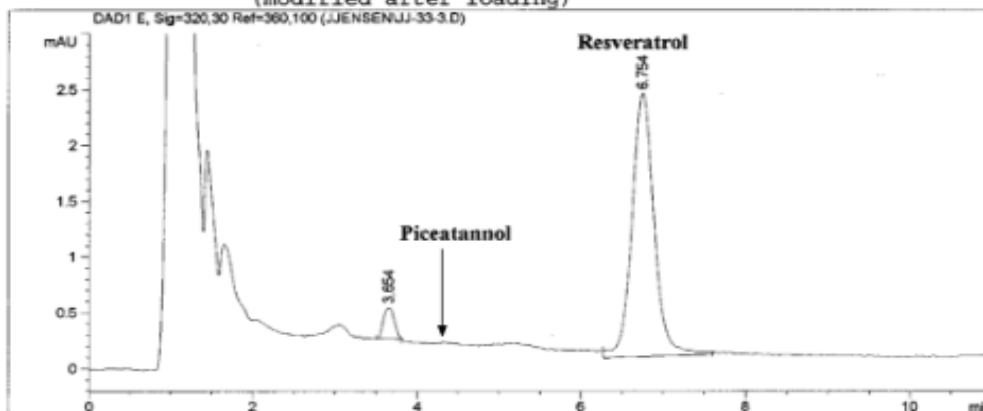
**Interaction of resveratrol 1 with CYP3A5 enzyme.** According to protocol A, interaction of resveratrol 1 (10 $\mu$ L) and CYP3A5 enzyme (20 $\mu$ L) produced the crude mixture which, according to HPLC, contained no piceatannol 7 (0%; anticipated  $t_r$  = 4.33min; resveratrol 1,  $t_r$  = 6.75min).

Data File C:\HPCHEM\1\DATA\JJENSEN\JJ-33-3.D

Sample Name: JJ-33-3

3.28.16 JJ-33-3, Crude, Isocratic-single bottle 1:3 AcN  
:Di-H2O mobile phase, 1.0 mL/min. flowrate  
Sample name:JJ-33 Crude RV/3A5 NS 3.28.16

```
=====
Injection Date   : 3/28/2016 4:40:12 PM
Sample Name      : JJ-33-3
Acq. Operator    : JJ
Vial             : 2
Inj Volume       : 30 ul
Acq. Method      : C:\HPCHEM\1\METHODS\SAMCAP1.M
Last changed     : 2/26/2016 7:10:36 PM by JJ
Analysis Method  : C:\HPCHEM\1\METHODS\SAMCAP1.M
Last changed     : 6/3/2016 3:34:54 PM by MP
                  (modified after loading)
=====
```



#### Area Percent Report

```
=====
Sorted By       : Signal
Multiplier      : 1.0000
Dilution        : 1.0000
Sample Amount   : 1.00000 [ng/ul] (not used in calc.)
=====
```

Signal 1: DAD1 E, Sig=320,30 Ref=360,100

Peak #	RetTime [min]	Type	Width [min]	Area [mAU*s]	Height [mAU]	Area %
1	3.654	MM	0.1542	2.58930	2.79845e-1	5.5051
2	6.754	BB	0.2878	44.44520	2.35897	94.4949

Totals : 47.03451 2.63881

Results obtained with enhanced integrator!

Instrument 1 6/3/2016 3:34:58 PM MP

Page 1 of 1

**Interaction of resveratrol 1 with CYP3A5 enzyme:** crude mixture spiked with 2 drops of piceatannol 7 ( $t_r = 4.33\text{min}$ ; resveratrol 1,  $t_r = 7.08\text{min}$ ).

Data File C:\HPCHEM\1\DATA\JJENSEN\JJ31-9.D

Sample Name: JJ31-9

5.13.16 JJ31-9, NS Crude, Pic-spiked 2drops, Isocratic single bottle delivery 1:3 AcN:Di-H2O mobile phase, 1.0 mL/min. flowrate  
Sample Name: RV/3A5 NS Crude 5.13.16

Injection Date : 5/13/2016 2:30:21 PM

Sample Name : JJ31-9

Vial : 1

Acq. Operator : JJ

Inj Volume : 30 ul

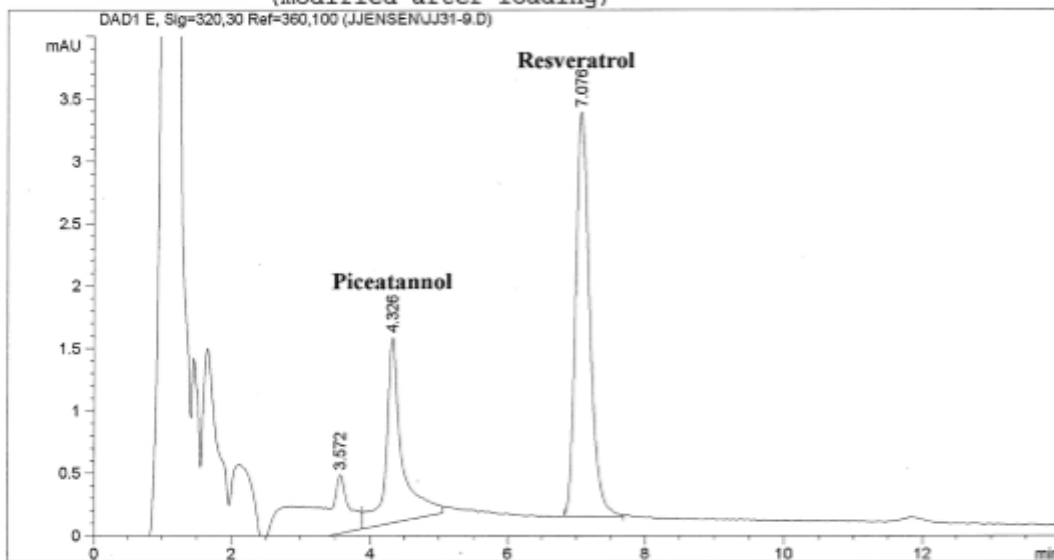
Acq. Method : C:\HPCHEM\1\METHODS\SAMCAP1.M

Last changed : 2/26/2016 7:10:36 PM by JJ

Analysis Method : C:\HPCHEM\1\METHODS\SAMCAP1.M

Last changed : 5/24/2016 4:02:55 PM by JJ

(modified after loading)



# Area Percent Report

Sorted By : Signal  
Multiplier : 1.0000  
Dilution : 1.0000  
Sample Amount : 1.00000 [ng/ul] (not used in calc.)

Signal 1: DAD1 E, Sig=320,30 Ref=360,100

Peak #	RetTime [min]	Type	Width [min]	Area [mAU*s]	Height [mAU]	Area %
1	3.572	VV	0.5579	21.24149	4.71197e-1	23.2929
2	4.326	VB	0.2224	24.00397	1.48610	26.3222
3	7.076	BB	0.2154	45.94742	3.24161	50.3849

**Interaction of resveratrol 1 with CYP2E1 enzyme.** According to protocol A, interaction of resveratrol 1 (10 $\mu$ L) and CYP2E1 enzyme (10 $\mu$ L) produced the crude mixture which, according to HPLC, contained piceatannol 7 (2%;  $t_r$  = 5.17min; resveratrol 1,  $t_r$  = 8.17min).

Data File C:\HPCHEM\1\DATA\JJENSEN\JJ35-4.D

Sample Name: JJ35-4

4.6.16 JJ35-4, NS from repos. (RV/2E1), Isocratic single bottle delivery 1:3 AcN:Di-H<sub>2</sub>O mobile phase, 1.0 mL/min. flowrate  
Sample name: JJ-35 Crude RV/2E1 4.7.16

Injection Date : 4/7/2016 1:52:02 PM

Sample Name : JJ35-4

Vial : 2

Acq. Operator : JJ

Inj Volume : 30  $\mu$ L

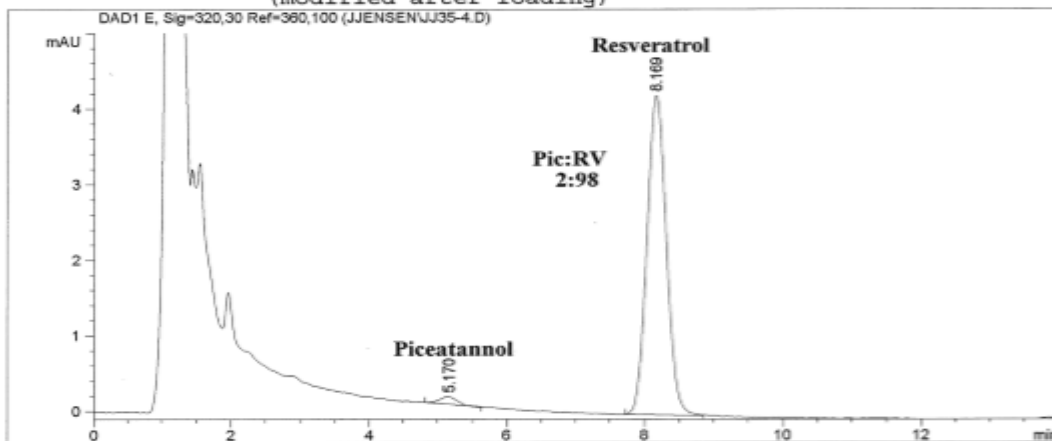
Acq. Method : C:\HPCHEM\1\METHODS\SAMCAP1.M

Last changed : 2/26/2016 7:10:36 PM by JJ

Analysis Method : C:\HPCHEM\1\METHODS\SAMCAP1.M

Last changed : 5/26/2016 8:27:45 PM by MP

(modified after loading)



#### Area Percent Report

Sorted By : Signal  
Multiplier : 1.0000  
Dilution : 1.0000  
Sample Amount : 1.00000 [ng/ $\mu$ L] (not used in calc.)

Signal 1: DAD1 E, Sig=320,30 Ref=360,100

Peak #	RetTime [min]	Type	Width [min]	Area [mAU*s]	Height [mAU]	Area %
1	5.170	BP	0.2090	1.66407	9.95701e-2	1.9871
2	8.169	BB	0.3048	82.08051	4.22166	98.0129

Totals : 83.74459 4.32123

Results obtained with enhanced integrator!

Instrument 1 5/26/2016 8:27:47 PM MP

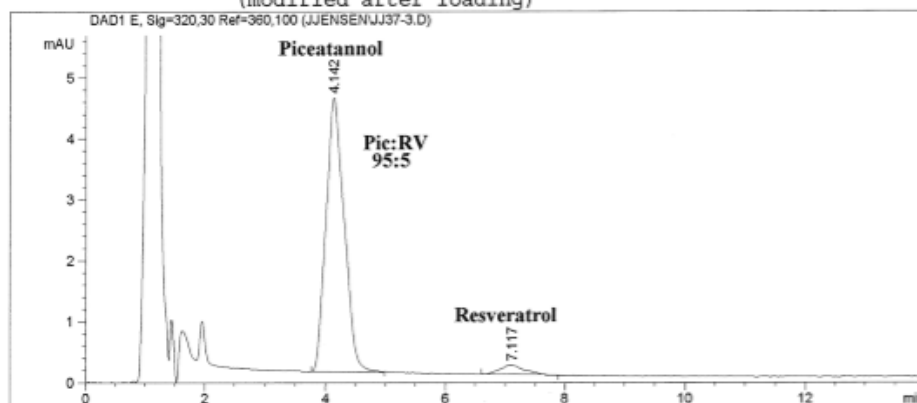
Page 1 of 1

**Interaction of resveratrol 1 with CYP2C18 enzyme.** According to protocol A, interaction of resveratrol 1 (10µL) and CYP2C18 enzyme (20µL) produced the crude mixture which, according to HPLC, contained piceatannol 7 (95%;  $t_r$  = 4.14min; resveratrol 1,  $t_r$  = 7.12min).

Data File C:\HPCHEM\1\DATA\JJENSEN\JJ37-3.D Sample Name: JJ37-3

4.22.16 JJ37-3, Isocratic single bottle delivery 1:3 Ac  
N:Di-H2O mobile phase, 1.0 mL/min. flowrate  
Sample name:JJ-37 RV/2C18 NS Crude 4.21.16

```
=====
Injection Date   : 4/22/2016 7:16:58 AM
Sample Name      : JJ37-3
Acq. Operator    : JJ
Vial             : 1
Inj Volume       : 30 ul
Acq. Method      : C:\HPCHEM\1\METHODS\SAMCAP1.M
Last changed     : 2/26/2016 7:10:36 PM by JJ
Analysis Method  : C:\HPCHEM\1\METHODS\SAMCAP1.M
Last changed     : 5/26/2016 8:47:53 PM by MP
                  (modified after loading)
=====
```



=====  
Area Percent Report  
=====

```
Sorted By      : Signal
Multiplier     : 1.0000
Dilution       : 1.0000
Sample Amount  : 1.00000 [ng/ul] (not used in calc.)
```

Signal 1: DAD1 E, Sig=320,30 Ref=360,100

Peak #	RetTime [min]	Type	Width [min]	Area [mAU*s]	Height [mAU]	Area %
1	4.142	PB	0.2937	94.67780	4.49619	95.3577
2	7.117	BP	0.3534	4.60925	1.57491e-1	4.6423

Totals : 99.28705 4.65368

Results obtained with enhanced integrator!

=====  
\*\*\* End of Report \*\*\*

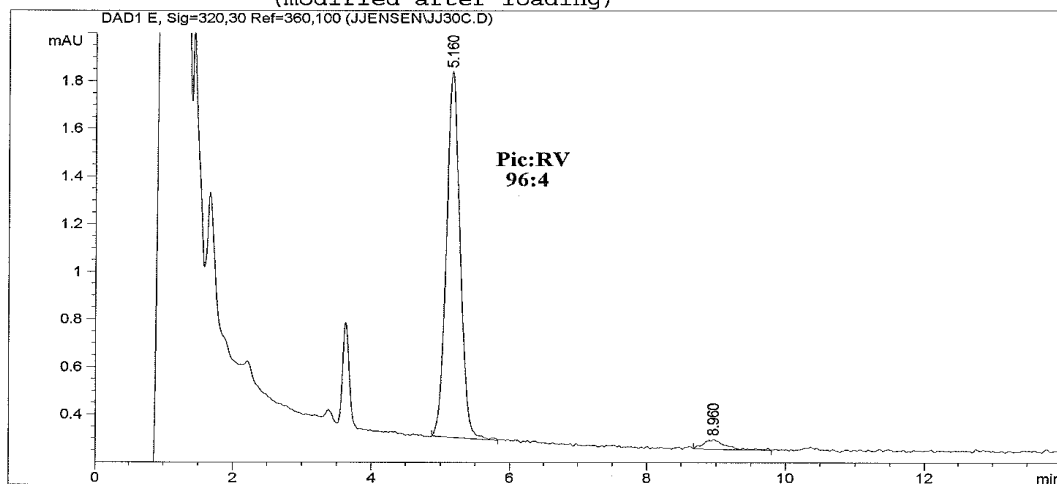
**Interaction of resveratrol 1 with CYP3A4 enzyme.** According to protocol A, interaction of resveratrol 1 (10µL) and CYP3A4 enzyme (10µL) produced the crude mixture which, according to HPLC, contained piceatannol 7 (96%;  $t_r$  = 5.16min; resveratrol 1,  $t_r$  = 8.96min).

Data File C:\HPCHEM\1\DATA\JJENSEN\JJ30C.D

Sample Name: JJ30C

3.10.16, JJ30C, RV/3A4 Crude, Isocratic-single bottle 1  
:3 AcN:Di-H2O mobile phase, 1.0 mL/min.  
Sample name:JJ-28 RV/3A4

```
=====
Injection Date   : 3/10/2016 12:31:44 PM
Sample Name      : JJ30C
Acq. Operator    : JJ
Vial             : 3
Inj Volume       : 30 ul
Acq. Method      : C:\HPCHEM\1\METHODS\SAMCAP1.M
Last changed     : 2/26/2016 7:10:36 PM by JJ
Analysis Method  : C:\HPCHEM\1\METHODS\SAMCAP1.M
Last changed     : 5/14/2016 1:57:16 PM by JJ
                  (modified after loading)
=====
```



```
=====
Area Percent Report
=====
```

```
Sorted By      : Signal
Multiplier     : 1.0000
Dilution       : 1.0000
Sample Amount  : 1.00000 [ng/ul] (not used in calc.)
```

Signal 1: DAD1 E, Sig=320,30 Ref=360,100

Peak #	RetTime [min]	Type	Width [min]	Area [mAU*s]	Height [mAU]	Area %
1	5.160	BB	0.2098	21.30284	1.53558	95.5870
2	8.960	VB	0.2888	9.83507e-1	4.14458e-2	4.4130

Instrument 1 5/14/2016 1:57:28 PM JJ

Page 1 of 2

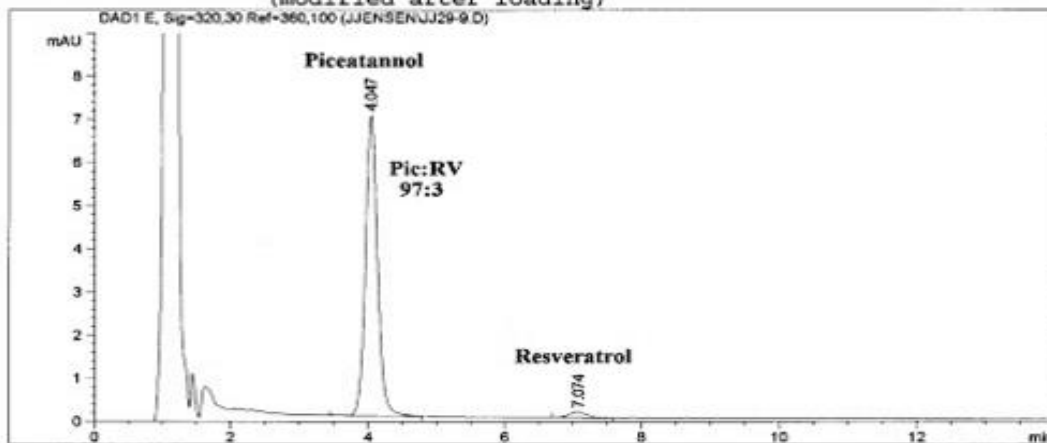
**Interaction of resveratrol 1 with CYP1A1 enzyme.** According to protocol A, interaction of resveratrol 1 (10 $\mu$ L) and CYP1A1 enzyme (20 $\mu$ L) produced the crude mixture which, according to HPLC, contained piceatannol 7 (97%;  $t_r$  = 4.05min; resveratrol 1,  $t_r$  = 7.07min).

Data File C:\HPCHEM\1\DATA\JJENSEN\JJ29-9.D Sample Name: JJ29-9

4.22.16 JJ29-9, Isocratic single bottle delivery 1:3 Ac  
N:Di-H2O mobile phase, 1.0 mL/min. flowrate  
Sample name:JJ-29 RV/1A1 NS Crude 4.21.16

=====

Injection Date	: 4/22/2016 7:37:33 AM	Vial	: 1
Sample Name	: JJ29-9		
Acq. Operator	: JJ	Inj Volume	: 30 ul
Acq. Method	: C:\HPCHEM\1\METHODS\SAMCAP1.M		
Last changed	: 2/26/2016 7:10:36 PM by JJ		
Analysis Method	: C:\HPCHEM\1\METHODS\SAMCAP1.M		
Last changed	: 6/1/2016 9:29:53 AM by MP		
	(modified after loading)		



=====  
Area Percent Report  
=====

Sorted By	:	Signal	
Multiplier	:	1.0000	
Dilution	:	1.0000	
Sample Amount	:	1.00000 [ng/ul]	(not used in calc.)

Signal 1: DAD1 E, Sig=320,30 Ref=360,100

Peak #	RetTime [min]	Type	Width [min]	Area [mAU*s]	Height [mAU]	Area %
1	4.047	BV	0.1864	85.05016	6.96655	96.9275
2	7.074	BP	0.2512	2.69602	1.42213e-1	3.0725

Totals : 87.74618 7.10877

Results obtained with enhanced integrator!

# Interaction of resveratrol 1 with CYP1A1 enzyme: HPLC analysis of the crude mixture

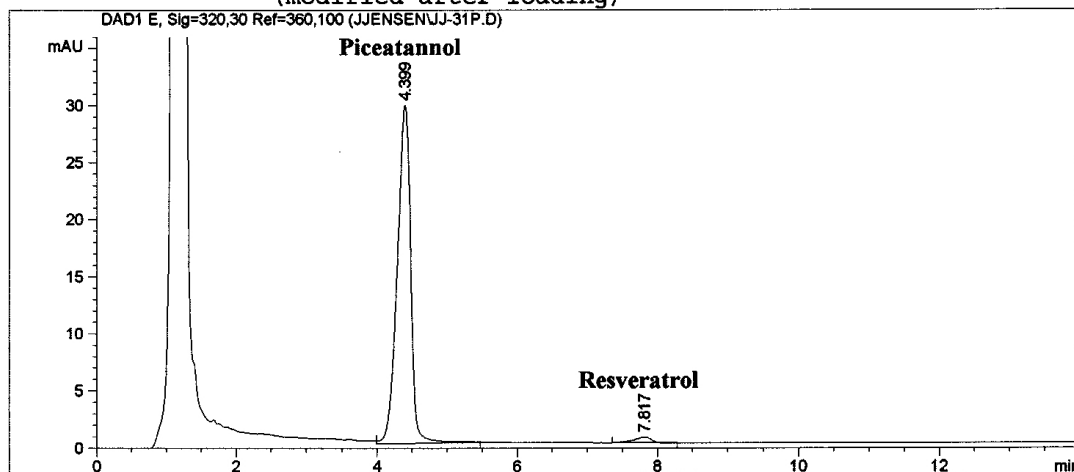
evacuated under reduced pressure overnight (protocol B).

Data File C:\HPCHEM\1\DATA\JJENSEN\JJ-31P.D

Sample Name: JJ-31P

3.1.16, JJ-31P (1A1), Isocratic-single bottle 1:3 AcN:D  
i-H<sub>2</sub>O mobile phase, 1.0 mL/min.  
Sample name:JJ-31 RV/1A1 Pump ON 1:3

=====  
Injection Date : 3/1/2016 12:40:35 PM  
Sample Name : JJ-31P Vial : 1  
Acq. Operator : JJ Inj Volume : 30 ul  
Acq. Method : C:\HPCHEM\1\METHODS\SAMCAP1.M  
Last changed : 2/26/2016 7:10:36 PM by JJ  
Analysis Method : C:\HPCHEM\1\METHODS\SAMCAP1.M  
Last changed : 6/1/2016 9:36:31 AM by MP  
(modified after loading)



## Area Percent Report

=====  
Sorted By : Signal  
Multiplier : 1.0000  
Dilution : 1.0000  
Sample Amount : 1.00000 [ng/ul] (not used in calc.)

Signal 1: DAD1 E, Sig=320,30 Ref=360,100

Peak #	RetTime [min]	Type	Width [min]	Area [mAU*s]	Height [mAU]	Area %
1	4.399	VB	0.2067	397.83682	29.62659	97.8766
2	7.817	BP	0.2517	8.63110	5.04171e-1	2.1234

Totals : 406.46792 30.13076

Results obtained with enhanced integrator!

Instrument 1 6/1/2016 9:36:57 AM MP

Page 1 of 1



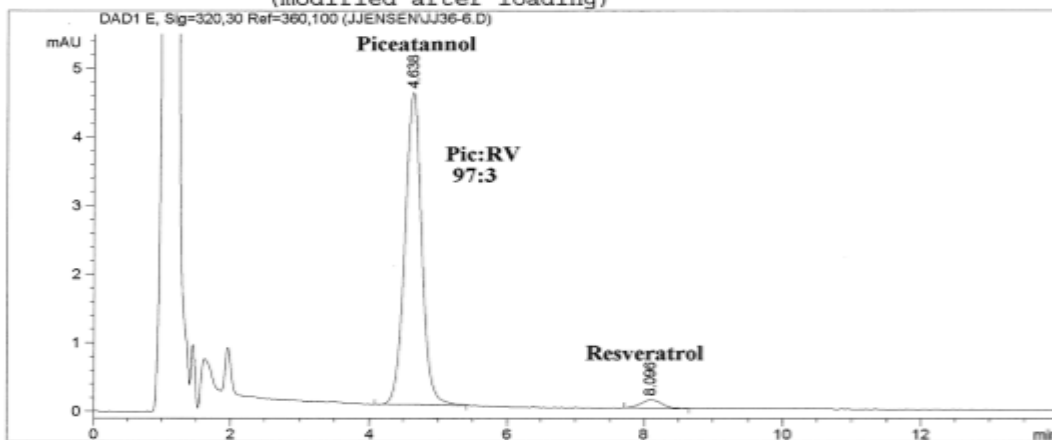
**Interaction of resveratrol 1 with CYP2A6 enzyme.** According to protocol A, interaction of resveratrol 1 (10µL) and CYP2A6 enzyme (10µL) produced the crude mixture which, according to HPLC, contained piceatannol 7 (97%;  $t_r$  = 4.64min; resveratrol 1,  $t_r$  = 8.10min).

Data File C:\HPCHEM\1\DATA\JJENSEN\JJ36-6.D Sample Name: JJ36-6

4.22.16 JJ36-6, Isocratic single bottle delivery 1:3 Ac  
N:Di-H2O mobile phase, 1.0 mL/min. flowrate  
Sample name:JJ-36 RV/2A6 NS Crude 4.21.16

=====

Injection Date	: 4/22/2016 9:43:24 AM	Vial	: 1
Sample Name	: JJ36-6		
Acq. Operator	: JJ	Inj Volume	: 30 ul
Acq. Method	: C:\HPCHEM\1\METHODS\SAMCAP1.M		
Last changed	: 2/26/2016 7:10:36 PM by JJ		
Analysis Method	: C:\HPCHEM\1\METHODS\SAMCAP1.M		
Last changed	: 5/26/2016 8:32:57 PM by MP		
	(modified after loading)		



=====  
Area Percent Report  
=====

Sorted By	:	Signal	
Multiplier	:	1.0000	
Dilution	:	1.0000	
Sample Amount	:	1.00000 [ng/ul]	(not used in calc.)

Signal 1: DAD1 E, Sig=320,30 Ref=360,100

Peak #	RetTime [min]	Type	Width [min]	Area [mAU*s]	Height [mAU]	Area %
1	4.638	PB	0.2631	77.74129	4.55450	96.6850
2	8.096	BP	0.3006	2.66547	1.22164e-1	3.3150

Totals : 80.40676 4.67667

Results obtained with enhanced integrator!

=====  
\*\*\* End of Report \*\*\*

## Interaction of resveratrol 1 with CYP2A6 enzyme: HPLC analysis of the crude mixture

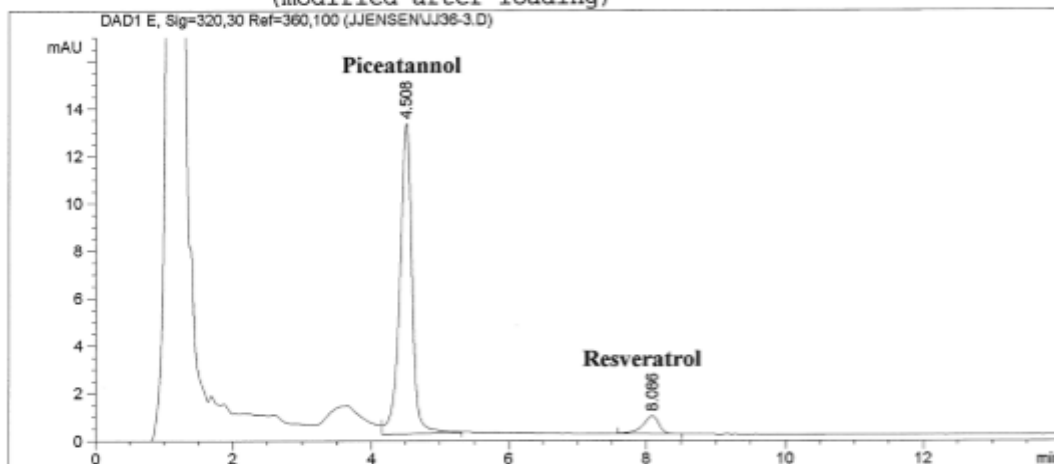
evacuated under reduced pressure overnight (protocol B).

Data File C:\HPCHEM\1\DATA\JJENSEN\JJ36-3.D

Sample Name: JJ36-3

3.24.16 JJ36-3, Pumped, Isocratic-single bottle 1:3 AcN  
:Di-H2O mobile phase, 1.0 mL/min. flowrate  
Sample name:JJ-36 PON RV/2A6

```
=====
Injection Date   : 3/24/2016 9:20:34 AM
Sample Name      : JJ36-3
Acq. Operator    : JJ
Vial             : 2
Inj Volume       : 30 ul
Acq. Method      : C:\HPCHEM\1\METHODS\SAMCAP1.M
Last changed     : 2/26/2016 7:10:36 PM by JJ
Analysis Method  : C:\HPCHEM\1\METHODS\SAMCAP1.M
Last changed     : 5/26/2016 8:38:20 PM by MP
                  (modified after loading)
=====
```



### Area Percent Report

```
=====
Sorted By       : Signal
Multiplier      : 1.0000
Dilution        : 1.0000
Sample Amount    : 1.00000 [ng/ul] (not used in calc.)
=====
```

Signal 1: DAD1 E, Sig=320,30 Ref=360,100

Peak #	RetTime [min]	Type	Width [min]	Area [mAU*s]	Height [mAU]	Area %
1	4.508	VB	0.1866	162.31223	13.09434	93.0066
2	8.086	BB	0.2375	12.20463	7.59205e-1	6.9934

Totals : 174.51685 13.85355

Results obtained with enhanced integrator!

Instrument 1 5/26/2016 8:38:56 PM MP

Page 1 of 1

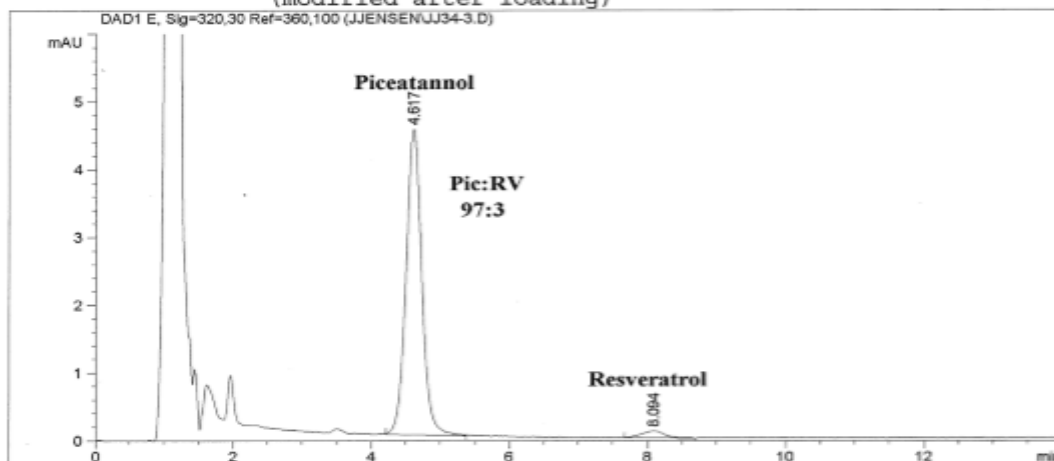
**Interaction of resveratrol 1 with CYP2C9 enzyme.** According to protocol A, interaction of resveratrol 1 (10 $\mu$ L) and CYP2C9 enzyme (20 $\mu$ L) produced the crude mixture which, according to HPLC, contained piceatannol 7 (97%;  $t_r$  = 4.62min; resveratrol 1,  $t_r$  = 8.10min).

Data File C:\HPCHEM\1\DATA\JJENSEN\JJ34-3.D

Sample Name: JJ34-3

4.22.16 JJ34-3, Isocratic single bottle delivery 1:3 Ac  
N:Di-H2O mobile phase, 1.0 mL/min. flowrate  
Sample name:JJ-34 RV/2C9 NS Crude 4.21.16

```
=====
Injection Date   : 4/22/2016 8:24:03 AM
Sample Name      : JJ34-3
Acq. Operator    : JJ
Vial             : 1
Inj Volume       : 30 ul
Acq. Method      : C:\HPCHEM\1\METHODS\SAMCAP1.M
Last changed     : 2/26/2016 7:10:36 PM by JJ
Analysis Method  : C:\HPCHEM\1\METHODS\SAMCAP1.M
Last changed     : 5/26/2016 7:45:20 PM by MP
                  (modified after loading)
=====
```



#### Area Percent Report

```
=====
Sorted By      : Signal
Multiplier     : 1.0000
Dilution       : 1.0000
Sample Amount  : 1.00000 [ng/ul] (not used in calc.)
=====
```

Signal 1: DAD1 E, Sig=320,30 Ref=360,100

Peak #	RetTime [min]	Type	Width [min]	Area [mAU*s]	Height [mAU]	Area %
1	4.617	BB	0.2410	71.45241	4.50609	96.5015
2	8.094	BP	0.3193	2.59039	1.03762e-1	3.4985

Totals : 74.04279 4.60985

Results obtained with enhanced integrator!

Instrument 1 5/26/2016 7:45:53 PM MP

Page 1 of 1

**Interaction of resveratrol 1 with CYP2C9 enzyme: HPLC analysis of the crude mixture**  
 evacuated under reduced pressure overnight (protocol B).

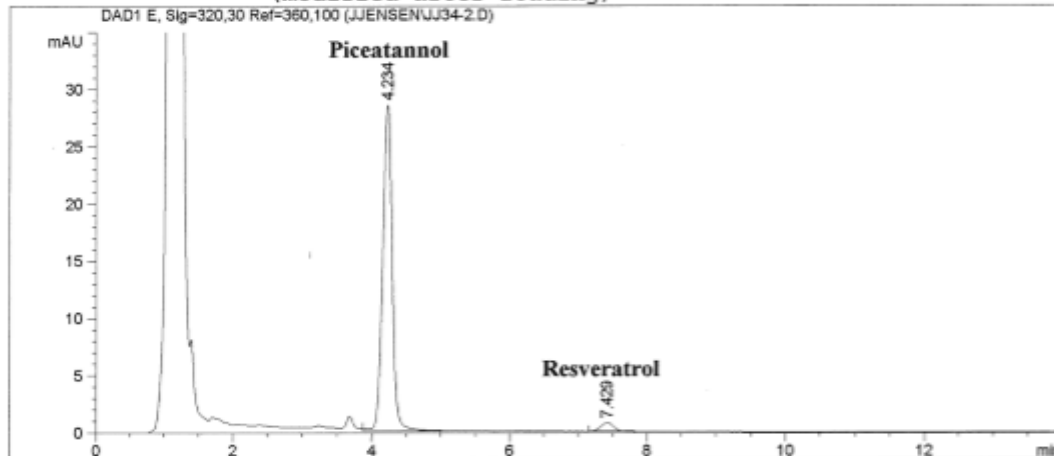
Data File C:\HPCHEM\1\DATA\JJJENSEN\JJ34-2.D

Sample Name: JJ34-2

3.22.16 JJ34-2 pumped, Isocratic-single bottle 1:3 AcN:  
 Di-H2O mobile phase, 1.0 mL/min. flowrate  
 Sample name:JJ-34 PON RV/2C9 3.22.16

=====

Injection Date	: 3/22/2016 10:32:20 AM	
Sample Name	: JJ34-2	Vial : 3
Acq. Operator	: JJ	
		Inj Volume : 30 ul
Acq. Method	: C:\HPCHEM\1\METHODS\SAMCAP1.M	
Last changed	: 2/26/2016 7:10:36 PM by JJ	
Analysis Method	: C:\HPCHEM\1\METHODS\SAMCAP1.M	
Last changed	: 5/26/2016 7:52:08 PM by MP	
	(modified after loading)	



=====  
 Area Percent Report  
 =====

Sorted By	:	Signal	
Multiplier	:	1.0000	
Dilution	:	1.0000	
Sample Amount	:	1.00000 [ng/ul]	(not used in calc.)

Signal 1: DAD1 E, Sig=320,30 Ref=360,100

Peak #	RetTime [min]	Type	Width [min]	Area [mAU*s]	Height [mAU]	Area %
1	4.234	VB	0.1478	273.31573	28.51952	96.5934
2	7.429	BP	0.2012	9.63915	7.43785e-1	3.4066

Totals : 282.95489 29.26330

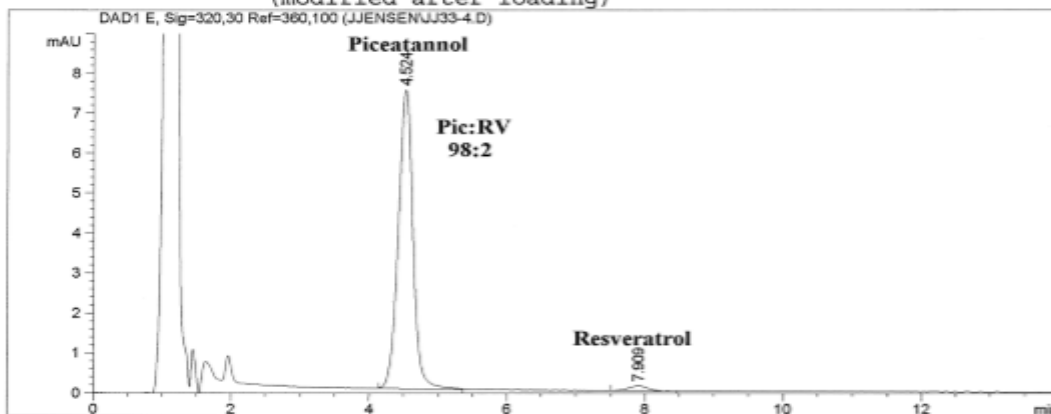
Results obtained with enhanced integrator!

**Interaction of resveratrol 1 with CYP2C8 enzyme.** According to protocol A, interaction of resveratrol 1 (10 $\mu$ L) and CYP2C8 enzyme (10 $\mu$ L) produced the crude mixture which, according to HPLC, contained piceatannol 7 (98%;  $t_r$  = 4.52min; resveratrol 1,  $t_r$  = 7.91min).

Data File C:\HPCHEM\1\DATA\JJENSEN\JJ33-4.D Sample Name: JJ33-4

4.22.16 JJ33-4, Isocratic single bottle delivery 1:3 Ac  
N:Di-H2O mobile phase, 1.0 mL/min. flowrate  
Sample name:JJ-33 RV/2C8 NS Crude 4.21.16

```
=====
Injection Date   : 4/22/2016 9:22:04 AM
Sample Name      : JJ33-4
Acq. Operator    : JJ
Vial             : 1
Inj Volume       : 30 ul
Acq. Method      : C:\HPCHEM\1\METHODS\SAMCAP1.M
Last changed     : 2/26/2016 7:10:36 PM by JJ
Analysis Method  : C:\HPCHEM\1\METHODS\SAMCAP1.M
Last changed     : 5/26/2016 7:30:28 PM by MP
                  (modified after loading)
=====
```



# Area Percent Report

```
=====
Sorted By      : Signal
Multiplier     : 1.0000
Dilution       : 1.0000
Sample Amount  : 1.00000 [ng/ul] (not used in calc.)
=====
```

Signal 1: DAD1 E, Sig=320,30 Ref=360,100

Peak #	RetTime [min]	Type	Width [min]	Area [mAU*s]	Height [mAU]	Area %
1	4.524	BB	0.2223	109.10845	7.47276	97.7971
2	7.909	BP	0.2620	2.45764	1.25773e-1	2.2029

Totals : 111.56609 7.59853

Results obtained with enhanced integrator!

\*\*\* End of Report \*\*\*

## Interaction of resveratrol 1 with CYP2C8 enzyme: HPLC analysis of the crude mixture

evacuated under reduced pressure overnight (protocol B).

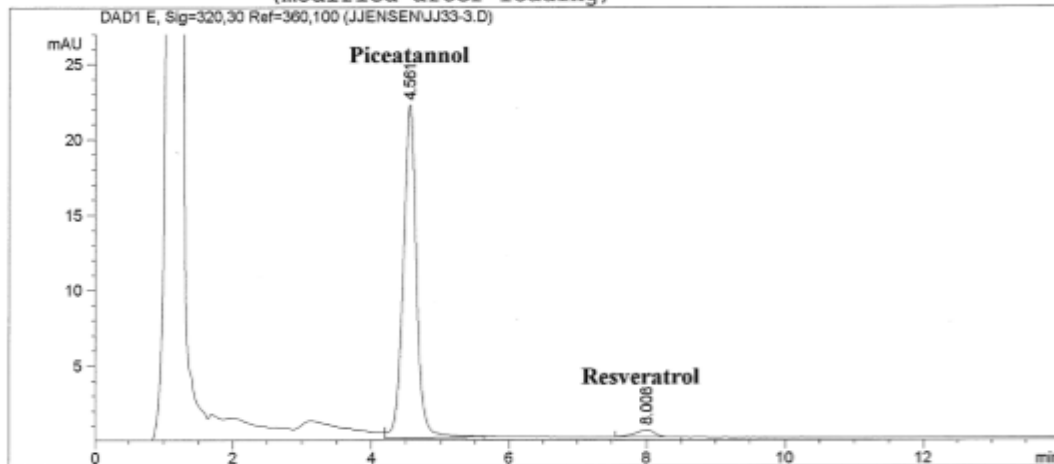
Data File C:\HPCHEM\1\DATA\JJENSEN\JJ33-3.D

Sample Name: JJ33-3

3.22.16 JJ33-3 pumped, Isocratic-single bottle 1:3 AcN:  
Di-H2O mobile phase, 1.0 mL/min. flowrate  
Sample name:JJ-33 PON RV/2C8 3.22.16

=====

Injection Date	: 3/22/2016 10:12:28 AM	
Sample Name	: JJ33-3	Vial : 2
Acq. Operator	: JJ	
		Inj Volume : 30 ul
Acq. Method	: C:\HPCHEM\1\METHODS\SAMCAP1.M	
Last changed	: 2/26/2016 7:10:36 PM by JJ	
Analysis Method	: C:\HPCHEM\1\METHODS\SAMCAP1.M	
Last changed	: 5/26/2016 6:58:32 PM by MP	
	(modified after loading)	



### Area Percent Report

Sorted By : Signal  
Multiplier : 1.0000  
Dilution : 1.0000  
Sample Amount : 1.00000 [ng/ul] (not used in calc.)

Signal 1: DAD1 E, Sig=320,30 Ref=360,100

Peak #	RetTime [min]	Type	Width [min]	Area [mAU*s]	Height [mAU]	Area %
1	4.561	VB	0.2008	293.05136	22.08678	96.8908
2	8.008	BP	0.2908	9.40384	4.88036e-1	3.1092

Totals : 302.45521 22.57481

Results obtained with enhanced integrator!

Instrument 1 5/26/2016 7:00:52 PM MP

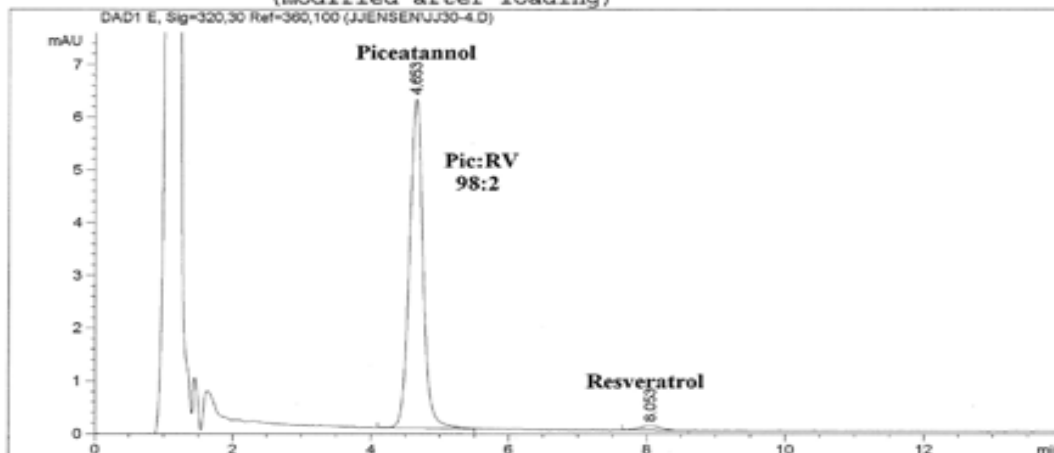
Page 1 of 1

**Interaction of resveratrol 1 with CYP4F12 enzyme.** According to protocol A, interaction of resveratrol 1 (10 $\mu$ L) and CYP4F12 enzyme (20 $\mu$ L) produced the crude mixture which, according to HPLC, contained piceatannol 7 (98%;  $t_r$  = 4.65min; resveratrol 1,  $t_r$  = 8.05min).

Data File C:\HPCHEM\1\DATA\JJENSEN\JJ30-4.D Sample Name: JJ30-4

4.22.16 JJ30-4, Isocratic single bottle delivery 1:3 Ac  
N:Di-H2O mobile phase, 1.0 mL/min. flowrate  
Sample name:JJ-30 RV/4F12 NS Crude 4.21.16

```
=====
Injection Date   : 4/22/2016 8:02:55 AM
Sample Name      : JJ30-4
Acq. Operator    : JJ
Vial             : 1
Inj Volume       : 30 ul
Acq. Method      : C:\HPCHEM\1\METHODS\SAMCAP1.M
Last changed     : 2/26/2016 7:10:36 PM by JJ
Analysis Method  : C:\HPCHEM\1\METHODS\SAMCAP1.M
Last changed     : 5/26/2016 6:31:09 PM by MP
                  (modified after loading)
=====
```



#### Area Percent Report

```
=====
Sorted By       : Signal
Multiplier      : 1.0000
Dilution        : 1.0000
Sample Amount   : 1.00000 [ng/ul] (not used in calc.)
=====
```

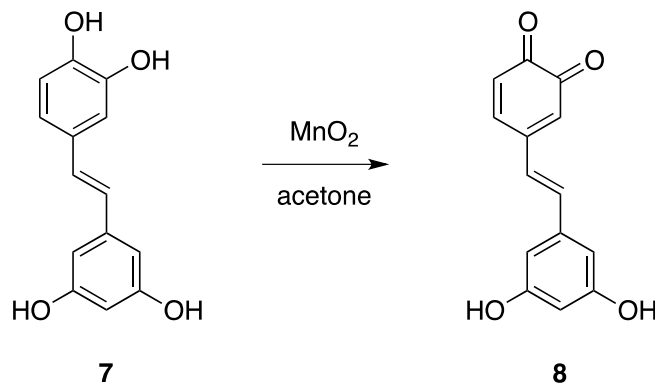
Signal 1: DAD1 E, Sig=320,30 Ref=360,100

Peak #	RetTime [min]	Type	Width [min]	Area [mAU*s]	Height [mAU]	Area %
1	4.653	PB	0.2125	85.73792	6.23170	97.7465
2	8.053	BB	0.2799	1.97667	8.48275e-2	2.2535

Totals : 87.71459 6.31652

Results obtained with enhanced integrator!

### Synthesis of piceatannol-*ortho*-quinone **8** (Pic-Q).



**(E)-4-(3',5'-Dihydroxystyryl)cyclohexa-3,5-diene-1,2-dione (**8**)**. Manganese (IV) oxide (39.2 mg, 0.45 mmol) was added to a solution of piceatannol **7** (12.2 mg, 0.05 mmol) in acetone- $d_6$  (3 mL) and stirred in an open air at 20 °C for 2 h (HPLC control, aliquot was centrifuged 25min; **7**  $t_r$  = 5.18min; **8**  $t_r$  = 6.30min). The reaction mixture was centrifuged for 25 min (2 test tubes) and red solution was analyzed by means of  $^1\text{H}/^{13}\text{C}$  NMR and MS spectroscopy (protected from light and kept at -78°C). Yield of individual *ortho*-quinone **8** (Pic-Q) cannot be determined because of its extreme instability: when pumped to dryness under reduced pressure, black solid undergoes partial decomposition when stored at room temperature over 30 min (NMR).

Pic-Q **8**: black solid (forms red solution in acetone).  $^1\text{H}$  NMR (400MHz,  $\delta$ , ac- $d_6$ ; sample is filtered in an open air through acetone-washed cotton): 6.43 (1H, t, 4'-H,  $J_{av}$  = 2.2), 6.45 (1H, spl d, 3-H,  $J$  = 1.6), 6.47 (1H, d, 6-H,  $J$  = 10.4), 6.70 (2H, d, 2'-H, 6'-H,  $J$  = 2.0), 7.15 (1H, d,  $\underline{\text{HC}}=\underline{\text{CH}}$ ,  $J$  = 16.4), 7.50 (1H, d,  $\underline{\text{HC}}=\underline{\text{CH}}$ ), 7.80 (1H, dd, 5-H,  $J$  = 2.0), 8.54 (2H, s, 2OH).  $^{13}\text{C}$  NMR (100MHz,  $\delta$ , ac- $d_6$ , -15 °C): 104.88 (C4'), 106.59 (C2'/C6'), 125.23, 126.38/126.48 (split signal supposedly due to the slow rotation at low T), 130.50, 137.29, 138.30, 139.32, 147.30 (C3-C6,  $\text{HC}=\text{CH}$ , C1'), 159.48 (C3'/C5'), 180.31, 180.99 (C1, C2). MS ESI/APCI+:  $m/z$  calcd



for  $C_{14}H_{10}O_4Na$   $MNa^+$  265.0471, found 265.0469. The  $MNa^+$  peak is of low intensity because of the instability of the compound in a pure form even at room temperature (in the course of MS analysis, compound is exposed to 200°C for several nanoseconds), and also supposedly because of the low ionization efficiency. Given the instability of *ortho*-quinone **8**, no diagnostic peaks were detected in the LIFDI analysis, or in an ESI/APCI probe *in the absence* of spiking with Na. For comparison, under analogous conditions piceatannol **7** shows an intense  $MH^+$  peak at 245.0834 along with a low intensity peaks at 267.0632 ( $MNa^+$ ) and 265.0502 ( $MNa^{+2}$ ; formed supposedly by oxidation of PIC **7** in the course of the MS analysis).

#### Stability studies:

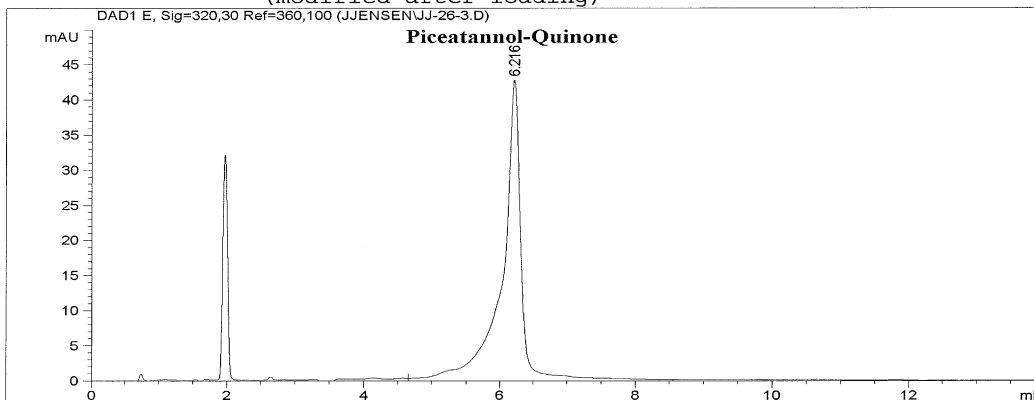
- **test #1** (stability in solution): by NMR, *ortho*-quinone **8** stable in acetone- $d_6$  solution at -15 °C for 20h;
- **test #2** (stability in solution): by NMR, *ortho*-quinone **8** stable in acetone- $d_6$  solution at -80 °C for 7 days;
- **test #3** (stability of *ortho*-quinone **8** in solid form at room temperature): solution of **8** in acetone- $d_6$  was evaporated to dryness under reduced pressure, black residue was kept in an open air for 5 min at room temperature (residue remained black with no visual changes in its appearance), then dissolved in acetone- $d_6$  and analyzed by NMR (red solution of a lesser intensity). Additional signals are visible in the NMR spectrum indicating a partial decomposition of *ortho*-quinone **8**;
- **test #4** (stability of *ortho*-quinone **8** in solid form at room temperature): solution of **8** in acetone- $d_6$  was evaporated to dryness under reduced pressure, black solid was kept in an open air for 30 min at room temperature (residue turned dark purple), then dissolved in

acetone-d<sub>6</sub> and analyzed by NMR (orange solution). Along with signals of *ortho*-quinone **8**, those of decomposition products became more prominent indicating a major decomposition of the former;

Data File C:\HPCHEM\1\DATA\JJENSEN\JJ-26-3.D Sample Name: JJ-26-3

12.15.15, JJ-26-3, find:Pic-Q retention time @ 1 mL flow rate, Isocratic-single bottle 100% 1:3 (A), Sample Names:JJ-26 Pic-Q Synthesized 12.11.15

```
=====
Injection Date   : 12/15/2015 7:00:15 PM
Sample Name      : JJ-26-3
Acq. Operator    : JJ
Vial             : 3
Inj Volume       : 1 ul
Acq. Method      : C:\HPCHEM\1\METHODS\SAMCAP1.M
Last changed     : 12/15/2015 6:59:02 PM by JJ
                  (modified after loading)
Analysis Method  : C:\HPCHEM\1\METHODS\SAMCAP1.M
Last changed     : 6/1/2016 9:40:55 AM by MP
                  (modified after loading)
=====
```



```
=====
Area Percent Report
=====
Sorted By      : Signal
Multiplier     : 1.0000
Dilution       : 1.0000
Sample Amount  : 1.00000 [ng/ul] (not used in calc.)
```

Signal 1: DAD1 E, Sig=320,30 Ref=360,100

Peak #	RetTime [min]	Type	Width [min]	Area [mAU*s]	Height [mAU]	Area %
1	6.216	VB	0.3786	1309.07776	45.11102	100.0000

Totals : 1309.07776 45.11102

Results obtained with enhanced integrator!

```
=====
*** End of Report ***
```

Instrument 1 6/1/2016 9:41:21 AM MP

Page 1 of 1

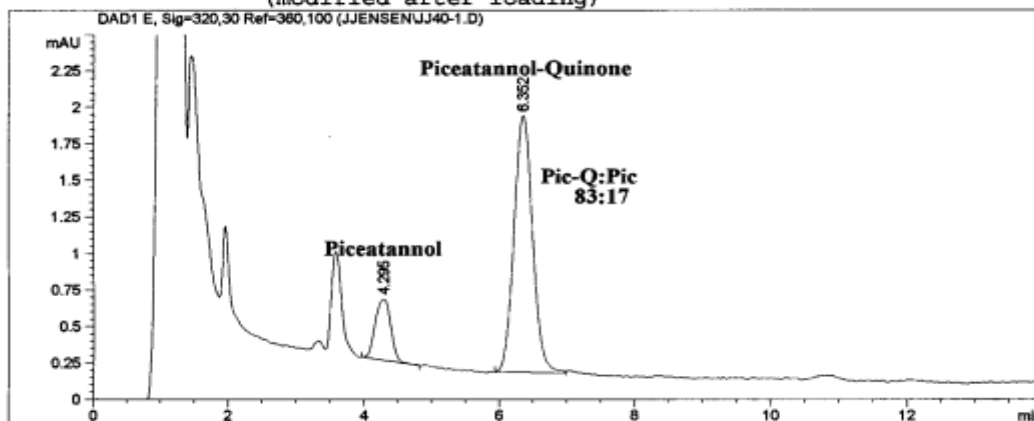
- **test #5** (stability on the TLC plate): red color instantaneously disappears when a solution of *ortho*-quinone **8** in acetone-d<sub>6</sub> is applied to silicagel. Development of TLC plate in acetone, as an eluent, did not show any mobile organic spots indicating a complete decomposition.

**Interaction of piceatannol 7 with CYP1A1 enzyme.** According to protocol A, interaction of piceatannol **7** (10μL) and CYP1A1 enzyme (20μL) produced the crude mixture, which according to HPLC, contained piceatannol-*ortho*-quinone **8** (83%; t<sub>r</sub> = 6.35min; piceatannol **7**, t<sub>r</sub> = 4.30min).

4.7.16 JJ40-1, Crude Pic/1A1, Isocratic single bottle delivery 1:3 AcN:Di-H2O mobile phase, 1.0 mL/min. flow rate  
Sample name: JJ-40 Crude Pic/1A1 4.6.16

=====

Injection Date	: 4/7/2016 5:10:43 PM	
Sample Name	: JJ40-1	Vial : 22
Acq. Operator	: JJ	Inj Volume : 30 ul
Acq. Method	: C:\HPCHEM\1\METHODS\SAMCAP1.M	
Last changed	: 4/7/2016 3:24:38 PM by JJ	
	(modified after loading)	
Analysis Method	: C:\HPCHEM\1\METHODS\SAMCAP1.M	
Last changed	: 6/1/2016 9:21:43 AM by MP	
	(modified after loading)	



=====

Area Percent Report

=====

Sorted By	:	Signal
Multiplier	:	1.0000
Dilution	:	1.0000
Sample Amount	:	1.00000 [ng/ul] (not used in calc.)

Signal 1: DAD1 E, Sig=320,30 Ref=360,100

Peak #	RetTime [min]	Type	Width [min]	Area [mAU*s]	Height [mAU]	Area %
1	4.295	VP	0.2595	6.68450	4.20497e-1	16.5650
2	6.352	BB	0.3033	33.66872	1.75877	83.4350

Totals : 40.35322 2.17927

Results obtained with enhanced integrator!

=====

## REFERENCES

1. (a) Stopper, H.; Schmitt, E.; Kobras, K. Genotoxicity of Phytoestrogens. *Mut. Res.* **2005**, *574*, 139-155. (b) Muqbil, I.; Beck, F. W. J.; Bao, B.; Sarkar, F. H.; Mohammad, R. M.; Hadi, S. M.; Azmi, A. S. Old Wine in a New Bottle: The Warburg Effect and Anticancer Mechanisms of Resveratrol. *Curr. Pharmaceut. Design* **2012**, *18*, 1645-1654. (c) Cos, P.; De Bruyne, T.; Apers, S.; Berghe, D. V.; Pieters, L.; Vlietinck, A. J. Phytoestrogens: Recent Developments. *Planta. Med.* **2003**, *69*, 589-599. (d) Yang, C. S.; Landau, J. M.; Huang, M-T; Newmark, H. L. Inhibition of Carcinogenesis by Dietary Polyphenolic Compounds. *Annu. Rev. Nutr.* **2001**, *21*, 381-406. (e) Bhat, K. P. L.; Pezzuto, J. M. Cancer Chemopreventive Activity of Resveratrol. *Ann. N. Y. Acad. Sci.* **2002**, *957*, 210-229. (f) de la Lastra, C. Alarcón; Villegas, I. Resveratrol as an Antioxidant and Pro-Oxidant Agent: Mechanisms and Clinical Implications. *Biochem. Soc. Trans.* **2007**, *35*, 1156-1160. (g) Gehm, B. D.; McAndrews, J. M.; Chien, P. Y.; Jameson, J. L. Resveratrol, a Polyphenolic Compound Found in Grapes and Wine, is an Agonist for the Estrogen Receptor. *Proc. Natl. Acad. Sci.* **1997**, *94*, 14138-14143. (h) Alzheimer's Association. 2015 Alzheimer's Disease Facts and Figures. *Alzheimer's Dement.* **2015**, *11*, 332-384.
2. (a) Collinge, D. B. *Plant Pathogen Resistance Biotechnology*, Edition 1; Wiley: Hoboken, 2016. (b) Langcake, P.; Pryce, R. J. The Production of Resveratrol by *Vitis vinefera* and Other Members of the Vitaceae as a Response to Infection or Injury. *Physiol. Plant Pathol.* **1976**, *9*, 77-86. (c) Kanagawa, N. Chemical Constituents of Polygonaceous Plants. I. Studies on the Components of Ko-jo-kon (*Polygonum cuspidatum* Sieb et Zucc. *Yakigaku Zasshi* **1963**, *83*, 988-990. (d) Lekli, I.; Ray, D.; Das, D. K. Longevity Nutrients Resveratrol, Wines, and Grapes. *Genes Nutr.* **2010**, *5*, 55-60.

3. (a) Soleas, G. J.; Diamandis, E. P.; Goldberg, D. M. Wine as a Biological Fluid: History, Production, and Role in Disease Prevention. *J. Clin. Lab Anal.* **1997**, *11*, 287-313. (b) Pennington Biomedical Research Center. Pennington Nutrition Series, Number 11. Resveratrol. [http://www.pbrc.edu/Division\\_of\\_Education/pdf/PNS\\_resveratrol.pdf](http://www.pbrc.edu/Division_of_Education/pdf/PNS_resveratrol.pdf). (accessed Feb 1, 2017). (c) Louisiana State University. Horticulture: Cultivar, Juice Extraction, Ultra Violet Irradiation and Storage Influence the Stilbene Content of Muscadine Grapes (*Vitis Rotundifolia* Michx.). <http://etd.lsu.edu/docs/available/etd-01202006-082858/> (accessed Feb 1, 2017). (d) Oregon State University. Linus Pauling Institute: Micronutrient Information Center. Resveratrol. <http://lpi.oregonstate.edu/infocenter/phytochemicals/resveratrol/> (accessed Feb 1, 2017). (e) Wang, Y.; Catana, F.; Yang, Y.; Roderick, R.; van Breemen, R. B. An LC-MS Method for Analyzing Total Resveratrol in Grape Juice, Cranberry Juice, and in Wine. *J. Agric. Food Chem.* **2002**, *50*, 431-435. (f) Rosemann, D.; Heller, W.; Sandermann, H. Biochemical Plant Responses to Ozone II Induction of Stilbene Biosynthesis in Scots Pine (*Pinus sylvestris* L.) Seedlings. *Plant Physiol.* **1991**, *97*, 1280-1286. (g) Ector, B. J.; Magee, J. B.; Hegwood, C. P.; Coign, M. J. Resveratrol Concentration in Muscadine Berries, Juice, Pomace, Purees, Seeds, and Wines. *Am. J. Enol. Vitic.* [Online] **1996**, *47*, 57-62 <http://www.ajevonline.org/cgi/content/abstract/47/1/57> (accessed Feb 1, 2017). (h) The Peanut Institute. Health and Nutrition: Protective Nutrients. <http://www.peanut-institute.org/health-and-nutrition/protective-nutrients/> (accessed Feb 1, 2017). (i) Lyons, M. M.; Yu, C.; Toma, R.B., Cho, S. Y.; Reiboldt, W.; Lee, J.; van Breemen, R. B. Resveratrol in Raw and Baked Blueberries and Bilberries. *J. Agric. Food Chem.* **2003**, *51*, 5867-5870. (j) Weiskirchen, S.; Weiskirchen, R. Resveratrol: How Much Wine Do You Have to Drink

- to Stay Healthy? *Adv. Nutr.* **2016**, 7, 706-718. (k) Frémont, L. Biological Effects of Resveratrol. *Life Sci.* **2000**, 66, 663-673. (l) Stervbo, U.; Vang, O.; Bonnesen, C. A Review of the Content of the Putative Chemopreventive Phytoalexin Resveratrol in Red Wine. *Food Chem.* **2007**, 101, 449-457.
4. (a) Bhat, K. P. L.; Kosmeder, J. W.; Pezzuto, J. M. Forum Review Article: Biological Effects of Resveratrol. *Antioxid. Redox Signal.* **2001**, 3, 1047-1064. (b) Alarcón de la Lastra, C.; Villegas, I.; Martin, A. R. In Resveratrol in Health and Disease Eds. Aggarwald, B. B.; Shishodia, S., CRC Press, Boca Raton, **2006**, 33-56. (c) Zini, R.; Morin, C.; Bertelli, A.; Bertelli, A. A.; Tillement, J. P. Effects of Resveratrol on the Rat Brain Respiratory Chain. *Drugs Exp. Clin. Res.* **1999**, 25, 87-97. (d) Athar, M.; Back, J. H.; Tang, X.; Kim, K. H.; Kopelovich, L.; Bickers, D. R.; Kim, A. L. Resveratrol: a Review of Preclinical Studies for Human Cancer Prevention. *Toxicol. Appl. Pharmacol.* **2007**, 224, 274-283. (e) Jang, M.; Pezzuto, J. M. Effects of Resveratrol on 12-*O*-Tetradecanoylphorbol-13-Acetate-Induced Oxidative Events and Gene Expression in Mouse Skin. *Cancer Lett.* **1998**, 134, 81-89. (f) Jang, M.; Cai, L.; Udeani, G. O.; Slowing, K. V.; Thomas, C. F.; Beecher, C. W.; Fong, H. H.; Farnsworth, N. R.; Kinghorn, A. D.; Mehta, R. G.; Moon, R. C. Cancer Chemopreventive Activity of Resveratrol, a Natural Product Derived from Grapes. *Science* **1997**, 275, 218-220. (g) Aziz, M. H.; Kumar, R.; Ahmad, N. Cancer Chemoprevention by Resveratrol: *in vitro* and *in vivo* Studies and the Underlying Mechanisms. *Int. J. Oncol.* **2003**, 23, 17-28. (h) Roemer, K.; Mahyar-Roemer, M. The Basis for the Chemopreventive Action of Resveratrol. *Drugs Today* **2002**, 38, 571-580. (i) Kueck, A.; Opipari, A. W.; Griffith, K. A.; Tan, L.; Choi, M.; Huang, J.; Wahl, H.; Liu, J. R. Resveratrol Inhibits Glucose Metabolism in Human Ovarian Cancer Cells. *Gynecol. Oncol.* **2007**, 107, 450-457.

- (j) Baur, J. A.; Sinclair, D. A. Therapeutic Potential of Resveratrol: the *in vivo* Evidence. *Nat. Rev. Drug Discov.* **2006**, *5*, 493-506. (k) Manna, S. K.; Mukhopadhyay, A.; Aggarwal, B. B. Resveratrol Suppresses TNF-Induced Activation of Nuclear Transcription Factors NF- $\kappa$ B, Activator Protein-1, and Apoptosis: Potential Role of Reactive Oxygen Intermediates and Lipid Peroxidation. *J. Immunol.* **2000**, *164*, 6509-6519. (l) Cadenas, S.; Barja, G. Resveratrol, Melatonin, Vitamin E, and PBN Protect Against Renal Oxidative DNA Damage Induced by the Kidney Carcinogen, KBrO<sub>3</sub>. *Free Radical Biol. Med.* **2000**, *26*, 1531-1537. (m) Kampa, M.; Hatzoglou, A.; Notas, G.; Damianaki, A.; Bakogeorgou, E.; Gemetzi, C.; Kouroumalis, E.; Martin, P. M.; Castanas, E. Wine Antioxidant Polyphenols Inhibit the Proliferation of Human Prostate Cancer Cell Lines. *Nutr. Cancer* **2000**, *37*, 223-233. (n) Martinez, J.; Moreno, J. J. Effect of Resveratrol, a Natural Polyphenolic Compound, on Reactive Oxygen Species and Prostaglandin Production. *Biochem. Pharmacol.* **2000**, *59*, 865-870. (o) Losa, G. A. Resveratrol Modulates Apoptosis and Oxidation in Human Blood Mononuclear Cells. *Eur. J. Clin. Invest.* **2003**, *33*, 818-823. (p) Yen, G. C.; Duh, P. D.; and Lin, C. W. Effects of Resveratrol and 4-Hexylresorcinol on Hydrogen Peroxide-Induced Oxidative DNA Damage in Human Lymphocytes. *Free Radical Res.* **2003**, *37*, 509-514.
5. (a) Sun, N. J.; Woo, S. H.; Cassady, J. M.; Snapka, R. M. DNA Polymerase and Topoisomerase II Inhibitors from *Psoralea corylifolia*. *J. Nat. Prod.* **1998**, *61*, 362-366. (b) Fontecave, M.; Lepoivre, M.; Elleingand, E.; Gerez, C.; Guittet, O. Resveratrol, a Remarkable Inhibitor of Ribonucleotide Reductase. *FEBS Lett.* **1998**, *421*, 277-279. (c) Reichard, P. Regulation of Deoxyribotide Synthesis. *Biochemistry* **1987**, *26*, 3245-3248. (d) Jordan, V. C.; Murphy, C. S. Endocrine Pharmacology of Antiestrogens as Antitumor



- Agents. *Endocr. Rev.* **1990**, *11*, 578-610. (e) Schwartz, S. A.; Hernandez, A.; Mark Evers, B. The Role of NF-kappaB/IkappaB Proteins in Cancer: Implications for Novel Treatment Strategies. *Surg. Oncol.* **1999**, *8*, 143-153. (f) Draczynska-Lusiak, B.; Chen, Y. M.; Sun, A. Y. Oxidized Lipoproteins Activate NF-kappaB Binding Activity and Apoptosis in PC12 Cell. *Neuroreport* **1998**, *9*, 527-532.
6. (a) Providencia, R. Cardiovascular Protection from Alcoholic Drinks: Scientific Basis of the French Paradox. *Rev. Port. Cardiol.* **2006**, *25*, 1043-1058. (b) Olsen, E. R.; Naugle, J. E.; Zhang, X.; Bomser, J. A.; Meszaros, J. G. Inhibition of Cardiac Fibroblast Proliferation and Myofibroblast Differentiation by Resveratrol. *Am. J. Physiol. Heart Circ. Physiol.* **2005**, *288*, H1131-1138. (c) Baur, J. A.; Pearson, K. J.; Price, N. L.; Jamieson, H. A.; Lerin, C.; Kalra, A.; Prabhu, V. V.; Allard, J. S.; Lopez-Lluch, G.; Lewis, K.; Pistell, P. J.; Poosala, S.; Becker, K. G.; Boss, O.; Gwinn, D.; Wang, M.; Ramaswamy, S.; Fishbein, K. W.; Spencer, R. G.; Lakatta, E. G.; Le Couteur D.; Shaw, R. J.; Navas, P.; Puigserver, P.; Ingram, D. K.; de Cabo, R.; Sinclair, D. A. Resveratrol Improves Health and Survival of Mice on a High-Calorie Diet. *Nature* **2006**, *444*, 337-342.
7. Lagouge, M.; Argmann, C.; Gerhart-Hines, Z.; Meziane, H.; Lerin, C.; Daussin, F.; Messadeq, N.; Milne, J.; Lambert, P.; Elliott, P.; Geny, B.; Laakso, M.; Puigserver, P.; Auwerx J. Resveratrol Improves Mitochondrial Function and Protects Against Metabolic Disease by Activating SIRT1 and PGC-1 $\alpha$ . *Cell* **2006**, *127*, 1109-1122.
8. Karuppagounder, S. S.; Pinto, J. T.; Xu, H.; Chen, H. L.; Beal, M. F.; Gibson, G. E. Dietary Supplementation with Resveratrol Reduces Plaque Pathology in a Transgenic Model of Alzheimer's Disease. *Neurochem. Int.* **2009**, *54*, 111-118.

9. (a) Elliott, P. J.; Jirousek, M. Sirtuins: Novel Targets for Metabolic Disease. *Curr. Opin. Invest. Drugs* **2008**, 9, 1472-4471. (b) Howitz, K. T.; Bitterman, K. J.; Cohen, H. Y.; Lamming, D. W.; Lavu, S.; Wood, J. G.; Zipkin, R. E.; Chung, P.; Kisielewski, A.; Zhang, L. L.; Scherer, B.; Sinclair, D. A. Small Molecule Activators of Sirtuins Extend *Saccharomyces cerevisiae* Lifespan. *Nature* **2003**, 425, 191-196. (c) Wood, J. G.; Rogina, B.; Lavul, S.; Howitz, K.; Helfand, S. L.; Tatar, M.; Sinclair, D. Sirtuin Activators Mimic Caloric Restriction and Delay Aging in Metazoans. *Nature* **2004**, 430, 686-689. (d) Gruber, J.; Tang, S. Y.; Halliwell, B. Evidence for a Trade-Off between Survival and Fitness Caused by Resveratrol Treatment of *Caenorhabditis elegans*. *Ann. N. Y. Acad. Sci.* **2007**, 1100, 530-542. (e) Bass, T. M.; Weinkove, D.; Houthoofd, K.; Gems, D.; Partridge, L. Effects of Resveratrol on Lifespan in *Drosophila melanogaster* and *Caenorhabditis elegans*. *Mech. Ageing Dev.* **2007**, 128, 546-552. (f) Pearson, K. J.; Baur, J. A.; Lewis, K. N.; Peshkin, L.; Price, N. L.; Labinskyy, N.; Swindell, W. R.; Kamara, D.; Minor, R. K.; Perez, E.; Jamieson, H. A. Resveratrol Delays Age-Related Deterioration and Mimics Transcriptional Aspects of Dietary Restriction without Extending Life Span. *Cell Metab.* **2008**, 8, 157-168.
10. (a) Merritt, R. J.; Jenks, B. H. Safety of Soy-Based Infant Formulas Containing Isoflavones: the Clinical Evidence. *J. Nutr.* **2004**, 134, 1220S-1224S. (b) Tuohy, P. G. Soy Infant Formula and Phytoestrogens. *J. Pediatr. Child Health* **2003**, 39, 401-405. (c) RevGenetics LLC. Resveratrol Research. <http://www.revgenetics.com/resveratrol/resveratrol-research> (accessed Feb 1, 2017). (d) Bowers, J. L.; Tyulmenkov, V. V.; Jernigan, S. C.; Klinge, C. M. Resveratrol Acts as a Mixed Agonist/Antagonist for Estrogen Receptors Alpha and Beta. *Endocrinology* **2000**,

- 141, 3657-3667. (e) Fischer, W. H.; Keiwan, A.; Schmitt, E.; Stopper, H. Increased Formation of Micronuclei after Hormonal Stimulation of Cell Proliferation in Human Breast Cancer Cells. *Mutagenesis* **2001**, *16*, 209-212. (f) Gregor, C.; Schmitt, E.; Fischer, W.; Stopper, H. Induction of Micronuclei Formation by Hormonal Stimulation of Cell Proliferation in BG-1 Cells. *Naunyn-Schmiedeberg's Arch. Pharmacol.* **2001**, *363* (Suppl.), R157. (g) Damianaki, A.; Bakogeorgou, E.; Kampa, M. Potent Inhibitory Action of Red Wine Polyphenols on Human Breast Cancer Cells. *J. Cell. Biochem.* **2000**, *78*, 429-441. (h) Bowers, J. L.; Tyulmenkov, V. V.; Jernigan, S. C.; Klinge, C. M. Resveratrol Acts as a Mixed Agonist/Antagonist for Estrogen Receptors  $\alpha$  and  $\beta$ . *Endocrinology*. **2000**, *141*, 3657-3667. (i) Bhat, K. P. L.; Pezzuto, J. M. Resveratrol Exhibits Cytostatic and Antiestrogenic Properties with Human Endometrial Adenocarcinoma (Ishikawa) Cells. *Cancer Res.* **2001**, *61*, 6137-6144. (j) Mizutani, K.; Ikeda, K.; Kawai, Y.; Yamori, Y. Resveratrol Stimulates the Proliferation and Differentiation of Osteoblastic MC3T3-E1 Cells. *Biochem. Biophys. Res. Commun.* **1998**, *253*, 859-863. (k) Bhat, K. P. L.; Lantvit, D.; Christov, K.; Mehta, R.G.; Moon, R. C.; Pezzuto, J. M. Estrogenic and Antiestrogenic Properties of Resveratrol in Mammary Tumor Models. *Cancer Res.* **2001**, *61*, 7456-7463.
11. (a) Fukuhara, K.; Miyata, N. Resveratrol as a New Type of DNA-Cleaving Agent. *Bioorg. Med. Chem. Lett.* **1998**, *8*, 3187-3192. (b) Ahmad, A.; Syed, F. A.; Singh, S.; Hadi, S. M. Prooxidant Activity of Resveratrol in the Presence of Copper Ions: Mutagenicity in Plasmid DNA. *Toxicol. Lett.* **2005**, *159*, 1-12. (c) Burkitt, M. J.; Duncan, J. Effects of Trans-Resveratrol on Copper-Dependent Hydroxyl Radical Formation and DNA Damage: Evidence for Hydroxyl-Radical Scavenging and a Novel Glutathione-Sparing Mechanism of Action. *Arch. Biochem. Biophys.* **2000**, *381*, 253-263. (d) Farber, J. L. Mechanisms of

- Cell Injury by Activated Oxygen Species. *Environ. Health Perspect.* **1994**, 102, 17-24. (e) Galati, G.; Sabzevari, O.; Wilson, J. X.; O'Brian, P. J. Prooxidant Activity and Cellular Effects of the Phenoxyl Radicals of Dietary Flavonoids and Other Polyphenolics. *Toxicology* **2002**, 177, 91-104. (f) De, S. R.; Festa, F.; Ricordy, R.; Perticone, P.; Cozzi, R. Resveratrol Affects in a Different Way Primary Versus Fixed DNA Damage Induced by H<sub>2</sub>O<sub>2</sub> in Mammalian Cells *in vitro*. *Toxicol. Lett.* **2002**, 135, 1-9. (g) Azmi, A. S.; Bhat, S. H.; Hadi, S. M. Resveratrol–Cu(II) Induced DNA Breakage in Human Peripheral Lymphocytes: Implications for Anticancer Properties. *FEBS Lett.* **2005**, 579, 3131-3135. (h) Azmi, A. S.; Bhat, S. H.; Hanif, S.; Hadi, S. M. Plant Polyphenols Mobilize Endogenous Copper in Human Peripheral Lymphocytes Leading to Oxidative DNA Breakage: a Putative Mechanism for Anticancer Properties. *FEBS Lett.* **2006**, 580, 533-538. (i) Shamim, U.; Hanif, S.; Ullah, M. F.; Azmi, A. S.; Bhat, S. H.; Hadi, S. M. Plant Polyphenols Mobilize Nuclear Copper in Human Peripheral Lymphocytes Leading to Oxidatively Generated DNA Breakage: Implications for an Anticancer Mechanism. *Free Radic. Res.* **2008**, 42, 764-772. (j) Khan, H. Y.; Zubair, H.; Ullah, M. F.; Ahmad, A.; Hadi, S. M. Oral Administration of Copper to Rats Leads to Increased Lymphocyte Cellular DNA Degradation by Dietary Polyphenols: Implication for a Cancer Preventive Mechanism. *Biometals* **2011**, 24, 1169-1178.
12. (a) Nelson, D. R.; Koymans, L.; Kamataki, T.; Stegeman, J. J.; Feyereisen, R.; Waxman, D. J.; Waterman, M. R.; Gotoh, O.; Coon, M. J.; Estabrook, R. W.; Gunsalus, I. C. P450 Superfamily: Update on New Sequences, Gene Mapping, Accession Numbers and Nomenclature. *Pharmacogenetics and Genomics*, **1996**, 6, 1-42. (b) Gonzales, F. J.; Gelboin, H. V. Role of Human Cytochromes P450 in the Metabolic Activation of Chemical

Carcinogens and Toxins. *Drug Metab. Rev.* **1994**, 26, 165-183. (c) Windmill, K. F.; McKinnon, R. A.; Zhu, X.; Gaedigk, A.; Grant, D. M.; McManus, M. E. The Role of Xenobiotic Metabolizing Enzymes in Arylamine Toxicity and Carcinogenesis: Functional and Localization Studies. *Mut. Res.* **1997**, 376, 153-160. (d) Murray, G. I. The Role of Cytochrome P450 in Tumor Development and Progression and its Potential in Therapy. *J. Pathol.* **2000**, 192, 419-426. (e) Murray, G. I.; Foster, C. O.; Barnes, T. S.; Weaver, R. J.; Ewen, S. W.; Melvin, W. T.; Burke, M. D. Expression of Cytochrome P450IA in Breast Cancer. *Br. J. Cancer* **1991**, 63, 1021-1023. (f) Mekhail-Ishak, K.; Hudson, N.; Tsao, M. S.; Batist, G. Implications for Therapy of Drug-Metabolizing Enzymes in Human Colon Cancer. *Cancer Res.* **1989**, 49, 4866-4869. (g) McLemore, T. L.; Adelberg, S.; Czerwinski, M.; Hubbard, W. C.; Yu, S. J.; Storeng, R.; Wood, T. G.; Hines, R. N.; Boyd, M. R. Altered Regulation of the Cytochrome P450IA1 Gene: Novel Inducer-Independent Gene Expression in Pulmonary Carcinoma Cell Lines. *J. Natl. Cancer Inst.* **1989**, 81, 1787-1794. (h) Ciolino, H. P.; Daschner, P. J.; Yeh, G. C. Resveratrol Inhibits Transcription of CYP1A1 *in vitro* by Preventing Activation of the Aryl Hydrocarbon Receptor. *Cancer Res.* **1998**, 58, 5707-5712. (i) Ciolino, H. P.; Yeh, G. C. Inhibition of Aryl-Hydrocarbon-Induced Cytochrome P-450 1A1 Enzyme Activity and CYP1A1 Expression by Resveratrol. *Mol. Pharmacol.* **1999**, 56, 760-767. (j) Casper, R. F.; Quesne, M.; Rogers, I. M.; Shirota, T.; Jolivet, A.; Milgrom, E.; Savouret, J. F. Resveratrol has Antagonist Activity on the Aryl Hydrocarbon Receptor: Implications for Prevention of Dioxin Toxicity. *Mol. Pharmacol.* **1999**, 56, 784-790. (k) Teel, R. W.; Huynh, H. Modulation by Phytochemicals of Cytochrome P450-Linked Enzyme Activity. *Cancer Lett.* **1998**, 133, 135-141. (l) Chang, T. K.; Lee, W. B.; Ko, H. H. Trans-Resveratrol Modulates the Catalytic Activity and

- mRNA Expression of the Procarcinogen-activating Human Cytochrome P450 1B1. *Can. J. Physiol. Pharmacol.* **2000**, 78, 874-881. (m) Chan, W. K.; Delucchi, A. B. Resveratrol, a Red Wine Constituent, is a Mechanism-Based Inactivator of Cytochrome P450 3A4. *Life Sci.* **2000**, 67, 3103-3112.
13. (a) Asensi, M.; Medina, I.; Ortega, A.; Carretero, J.; Baño, M. C.; Obrador, E.; Estrela, J. M. Inhibition of Cancer Growth by Resveratrol is related to its Low Bioavailability. *Free Radic. Biol. Med.* **2002**, 33, 387-398. (b) Walle, T.; Hsieh, F.; DeLegge, M. H.; Oatis, J. E.; Walle, U. K. High Absorption but Very Low Bioavailability of Oral Resveratrol in Humans. *Drug Metab. Dispos.* **2004**, 32, 1377-1382. (c) Boocock, D. J.; Faust, G. E.; Patel, K. R.; Schinas, A. M.; Brown, V. A.; Ducharme, M. P.; Booth, T. D.; Crowell, J. A.; Perloff, M.; Gescher, A. J.; Steward, W. P. Phase I Dose Escalation Pharmacokinetic Study in Healthy Volunteers of Resveratrol, a Potential Cancer Chemopreventive Agent. *Cancer Epidemiol. Biomarkers Prev.* **2007**, 16, 1246-1252.
14. (a) Whole Health. Vitamins and Supplements: Antioxidants. <http://www.wholehealth.com/vitamins-supplements/antioxidants.html> (accessed Feb 1, 2017). (b) Oregon State University. Linus Pauling Institute: Micronutrient Information Center. Resveratrol. <http://lpi.oregonstate.edu/mic/dietary-factors/phytochemicals/resveratrol#safety> (accessed Feb 1, 2017).
15. (a) Potter, G. A.; Patterson, L. H.; Wahogho, E.; Perry, P. J.; Butler, P. C.; Ijaz, T.; Ruparelia, K. C.; Lamb, J. H.; Farmer, P. B.; Stanley, L. A.; Burke, M. D. The Cancer Preventive Agent Resveratrol is Converted to the Anticancer Agent Piceatannol by the Cytochrome P450 Enzyme CYP1B1. *British J. Cancer* **2002**, 86, 774-778. (b) Melikyan, G. Guilty Until Proven Innocent: Antioxidants, Foods, Supplements, and Cosmetics, 1<sup>st</sup> ed.;

- Delta: California 2010, pp 368. (c) Piver, B.; Fer, M.; Vitrac, X.; Merillon, J.-M.; Dreano, Y.; Berthou, F.; Lucas, D. Involvement of Cytochrome P450 1A2 in the Biotransformation of trans-Resveratrol in Human Liver Microsomes. *Biochem. Pharm.* **2004**, *68*, 773-782.
16. (a) National Library of Medicine. National Institutes of Health: Genetics Home Reference. <https://ghr.nlm.nih.gov/gene/CYP2C19> (accessed Feb 1, 2017). (b) Fer, M.; Corcos, L.; Dréano, Y.; Plée-Gautier, E.; Salaün, J. P.; Berthou, F.; Amet, Y. Cytochromes P450 from Family 4 are the Main Omega Hydroxylating Enzymes in Humans: CYP4F3B is the Prominent Player in PUFA Metabolism. *J Lipid Res.* **2008**, *49*, 2379-2389.
17. (a) Wang, B.; Yang, L. P.; Zhang, X. Z.; Huang, S. Q.; Bartlam, M.; Zhou, S. F. New Insights into the Structural Characteristics and Functional Relevance of the Human Cytochrome P450 2D6 Enzyme. *Drug Metab. Rev.* **2009**, *41*, 573-643. (b) Corning Discovery Labware, Inc. (catalog number 456219, Human CYP2C19 + P450 Reductase Supersomes), [www.corning.com/lifesciences](http://www.corning.com/lifesciences) (accessed Mar 25, 2015). (c) Otten, S.; Schadel, M.; Cheung, S. W.; Kaplan, H. L.; Busto, U. E.; Sellers, E. M. CYP2D6 Phenotype Determines the Metabolic Conversion of Hydrocodone to Hydromorphone. *Clin. Pharmacol. Ther.* **1993**, *54*, 463-472. (d) Teh, L. K.; Bertilsson, L. Pharmacogenomics of CYP2D6: Molecular Genetics, Interethnic Differences and Clinical Importance. *Drug Metab. Pharmacokinet.* **2012**, *27*, 55-67.
18. (a) "P08684-CP3A4 Human". *UniProt*. Retrieved November 2014. (b) Corning Discovery Labware, Inc. (catalog number 456256, Human CYP3A5 + P450 Reductase + Cytochrome b<sub>5</sub> Supersomes), [www.corning.com/lifesciences](http://www.corning.com/lifesciences) (accessed Mar 25, 2015). (c) Emoto, C.; Nishida, H.; Hirai, H.; Iwasaki, K. CYP3A4 and CYP3A5 Catalyse the Conversion of the N-Methyl-D-Aspartate (NMDA) Antagonist CJ-036878 to Two Novel Dimers. *Xenobiotica*

- 2007**, 37, 1408-1420. (d) Zanger, U. M.; Turpeinen, M.; Klein, K.; Schwab, M. Functional Pharmacogenetics/genomics of Human Cytochromes P450 Involved in Drug Biotransformation. *Analytical and Bioanalytical Chemistry*. **2008**, 392, 1093-1108.
19. (a) Fer, M.; Corcos, L.; Dréano, Y.; Plée-Gautier, E.; Salaün, J. P.; Berthou, F.; Amet, Y. Cytochromes P450 from Family 4 are the Main Omega Hydroxylating Enzymes in Humans: CYP4F3B is the Prominent Player in PUFA Metabolism. *J. Lipid Res.* **2008**, 49, 2379-2389. (b) Sanders, R. J.; Ofman, R.; Dacremont, G.; Wanders, R. J.; Kemp, S. Characterization of the Human  $\omega$ -Oxidation Pathway for  $\omega$ -Hydroxy-Very-Long-Chain Fatty Acids. *FASEB J.* **2008**, 22, 2064-2071. (c) BD Biosciences-Discovery Labware, (catalog number 456273, Human CYP4F3A + P450 Reductase + Cytochrome b<sub>5</sub> Supersomes.) bdbiosciences.com (accessed Mar 25, 2015). (d) National Library of Medicine. National Institutes of Health: National Center for Biotechnology Information. <https://www.ncbi.nlm.nih.gov/gene/4051> (accessed Feb 1, 2017).
20. (a) Lewis, D. F.; Lake, B. G.; Bird, M. G.; Loizou, G. D.; Dickins, M.; Goldfarb, P. S. Homology Modelling of Human CYP2E1 Based on the CYP2C5 Crystal Structure: Investigation of Enzyme-Substrate and Enzyme-Inhibitor Interactions." *Toxicology in Vitro* **2003**, 17, 93–105. (b) Westphal, C.; Konkel, A.; Schunck, W. H. CYP-Eicosanoids - a New Link Between Omega-3 Fatty Acids and Cardiac Disease?" *Prostaglandins & Other Lipid Mediators* **2011**, 96, 99–108. (c) Rendic, S.; Di Carlo, F. J. Human Cytochrome P450 Enzymes: a Status Report Summarizing Their Reactions, Substrates, Inducers, and Inhibitors. *Drug Metabolism Reviews* **1997**, 29, 413–580. (d) Desai, H. D.; Seabolt, J.; Jann, M. W. Smoking in Patients Receiving Psychotropic Medications: a Pharmacokinetic Perspective. *CNS Drugs* **2001**, 15, 469–494. (e) Porubsky, P. R.; Meneely, K. M.; Scott, E.



- E. Structures of Human Cytochrome P-450 2E1. Insights Into the Binding of Inhibitors and Both Small Molecular Weight and Fatty Acid Substrates. *The Journal of Biological Chemistry* **2008**, 283, 33698-33707. (f) Hayashi, S.; Watanabe, J.; Kawajiri, K. Genetic Polymorphisms in the 5'-Flanking Region Change Transcriptional Regulation of the Human Cytochrome P450IIE1 Gene. *Journal of Biochemistry*. **1991**. 110, 559-565.
21. (a) Stresser, D. M.; Kupfer, D. Human Cytochrome P450–Catalyzed Conversion of the Pro-Estrogenic Pesticide Methoxychlor into an Estrogen Role of CYP2C19 and CYP1A2 in O-Demethylation. *Drug Metab Dispos*. **1998**, 26, 868-874. (b) Spector, A. A.; Kim, H. Y. Cytochrome P450 Epoxygenase Pathway of Polyunsaturated Fatty Acid Metabolism. *Biochimica et Biophysica Acta*. **2015**, 1851, 356-365. (c) Fleming, I. The Pharmacology of the Cytochrome P450 Epoxygenase/Soluble Epoxide Hydrolase Axis in the Vasculature and Cardiovascular Disease. *Pharmacological Reviews* **2014**, 66, 1106-1140. (d) Wagner, K.; Vito, S.; Inceoglu, B.; Hammock, B. D. The Role of Long Chain Fatty Acids and their Epoxide Metabolites in Nociceptive Signaling. *Prostaglandins & Other Lipid Mediators* **2014**, 113-115, 2-12. (e) Fischer, R.; Konkel, A.; Mehling, H.; Blossey, K.; Gapelyuk, A.; Wessel, N.; von Schacky, C.; Dechend, R.; Muller, D. N.; Rothe, M.; Luft, F. C.; Weylandt, K.; Schunck, W. H. Dietary Omega-3 Fatty Acids Modulate the Eicosanoid Profile in Man Primarily via the CYP-Epoxygenase Pathway. *Journal of Lipid Research* **2014**, 55, 1150-1164. (f) McMaster University. Poster: Cytochrome P450 Metabolites of Arachidonic Acid: Potential Roles in Intestinal Ion Transport. <http://mcmaster.ca/inabis98/rangacharipharm/schleihauf0148/index.html> (accessed Feb 1, 2017).

22. (a) Corning Discovery Labware, Inc. (catalog number 456207, Human CYP3A4 + P450 Reductase Supersomes. [www.corning.com/lifesciences](http://www.corning.com/lifesciences) (accessed Mar 25, 2015). (b) Chen, H.; Howald, W. N.; Juchau, M. R. Biosynthesis of All-Trans-Retinoic Acid from All-Trans-Retinol: Catalysis of All-Trans-Retinol Oxidation by Human P-450 Cytochromes. *Drug Metab. Dispos.* **2000**, *28*, 315-322. (c) Bishop-Bailey, D.; Thomson, S.; Askari, A.; Faulkner, A.; Wheeler-Jones, C. Lipid-Metabolizing CYPs in the Regulation and Dysregulation of Metabolism. *Annual Review of Nutrition* **2014**, *34*, 261–279. (d) Bidstrup, T. B.; Bjørnsdottir, I.; Sidelmann, U. G.; Thomsen, M. S.; Hansen, K. T. CYP2C8 and CYP3A4 are the Principal Enzymes Involved in the Human In Vitro Biotransformation of the Insulin Secretagogue *Repaglinide*. *Br. J. Clin. Pharmacol.* **2003**, *56*, 305-314. (e) Shahrokh, K.; Cheatham, T. E.; Yost, G. S. Conformational Dynamics of CYP3A4 Demonstrate the Important Role of Arg212 Coupled with the Opening of Ingress, Egress, and Solvent Channels to Dehydrogenation of 4-Hydroxy-tamoxifen. *Biochimica et Biophysica Acta* **2012**, *1820*, 1605–1617. (f) Flockhart, D. A. Drug Interactions: Cytochrome P450 Drug Interaction Table (2007).
23. (a) Corning Discovery Labware, Inc. (catalog number 456211, Human CYP1A1 + P450 Reductase Supersomes.) [www.corning.com/lifesciences](http://www.corning.com/lifesciences) (accessed Mar 25, 2015). (b) Doostdar, H.; Burke, M. D.; Mayer, R. T. Bioflavonoids: Selective Substrates and Inhibitors for Cytochrome P450 CYP1A and CYP1B1. *Toxicology*. **2000**, *144*, 31-38. (c) Beresford, A. P. CYP1A1: Friend or Foe? *Drug Metabolism Reviews* **1993**, *25*, 503-517.
24. (a) Mwenifumbo, J. C.; Lessov S. C. N.; Zhou, Q.; Krasnow, R. E.; Swan, G. E.; Benowitz, N. L.; Tyndale, R. F. Identification of Novel CYP2A6\* 1B variants: the CYP2A6\* 1B Allele is Associated with Faster In Vivo Nicotine Metabolism. *Clin. Pharmacol. Ther.*

- 2008**, 83, 115-121. (b) McGraw, J. E; Waller, D. P. Specific Human CYP450 Isoform Metabolism of a Pentachlorobiphenol (PCB-IUPAC#101). *Biochem. Biophys. Res. Commun.* **2006**, 344, 129-133. (c) Lacy, C. F.; Armstrong, L. L.; Goldman, M. P.; Lance, L. L. Cytochrome P450 Enzymes: Substrates, Inhibitors, and Inducers. Hudson, OH: LexiComp Inc.; 2007, pp. 1899-1912.
25. (a) BD Biosciences-Discovery Labware, (catalog number 456258, Human CYP2C9\*1 (Arg<sub>144</sub>) + P450 Reductase + Cytochrome b<sub>5</sub> Supersomes. bdbiosciences.com (accessed Mar 25, 2015). (b) Rettie, A. E.; Wienkers, L. C.; Gonzalez, F. J.; Trager, W. F.; Korzekwa, K. R. Impaired (S)-Warfarin Metabolism Catalysed by the R144C Allelic Variant of CYP2C9. *Pharmacogenet. Genomics* **1994**, 4, 39-42. (c) Bland, T. M.; Haining, R. L.; Tracy, T. S.; Callery, P. S. CYP2C-Catalyzed Delta (9)-Tetrahydrocannabinol Metabolism: Kinetics, Pharmacogenetics and Interaction with Phenytoin. *Biochem. Pharmacol.* **2005**, 70, 1096-1103. (d) Rettie, A. E.; Jones, J. P. Clinical and Toxicological Relevance of CYP2C9: Drug-Drug Interactions and Pharmacogenetics. *Annual Review of Pharmacology and Toxicology.* **2005**, 45, 477-494.
26. Westphal, C.; Konkel, A.; Schunck, W. H. CYP-Eicosanoids - a New Link Between Omega-3 Fatty Acids and Cardiac Disease? *Prostaglandins and Other Lipid Mediators* **2011**, 96, 99-108.
27. (a) Eksterowicz, J.; Rock, D. A.; Rock, B. M.; Wienkers, L. C.; Foti, R. S. Characterization of the Active Site Properties of CYP4F12. *Drug Metab. Dispos.* **2014**, 42, 1698-1707. (b) BD Biosciences – Discovery Labware (catalog number 456275, CYP4F12 + P450 Reductase + Cytochrome b<sub>5</sub> Supersomes), bdbiosciences.com (accessed Mar 25, 2015). (c) Johnson, A. L.; Edson, K. Z.; Totah, R. A.; Rettie, A. E. Cytochrome P450  $\omega$ -Hydroxylases

- in Inflammation and Cancer. *Advances in Pharmacology* **2015**, 74, 223-262. (d) Westphal, C.; Konkel, A.; Schunck, W. H. CYP-Eicosanoids - a New Link Between omega-3 Fatty Acids and Cardiac Disease? *Prostaglandins and Other Lipid Mediators* **2001**, 96, 99–108.
- (e) Fleming, I. The Pharmacology of the Cytochrome P450 Epoxygenase/Soluble Epoxide Hydrolase Axis in the Vasculature and Cardiovascular Disease. *Pharmacological Reviews* **2014**, 66, 1106-1140. (f) Zhang, G.; Kodani, S.; Hammock, B. D. Stabilized Epoxygenated Fatty Acids Regulate Inflammation, Pain, Angiogenesis and Cancer. *Progress in Lipid Research* **2014**, 53, 108-123.
28. Cavalieri, E. L.; Li, K.; Balu, M.; Saeed, M.; Devanesan, P.; Higginbotham, S.; Zhao, J.; Gross, M. L.; Rogan, E. G. Catechol ortho-Quinones: the Electrophilic Compounds that Form Depurinating DNA Adducts and Could Initiate cancer and Other Diseases. *Carcinogenesis* **2002**, 23, 1071-1077.
29. Masuda, T.; Inaba, Y.; Maekawa, T.; Takeda, Y.; Tamura, H.; Yamaguchi, H. Recovery Mechanism of the Antioxidant Activity from Carnosic Acid Quinone, an Oxidized Sage and Rosemary Antioxidant. *J. Agric. Food Chem.* **2002**, 50, 5863-5869.